Even-tempered Gaussian atomic orbital bases in quantum chemistry: *Ab initio* calculations on atoms hydrogen through krypton and on molecules containing carbon, hydrogen, and oxygen

by

Richard Dale Bardo

A Dissertation Submitted to the
Graduate Faculty in Partial Fulfillment of
The Requirements for the Degree of
DOCTOR OF PHILOSOPHY

Department: Chemistry
Major: Physical Chemistry

Approved:

Signature was redacted for privacy.

In Charge of Major Work

Signature was redacted for privacy.

For the Major Department

Signature was redacted for privacy.

For the Graduate College

Iowa State University
Ames, Iowa
1973

TABLE OF CONTENTS

FORMULATION OF PROBLEM

Ab initio calculations on systems of chemical interest require solutions to the Schroedinger equation. Although exact wave functions cannot be obtained for systems containing more than one electron, considerable progress has been made by quantum chemists in the development of mathematical methods from which rather accurate, approximate wave functions can be generated. Programming these methods on high-speed computers has enabled the quantum chemist to provide quantitatively meaningful results of importance to the field of chemistry. However, the need for calculations on molecular systems with ever-increasing numbers of electrons will continue to strain the capabilities of computers. Therefore, refinements in the existing methods as well as the search for new techniques must be continually made so that accurate calculations on large systems will become more accessible.

The most versatile ab initio treatments for atoms and molecules include the concept of the complete set of spin orbitals for constructing wave functions. Each spin orbital is defined as a product of a one-electron space orbital $\varphi_{i_{\mu\mu}}(r)$ and a spin function (1). Since a complete set of spin orbitals is usually infinite, the theoretician must resort to the use of finite subsets in performing calculations. From these orbital subsets approximate wave functions are constructed by any one of a number of ab initio theories. Of these, the most widely used one is the Hartree-Fock method (2) in which the wave function is an antisymmetrized product of spin orbitals u_i,

$$\psi(1,2,\ldots,N) = A\{u_1(1)u_2(2)\ldots u_N(N)\} \ . \qquad (1)$$

The space orbitals $\varphi_i(\underset{\sim}{r})$ may be expanded in terms of a finite number of suitably chosen basis functions χ_k,

$$\varphi_i(\underset{\sim}{r}) = \sum_k \chi_k(\underset{\sim}{r})\, C_{ki}. \qquad (2)$$

Once the analytic form for $\chi_k(\underset{\sim}{r})$ is specified, the variational principle is invoked in order to determine the optimal $\chi_k(\underset{\sim}{r})$ and expansion coefficients C_{ki} which give the lowest total energy of the atomic or molecular system. If one is interested in obtaining in this manner the minimum total energy corresponding to Equation (1), approximate Hartree-Fock solutions are produced.

A variety of basis functions have been introduced in the past and used in atomic and molecular calculations. The type of basis set to be investigated in the present work is the even-tempered basis of primitive atomic orbitals defined by

$$p(k\ell m|\underset{\sim}{r}) = N_\ell^\varepsilon \cdot (\alpha_\ell \beta_\ell^{\,k})^{[(2\ell+3)/2\varepsilon]} \cdot \exp(-\alpha_\ell \beta_\ell^{\,k} r^\varepsilon) \cdot r^\ell \cdot S_\ell^m(\theta,\varphi),$$

$$\alpha_\ell, \beta_\ell > 0, \quad \beta_\ell \neq 1, \quad k = 1,2,\ldots,M. \qquad (3)$$

Two choices of the power ε are of particular interest. The choice $\varepsilon = 1$ yields even-tempered exponential-type primitive atomic orbitals (ETEPAO's); the choice $\varepsilon = 2$ yields even-tempered Gaussian-type primitive atomic orbitals (ETGPAO's). The parameters α_ℓ and β_ℓ are, in general,

different for different values of the quantum number ℓ, although the possibility of using the same α and β for all values of ℓ will also be considered. The symbol β_ℓ^k denotes the k-th power of β_ℓ. The factors N_ℓ^ϵ contain the necessary numerical normalization constants. The $S_\ell^m(\theta,\varphi)$ are normalized spherical harmonic functions which may be real or complex. As discussed in Reference (3), treating $r^\ell \cdot S_\ell^m(\theta,\varphi)$ as a unit (a solid spherical harmonic) facilitates the formulation of mathematical expressions for integral evaluation. The normalization constants are

$$N_\ell^1 = 2^{\ell+3/2}\,[(2\ell+2)!]^{-1/2},$$

$$N_\ell^2 = 2^{\ell+7/4}\pi^{-1/4}\,[(2\ell+1)!!]^{-1/2}.$$

The special form for the exponent parameters, $\alpha_\ell\beta_\ell^k$, which suggests the name "even-tempered", is of particular importance for atomic and molecular calculations. A basis set of M even-tempered primitives, instead of having one optimizable orbital exponent per basis function, has at most only two such parameters for each value of ℓ. Such a large decrease in the number of optimizable parameters greatly increases the feasibility of performing full optimizations in atoms and molecules. Except for calculations on atoms, full-scale molecular optimizations employing the most widely-used bases with ζ_k replacing $\alpha_\ell\beta_\ell^k$ have been found to be unfeasible in the past. This is due to the fact that optimization methods are iterative and based on quadratic fits where, for a given number of free parameters n, each fit requires $(n+1)(n+2)/2$ function evaluations per independent group.

In Reference (4) linear combinations of ETEPAO's ($\varepsilon = 1$ in Equation (3)) were found to give close approximations to atomic SCF orbitals. The ETEPAO's would be the best basis functions for molecular calculations, too. However, the difficulties encountered with exponential-type functions such as the ETEPAO's in calculating molecular multi-centered integrals, is the main deterent to their use. On the other hand, the multi-center integrals over primitive Gaussians are much simpler and more tractable as detailed in Reference (5). Therefore, in spite of the fact that more Gaussian than exponential primitives are needed, the majority of molecular calculations have used Gaussian basis sets.

The present work is concerned primarily with the construction of bases of ETGPAO's for use in molecular calculations. Chapter I deals with the economic deployment of ETGPAO's in expanding atomic SCF orbitals. In Chapter II, use is made of the geometric progression of orbital exponents, Equation (3), to devise a method for constructing primitive and contracted even-tempered Gaussian atomic orbitals which allow the atomic orbitals to expand or contract in molecular calculations. Finally, in Chapter III full optimizations of the parameters α_ℓ and β_ℓ are made in molecules. For this purpose, minimization schemes are implemented and used in conjunction with the LCAO-MO-SCF technique for solving the Hartree-Fock equations (6). With the techniques developed here, bases of ETGPAO's are found to be very well suited for use in molecular calculations.

CHAPTER I. ECONOMIC DEPLOYMENT OF EVEN-TEMPERED GAUSSIAN PRIMITIVES IN EXPANDING ATOMIC SCF ORBITALS

Introduction

The economic deployment of all available atomic-orbital-type basis functions is an important consideration when Gaussian-type primitives are used to expand molecular orbitals, and an important first step in attaining this effectiveness is the optimal determination of accurate as well as economic expansions of atomic self-consistent-field orbitals. This is so no matter which course molecular calculations follow. A variety of Gaussian expansions for atomic self-consistent-field orbitals have therefore been published in recent years (7-16). But there still is a need for systematic analyses comparing the efficiency of such expansions.

Of particular interest is the problem of the optimal lengths of the individual atomic-orbital expansions for a given total number of basis functions. While highest accuracy results, of course, when all primitives are used for all atomic orbitals, a substantial reduction in the lengths of the individual AO expansion is in fact possible with only a negligible effect on the overall accuracy. The examination of this question for different numbers of total primitives and for different atoms is the main object of the present investigation.

Even-tempered Gaussian atomic-basis sets are used in these calculations. As has been discussed in References (17) and (18), the loss in accuracy incurred by the limitation to even-temperedness is negligible as compared to the substantial advantages of such basis sets. In the present

context, the systematic formal uniformity of the expansions obtained for various cases is particularly useful. We are confident that the general conclusions deduced here are also valid for other types of Gaussian-type basis sets.

Expansion of SCF-AO's in Terms of Even-Tempered Gaussian Primitives

In Reference (17), we have introduced the even-tempered Gaussian primitives (ETGPAO's)

$$g(k\ell m|\underset{\sim}{r}) = N_\ell \cdot (\alpha_\ell \beta_\ell^k)^{(2\ell+3)/4} \exp(-\alpha_\ell \beta_\ell{}^k r^2) \cdot r^\ell Y_{\ell m}(\Theta,\phi) \quad (4a)$$

$$N_\ell = 2^{(4\ell+7)/4} \pi^{-\frac{1}{2}} [(2\ell+1)!!]^{-\frac{1}{2}} \quad (4b)$$

where β_ℓ^k denotes the k-th power of the spacing parameter β_ℓ and $Y_{\ell m}$ are normalized spherical harmonics.

Energetically optimal even-tempered representations of canonical SCF-AO's result from solving the matrix form of the Hartree-Fock equations in a basis of even-tempered Gaussian primitives. We have found, however, that atomic orbitals of nearly equal quality are obtained by suitable least mean square fitting of even-tempered expansions to known accurate exponential-type representations of SCF-AO's. The fitting procedure is based on the weighted mean square deviations

$$d_{n\ell}(\alpha_\ell,\beta_\ell) = \int dV[\psi(n\ell m|\underset{\sim}{r}) - \varpi(n\ell m|\underset{\sim}{r})]^2/r \quad (5)$$

of the even-tempered expansions

$$\phi(n\ell m|r) = \sum_k g(k\ell m|r)c(k|n\ell) \qquad (6)$$

from "accurate" orbitals $\psi(n\ell m)$. Minimization of Equation 5 for fixed α_ℓ,β_ℓ yields the orbital expansion coefficients $c(k|n\ell)$ of α_ℓ and β_ℓ. Nonlinear minimization of the weighted averages

$$D(\alpha_\ell,\beta_\ell) = \sum_n w_{n\ell} d_{n\ell}(\alpha_\ell,\beta_\ell) \qquad (7)$$

yields the optimal parameters α_ℓ,β_ℓ for each symmetry ℓ.

The weight factors in these equations, namely r^{-1} in Equation (5) and $w_{n\ell}$ in Equation (7) were chosen so as to make the total energies resulting from these wavefunctions as close as possible to the accurate SCF energies. It was found that r^{-1} was superior to any other power of r and that the most effective choice for the $w_{n\ell}$ was

$$w_{n\ell} = (2 - \delta_{1n})10^{1-n} \times (\text{orbital occupation number}). \qquad (8)$$

This choice favors the inner orbitals and, in most cases, results in a somewhat better relative fit for them. Nonetheless, the values of orbital energies of the outer orbitals are, in general, still better than those of the inner orbitals. The relative emphasis on the accuracy of the inner orbitals is considered desirable for use of the resulting expansions in molecular calculations, because the inner orbitals remain much the same, when atoms form different molecules. Valence orbitals, on the other hand, vary greatly when atoms enter various bonds, and for them, flexibility and adaptability of the basis set would seem to be more appropriate than an extremely accurate reproduction of particular atomic or molecular orbitals in any one system.

Equations (5) and (7) yield the best possible fitted even-tempered Gaussian bases. However, for the purpose of the present investigation, it is found that no substantial deterioration in accuracy occurs if one assumes $\alpha_\ell = \alpha$ and $\beta_\ell = \beta$ to be independent of ℓ and determines α and β by minimizing

$$\tilde{D}(\alpha,\beta) = \sum_{n\ell}\sum w_{n\ell}\tilde{d}_{n\ell}(\alpha,\beta). \tag{9}$$

This is substantiated in Table 1 which provides a comparison of the absolute and relative deviations of the total energies and of the individual orbital energies for the atoms nitrogen and aluminum obtained by the following procedures:

(1) weighted least mean square fitting of accurate SCFAO's by even-tempered Gaussian-type expansions with different α_ℓ and β_ℓ for different ℓ, based on Equation (7);

(2) weighted least mean square fitting of accurate SCFAO's by even-tempered Gaussian-type expansions with $\alpha_\ell = \alpha$ and $\beta_\ell = \beta$ the same for all ℓ, based on Equation (9).

The poorer energies of the 1s orbitals result because in procedure (2), a larger number of outer orbitals influence the values of α and β (which the 1s orbital, too, must use).

Comparisons of total and individual orbital energies for expansions obtained by procedure (2) with those of the energies optimized SCFAO's of Huzinaga (7) and Clementi (18) are presented in Tables 2, 3, 4, and 5. Each table contains information pertaining to one atom or a group of atoms all having the same number and kinds of SCFAO's. For each atom in

Table 1. Comparison of even-tempered Gaussian bases with different α_ℓ, β_ℓ for different ℓ and with $\alpha_\ell = \alpha$, $\beta_\ell = \beta$ the same for all ℓ

Absolute Deviations (in atomic units) from Accurate SCF Energies[a]

Atom	Basis[b]	$\Delta\epsilon$ (3s)	$\Delta\epsilon$ (3p)	$\Delta\epsilon$ (2s)	$\Delta\epsilon$ (2p)	$\Delta\epsilon$ (1s)	ΔE
N	$(\alpha_\ell,\beta_\ell \mid 7,7,4;11,11)$			.0032	.0050	.029	.075
	$(\alpha\beta \mid 7,7,4;11,7)$			.0037	.0041	.031	.078
	$(\alpha_\ell,\beta_\ell \mid 7,7,7;17,17)$			.00011	-.00017	.0025	.0090
	$(\alpha\beta \mid 7,7,7;17,10)$			.00007	-.00019	.0026	.0092
Al	$(\alpha_\ell,\beta_\ell \mid 6,6,6,6,6;18,18)$	.0070	.0059	.013	.0083	.039	.098
	$(\alpha\beta \mid 6,6,6,6,6;18,10)$	.0060	.0043	.014	.011	.057	.12
	$(\alpha_\ell,\beta_\ell \mid 7,7,7,7,7;21,21)$	.00071	.00029	.0014	-.00018	.011	.038
	$(\alpha\beta \mid 7,7,7,7,7;21,12)$	.00056	.00020	.0011	-.00029	.012	.039

Percent Deviations from Accurate SCF Energies[a]

Atom	Basis[b]	$\lvert\%\Delta\epsilon$ (3s)$\rvert$	$\lvert\%\Delta\epsilon$ (3p)$\rvert$	$\lvert\%\Delta\epsilon$ (2s)$\rvert$	$\lvert\%\Delta\epsilon$ (2p)$\rvert$	$\lvert\%\Delta\epsilon$ (1s)$\rvert$	$\lvert\%\Delta E\rvert$
N	$(\alpha_\ell,\beta_\ell \mid 7,7,4;11,11)$			.33	.88	.19	.14
	$(\alpha\beta \mid 7,7,4;11,7)$			.39	.71	.20	.14
	$(\alpha_\ell,\beta_\ell \mid 7,7,7;17,17)$			.011	.029	.016	.016
	$(\alpha\beta \mid 7,7,7;17,10)$			.010	.033	.017	.017
Al	$(\alpha_\ell,\beta_\ell \mid 6,6,6,6,6;18,18)$	1.8	2.8	.27	.26	.066	.040
	$(\alpha\beta \mid 6,6,6,6,6;18,10)$	1.5	2.0	.28	.34	.097	.050
	$(\alpha_\ell,\beta_\ell \mid 7,7,7,7,7;21,21)$	.18	.14	.027	.0050	.018	.015
	$(\alpha\beta \mid 7,7,7,7,7;21,12)$	.14	.10	.022	.0090	.019	.016

[a] The accurate SCF energies are taken from Clementi (see Ref. 18). The absolute deviation and absolute value of the percent deviation are defined as $\Delta\epsilon = \epsilon - \epsilon$ (Clementi) and $\lvert\%\Delta\epsilon\rvert = \lvert\Delta\epsilon/\epsilon$ (Clementi)$\rvert \times 100$, respectively, and similarly for ΔE.

[b] The symbols α_ℓ,β_ℓ and $\alpha\beta$ to the left of the vertical line within the parentheses distinguish bases with different $\alpha_\ell\beta_\ell$ for different ℓ and with $\alpha_\ell = \alpha$, $\beta_\ell = \beta$ for all ℓ, respectively. The number of primitives for each AO is given between the vertical line and the semicolon according to the order: 1s, 2s, 3s, 2p, 3p. To the right of the semicolon, the number of basis functions and the number of exponents are given.

Table 2. Absolute and relative errors in orbital and total energies of even-tempered and optimal Gaussian bases for Li

Atom	Basis[b]	Absolute Deviations (in atomic units) from Accurate SCF Energies[a] $\Delta\varepsilon(2s)$	$\Delta\varepsilon(1s)$	ΔE
Li	H(7,7;7,7)	.0014	.00027	.0024
	BR(7,7;7,7)	.00049	.0053	.0097
	H(10,10;10,10)	.00002	.00012	.00022
	BR(7,6;10,10)	.00006	.00051	.0015

[a]The accurate SCF energies are taken from Clementi (18). The absolute deviation and absolute value of the percent deviation are defined as $\Delta\varepsilon = \varepsilon - \varepsilon$ (Clementi) and $|\%\Delta\varepsilon| = |\Delta\varepsilon/\varepsilon \text{ (Clementi)}| \times 100$, respectively, and similarly for ΔE.

[b]The codes H and BR reference Huzinaga's bases (7) and this work, respectively. The number of primitives for each AO is given in parentheses to the left of the semicolon according to the order: 1s, 2s, 2p, 3p. For code BR the value of k, which subscripts the initial primitive Gaussian in Equation (6), is different for each orbital corresponding to a given value of ℓ. These initial subscripts are not given here, but are available in Table 7. To the right of the semicolon the number of basis functions (=N, as defined on p. 15) and the number of distinct exponents (=M, as defined on p. 15) are given.

Table 2. (Continued)

Atom	Basis[b]	Percent Deviations from Accurate SCF Energies[a] $\lvert\%\Delta\varepsilon(2s)\rvert$	$\lvert\%\Delta\varepsilon(1s)\rvert$	$\lvert\%\Delta E\rvert$
Li	H(7,7;7,7)	.70	.011	.032
	BR(7,7;7,7)	.25	.21	.13
	H(10,10;10,10)	.01	.0048	.0029
	BR(7,6;10,10)	.03	.020	.019

Table 3. Absolute and relative errors in orbital and total energies of even-tempered and optimal Gaussian bases for Na

Atom	Basis[b]	$\Delta\epsilon$ (3s)	$\Delta\epsilon$ (2s)	$\Delta\epsilon$ (2p)	$\Delta\epsilon$ (1s)	ΔE
	Absolute Deviations (in atomic units) from Accurate SCF Energies[a]					
Na	H(9,9,9,5;14,14)	.0017	.0068	.0074	.012	.030
	BR(5,5,6,5;14,9)	.0013	.012	.0063	.096	.22
	H(12,12,12,6;18,18)	.00037	.0018	.0020	.0026	.0063
	BR(7,7,7,7;19,12)	.00016	.0012	.00047	.0089	.026
	Percent Deviations from Accurate SCF Energies[a]					
Atom	Basis[b]	$\lvert\%\Delta\epsilon$ (3s)$\rvert$	$\lvert\%\Delta\epsilon$ (2s)$\rvert$	$\lvert\%\Delta\epsilon$ (2p)$\rvert$	$\lvert\%\Delta\epsilon$ (1s)$\rvert$	$\lvert\%\Delta E\rvert$
Na	H(9,9,9,5;14,14)	.92	.24	.49	.028	.018
	BR(5,5,6,5;14,9)	.71	.42	.41	.23	.13
	H(12,12,12,6;18,18)	.20	.064	.13	.0065	.0038
	BR(7,7,7,7;19,12)	.088	.042	.031	.022	.016

[a]See Table 2 for this footnote.

[b]See Table 2 for this footnote.

Table 4. Absolute and relative errors in orbital and total energies of even-tempered and optimal Gaussian bases for B, N, and F

Atom	Basis[b]	$\Delta\epsilon$ (2s)	$\Delta\epsilon$ (2p)	$\Delta\epsilon$ (1s)	ΔE
	Absolute Deviations (in atomic units) from Accurate SCF Energies[a]				
B	H(7,7,3;10,10)	.0013	.0063	.0030	.015
	BR(7,7,4;11,7)	.0016	.00085	.015	.034
	H(10,10,6;16,16)	.00003	.00009	.00021	.00076
	BR(7,7,7;17,10)	.00002	-.00009	.0010	.0044
N	H(7,7,3;10,10)	.0070	.019	.0048	.061
	BR(7,7,4;11,7)	.0037	.0041	.031	.078
	H(10,10,6;16,16)	.00021	.00044	.00044	.0020
	BR(7,7,7;17,10)	.00007	-0.00019	.0026	.0092
F	H(7,7,3;10,10)	.021	.047	.012	.17
	BR(7,7,4;11,7)	.0090	.010	.056	.16
	H(10,10,6;16,16)	.00076	.0010	.0012	.0043
	BR(7,7,7;17,10)	.00051	.00001	0061	.016
	Percent Deviations from Accurate SCF Energies[a]				
Atom	Basis[b]	$\lvert\%\Delta\epsilon$ (2s)$\rvert$	$\lvert\%\Delta\epsilon$ (2p)$\rvert$	$\lvert\%\Delta\epsilon$ (1s)$\rvert$	$\lvert\%\Delta E\rvert$
B	H(7,7,3;10,10)	.26	2.0	.039	.059
	BR(7,7,4;11,7)	.32	.27	.20	.14
	H(10,10,6;16,16)	.006	.03	.0027	.0030
	BR(7,7,7;17,10)	.004	.03	.013	.018
N	H(7,7,3;10,10)	.74	3.4	.031	.11
	BR(7,7,4;11,7)	.39	.71	.20	.143
	H(10,10,6;16,16)	.022	.077	.0028	.0036
	BR(7,7,7;17,10)	.01	.033	.017	.017
F	H(7,7,3;10,10)	1.3	6.4	.045	.18
	BR(7,7,4;11,7)	.57	1.4	.21	.16
	H(10,10,6;16,16)	.048	.14	.0046	.0043
	BR(7,7,7;17,10)	.032	.003	.023	.016

[a] See Table 2 for this footnote.

[b] See Table 2 for this footnote.

Table 5. Absolute and relative errors in orbital and total energies of even-tempered and optimal Gaussian bases for Al, P, and Ar

Absolute Deviations (in atomic units) from Accurate SCF Energies[a]

Atom	Basis[b]	$\Delta\epsilon$ (3s)	$\Delta\epsilon$ (3p)	$\Delta\epsilon$ (2s)	$\Delta\epsilon$ (2p)	$\Delta\epsilon$ (1s)	ΔE
Al	H(10,10,10,6,6,;16,16)	.0071	.015	.0075	.0099	.0087	.052
	BR(6,6,6,6,6;18,10)	.0060	.0043	.014	.011	.057	.12
	H(12,12,12,8,8;20,20)	.0031	.0018	.0066	.0067	.0082	.0083
	BR(7,7,7,7,7;21,12)	.00056	.00020	.0011	-.00029	.011	.039
P	H(10,10,10,6,6;16,16)	.013	.013	.024	.031	.029	.091
	BR(6,6,6,6,6;18,10)	.0095	.0079	.016	.010	.056	.15
	H(12,12,12,8,8;20,20)	.0030	.0029	.0047	.0048	.0057	.011
	BR(7,7,7,7,7;21,12)	-.00004	-.00016	-.00029	-.0029	.012	.058
Ar	H(10,10,10,6,6;16,16)	.012	.015	.017	.028	.020	.14
	BR(6,6,6,6,6;18,10)	.016	.016	.029	.020	.086	.24
	H(12,12,12,8,8;20,20)	.0060	.0067	.0036	.0079	.0082	.021
	BR(7,7,7,7,7;21,12)	-.00079	-.00099	-.0029	-.0077	.013	.094

Percent Deviations from Accurate SCF Energies[a]

Atom	Basis[b]	$\lvert\%\Delta\epsilon$ (3s)$\rvert$	$\lvert\%\Delta\epsilon$ (3p)$\rvert$	$\lvert\%\Delta\epsilon$ (2s)$\rvert$	$\lvert\%\Delta\epsilon$ (2p)$\rvert$	$\lvert\%\Delta\epsilon$ (1s)$\rvert$	$\lvert\%\Delta E\rvert$
Al	H(10,10,10,6,6;16,16)	1.8	7.1	.15	.31	.015	.021
	BR(6,6,6,6,6;18,10)	1.5	2.0	.28	.34	.097	.050
	H(12,12,12,8,8;20,20)	.79	.86	.13	.21	.014	.0034
	BR(7,7,7,7,7;21,12)	.14	.10	.022	.0090	.019	.016
P	H(10,10,10,6,6;16,16)	1.9	3.3	.32	.57	.036	.027
	BR(6,6,6,6,6;18,10)	1.3	2.0	.21	.18	.069	.045
	H(12,12,12,8,8;20,20)	.43	.74	.062	.089	.0071	.0031
	BR(7,7,7,7,7;21,12)	.01	.041	.0038	.052	.015	.017
Ar	H(10,10,10,6,6;16,16)	.94	2.5	.14	.29	.017	.026
	BR(6,6,6,6,6;18,10)	1.2	2.6	.24	.21	.071	.046
	H(12,12,12,8,8;20,20)	.47	1.1	.029	.082	.0069	.0039
	BR(7,7,7,7,7;21,12)	.061	.17	.023	.080	.011	.018

[a]See Table 2 for this footnote.

[b]See Table 2 for this footnote.

the tables, shell-by-shell energy comparisons are given for two even-tempered expansions. The percent deviations show that even-tempered Gaussian bases provide good representations of accurate SCFAO's, even if there is a substantial reduction in the number of primitives expanding each SCFAO. This reduction in the size of the basis set will be dealt with in greater detail in the next two sections. Moreover, these tables confirm that the procedure based on Equation (9) will be very adequate for establishing the information sought in the present investigation. It can also be seen that the deviations depend upon the expansion length and the orbital type in a consistent manner.

As has been discussed in a separate investigation (19), there exist advantages in using nonorthogonal SCFAO's rather than orthogonal canonical SCFAO's. Firstly, scaling in a molecular context is more appropriate for the nonorthogonal SCFAO's. Secondly, shorter expansions in terms of primitives result for the latter. It is this latter property which furnishes the very basis for the present investigation. We ask: How short can the expansions of these nonorthogonal SCFAO's be chosen without loss of accuracy? The even-tempered SCFAO's to be discussed in the sequel are therefore obtained by the following procedure. First, accurate expansions of canonical SCFAO's in terms of exponential type primitives, such as given by Clementi (18) or by Raffenetti (4) are deorthogonalized by the technique developed in Reference (19). These accurate exponential expansions of nonorthogonal SCFAO's are then expressed in terms of even-tempered Gaussian expansions of various lengths by the fitting procedures described in connection with Equations (5) to (9), with $\alpha_\ell = \alpha$, $\beta_\ell = \beta$ the

same for all ℓ.

Determination of Optimal Expansions

Criteria

The efficiency of an atomic orbital basis is roughly given by the ratio of the "quality" of the generated SCF wavefunction to the "number of AO's deployed." As a criterion for judging the "quality" of an approximate SCF wavefunction, we shall use the total weighted mean square deviation (TWMSQD) introduced in Equation (9) of the preceding section, since it appears to represent a satisfactory compromise between an energy and a wavefunction criterion. The concept of "the number of AO's deployed" is complicated by the fact that one must distinguish between the total number of basis AO's and the number of basis AO's used to represent the individual SCFAO's. Fortunately, the analysis is clarified by the fact that the even-tempered parameters α,β are chosen independent of ℓ. An examination of the calculated expansions shows that (1) the total number M of exponents $\alpha\beta^k[k = 1, 2, \ldots M]$ determines the optimal quality possible for a given basis, and (2) this quality can be closely approximated even if each of the individual AO's does not contain all M exponents.

The discussion is facilitated by defining the following quantities:

$x(n\ell)$ = the number of even-tempered basis AO's used to represent any one of the SCFAO's $\psi(n\ell m)$. (The expansions for different m-values are entirely analogous to each other.)

$N(\ell)$ = The number of even-tempered basis AO's used to represent all SCF

AO's $\psi(n\ell m)$ for $n = (\ell+1), (\ell+2), \ldots$ with ℓ and m fixed. Since the same basis AO's may be used by different SCFAO's, the number $N(\ell)$ is in general smaller than the sum $\Sigma_n x(n\ell)$.

$N = \Sigma_n \Sigma_\ell x(n,\ell)$ = the "total number" of basis functions occurring in all SCFAO's counting, however, each ℓ-symmetry only once and not $(2\ell+1)$ times.

Since the representation of the s-orbitals requires basis AO's with highest and lowest exponents, it is apparent that $N(0) = N(s) = M$ = the total number of exponents $\alpha\beta^k$. However, for $\ell \geq 1$, we have in general $N(\ell) < M$.

Discussion of a prototype

To illustrate the quantitative situation, we shall work through the explicit results of the oxygen atom groundstate. Figure 1 contains plots of TWMSQD against N. Each point corresponds to a particular choice of x(1s), x(2s), x(2p), and M. The number triple next to each point is in fact [x(1s), x (2s), x(2p)]. The points on the dashed curve are obtained when all exponents are used in the expansion of each individual SCFAO, i.e., x(1s) = x(2s) = x(2p) = M. Thus, the number triples next to these points are in fact (M, M, M). Since all coefficients as well as α and β are completely optimized, this clearly represents the lowest TWMSQD obtainable for the chosen set of primitives. Plotted are results for $3 \leq M \leq 13$ because, for $M < 3$, the calculated energy becomes positive, and for $M > 13$, TWMSQD improves by less than 10^{-5}.

From any one of these expansions more efficient expansions are derived by the following procedure. In each SCFAO, primitives with

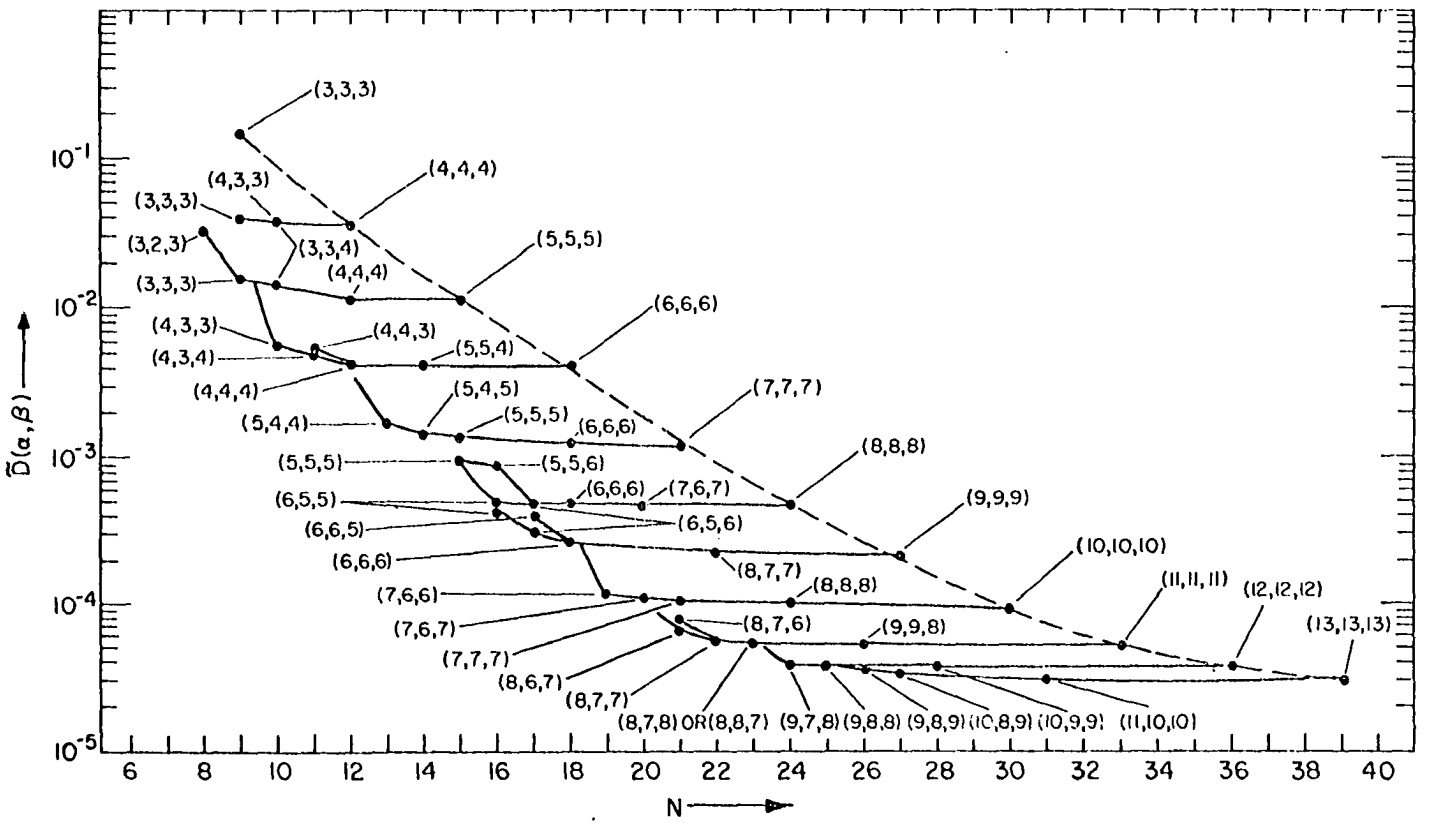

Figure 1. Total weighted mean square deviation (TWMSQD) for even-tempered Gaussian expansions of various lengths for nonorthogonal SCFAO's of the oxygen groundstate

the highest and/or, lowest exponents are eliminated if the magnitudes of their coefficients are < 10^{-4} and two coefficients of nearly the same magnitude have alternate signs. Thus a new expansion [x'(1s), x'(2s), x'(2p)] is defined in which each SCFAO contains only part of the primitive set. Coefficients and parameters (α,β) are again optimized, and the resulting TWMSQD is plotted and connected to the (M,M,M) point by a solid line. For M = 11, this yields the second expansion (9,9,8). The expansion (9,9,8) is then re-examined: now all primitives with coefficient magnitudes < 10^{-3} are deleted, and the coefficients and (α,β) re-optimized. It corresponds to the expansion (8,7,7). Explicit information about the expansions (11,11,11), (9,9,8), and (8,7,7) of oxygen are given in Table 6. An examination of the orbital mean square deviations shows that the deterioration in the TWMSQD is primarily due to the elimination of the 2p primitive from the expansion (9,9,8). Adding again the 2p primitive yields an expansion (8,7,8), also shown in Table 6, that is about as good as the expansion (9,9,8). It is apparent that hardly any accuracy has been lost until now. The situation changes, however, when one or several of the SCFAO expansions are further shortened. Hence, primitives are now removed one by one from each SCFAO in order to determine the effect on the TWMSQD. In this manner the additional points (8,6,7), (8,7,6), and (7,7,7) are determined on the branch that originates from (11,11,11). It is seen that, while the branch is fairly horizontal until (8,7,8) or (8,7,7), it turns up to the left of these points. In fact, for the expansion (7,7,7), the TWMSQD increases so much that it becomes identical to the TWMSQD obtained for the expansions based on M = 10.

Table 6. Even-tempered Gaussian expansions of nonorthogonal SCFAO's corresponding to M = 11 for oxygen (^3P)

Expansions of Nonorthogonal SCFAO's

(11,11,11)-Basis				(9,9,8)-Basis			
Exponents[a]	1s	2s	2p	Exponents[a]	1s	2s	2p
0.145136	-0.001681	0.123734	0.171842	0.139534	0.0	0.109796	0.159111
0.415342	0.006109	0.582929	0.416577	0.397053	0.0	0.567091	0.409299
1.188598	-0.007452	0.418179	0.395410	1.129840	-0.000628	0.439765	0.399613
3.401451	0.149088	-0.037437	0.202651	3.215034	0.125773	-0.022548	0.212506
9.734045	0.467363	-0.082339	0.058118	9.148589	0.458871	-0.086765	0.062677
27.856242	0.347250	-0.013996	0.014121	26.032909	0.360612	-0.015983	0.015576
79.717139	0.135246	-0.003109	0.002316	74.078345	0.145340	-0.003381	0.002516
228.129201	0.042161	0.000188	0.000523	210.794774	0.045810	0.000055	0.000693
652.844964	0.012637	-0.000205	0.000032	599.830312	0.014038	-0.000114	0.0
1868.268265	0.002356	0.000060	0.000024	1706.856367	0.002566	0.0	0.0
5346.485767	0.001663	-0.000015	-0.000001	4856.971382	0.001884	0.0	0.0
MSQ-DEV	2.12(-5)	6.16(-6)	7.61(-6)		2.30(-5)	5.75(-6)	6.59(-6)
TWHSQD	5.10(-5)				5.36(-5)		

(8,7,7)-Basis				(8,7,8)-Basis			
Exponents[a]	1s	2s	2p	Exponents[a]	1s	2s	2p
0.141502	0.0	0.114294	0.163408	0.140186	0.0	0.111029	0.159280
0.402524	0.0	0.571097	0.410417	0.398189	0.0	0.567145	0.408863
1.145042	0.0	0.433226	0.398366	1.131024	0.0	0.438287	0.398826
3.257253	0.128883	-0.025837	0.209196	3.212585	0.124415	-0.022019	0.212274
9.265772	0.461290	-0.086047	0.062559	9.125100	0.458343	-0.087143	0.062784
26.357952	0.357144	-0.015293	0.014116	25.919142	0.360670	-0.015759	0.015647
74.979358	0.143741	-0.003492	0.003664	73.621318	0.146173	-0.003612	0.003539
213.290632	0.045071	0.0	0.0	209.115659	0.046072	0.0	0.000702
606.738903	0.013883	0.0	0.0	593.976858	0.014227	0.0	0.0
1725.964678	0.002514	0.0	0.0	1687.145328	0.002577	0.0	0.0
4909.779239	0.001862	0.0	0.0	4792.205826	0.001920	0.0	0.0
MSQ-DEV	2.30(-5)	5.92(-6)	8.80(-6)		2.31(-5)	5.84(-6)	6.60(-6)
TWHSQD	5.54(-5)				5.38(-5)		

[a]The exponent parameters are as follows: (11,11,11)-Basis, α = 0.0507163, β = 2.861733; (9,9,8)-Basis, α = 0.0490356, β = 2.845565; (8,7,7)-Basis, α = 0.0497429, β = 2.844658; (8,7,8)-Basis, α = 0.0493541, β = 2.840423.

Thus the following conclusions can be drawn: (i) For M = 11 it is wasteful to choose x(1s), x(2s), x(2p) larger than (8,7,8) since no accuracy is gained; (ii) if x(1s), x(2s), x(20) are chosen as (7,7,7), then it is wasteful to choose M larger than 10; choosing M = 11 does not yield additional accuracy. The most effective expansion for M = 11 is therefore (8,7,8) or (8,7,7). From Figure 1 it is apparent that the situation is similar for other values of M. In each case, the branch originating at (M,M,M) starts out to be horizontal and then turns up. The most effective expansions occur for the points where the upturn begins.

The selection of the most effective expansion for a given M value is made with the help of the following criterion. First, it is required that the TWMSQD of the reduced expansion is $\leq$ 1.4 times the TWMSQD of the (M,M,M) expansion. In general, this leads to expansion coefficients $\geq 10^{-3}$. In cases where two expansions with similar TWMSQD exist, the WMSQD's for the individual orbitals are examined and the smallest basis is chosen consistent with the requirements that the WMSQD's of the individual orbitals, too, are $\leq$ 1.4 times the corresponding values for the (M,M,M) expansions. If there is still ambiguity, the expansion giving the best accuracy to the inner shell is chosen. In this manner one finds the expansion (8,7,8) for oxygen and M = 11. It is characterized by the following data:

M = 11, i.e., exponents $\alpha\beta^k$ with k = 1, 2, . . . 11

x(1s) = 8, i.e., exponents for k = 4, 5, 6, . . . 11

x(2s) = 7, i.e., exponents for k = 1, 2, . . . 7

x(2p) = 8, i.e., exponents for k = 1, 2, . . . 8

N(s) = 11, i.e., exponents for k = 1, 2, . . . 11

N(p) = 8, i.e., exponents for k = 1, 2, . . . 8

N = 8 + 7 + 8 = 23

TWMSQD $\simeq 5 \times 10^{-5}$.

Most Effective Expansions for Various Atoms

Expansion lengths

A graph of the type discussed for oxygen can be obtained for every atom. It then can be used to determine the most economical expansion for each value of M. The results of this analysis for all atoms up to krypton are presented in Table 7. Each column in this table contains data corresponding to a group of atoms, for which the most economical expansions have similar characteristics regarding the $x(n,\ell)$ numbers. Atoms with the same number and kinds of SCFAO's belong to one group. For each value of M, there are given the values of $x(n,\ell)$ and, in parentheses, also the k-value of the lowest exponent k for each (n,ℓ). For example, the atoms Sc through Zn in the periodic system form a group and, for them, the most effective expansions based on a total of M = 10 primitive exponents $\alpha\beta^k$ are as follows:

x(1s) = 6, with k = 5, 6, 7, 8, 9, 10,

x(2s) = 5, with k = 4, 5, 6, 7, 8,

x(3s) = 5, with k = 2, 3, 4, 5, 6,

x(3s) = 5, with k = 1, 2, 3, 4, 5,

x(2p) = 5, with k = 4, 5, 6, 7, 8,

x(3p) = 5, with k = 2, 3, 4, 5, 6,

x(3d) = 5, with k = 2, 3, 4, 5, 6.

Table 7. Expansion lengths of even-tempered Gaussian bases for the most economic representations of nonorthogonal SCFAO's[a]

No. of Exponents	Li, Be (▽)	B, C, N, O, F, Ne (△)	Na (◇), Mg	Al, Si (□), P, S, Cl, Ar (⊡)
3	3(1)3(1)	3(1)3(1),3(1)		
4	3(2)3(1)	3(2)3(1),3(1)	3(2)3(2)3(1),3(2)	3(2)3(2)3(1),3(2)3(1)
5	4(2)3(1)	3(3)3(1),3(1)	3(3)3(2)4(1),3(2)	3(3)3(2)4(1),3(2)4(1)
6	4(3)4(1)	4(3)4(1),4(1)	4(3)4(2)4(1),4(2)	4(3)4(2)4(1),4(2)4(1)
7	5(3)4(1)	5(3)5(1),5(1)	4(4)4(2)5(1),5(2)	4(4)4(2)5(1),5(2)5(1)
8	6(3)5(1)	6(3)5(1),6(1)	5(4)5(2)5(1),5(2)	5(4)5(2)5(1),5(2)5(1)
9	7(3)5(1)	6(4)6(1),6(1)	5(5)5(3)6(1),5(3)	5(5)5(3)6(1),5(3)6(1)
10	7(4)6(1)	7(4)7(1),7(1)	6(5)6(3)6(1),6(3)	6(5)6(3)6(1),6(3)6(1)
11	8(4)6(1)	8(4)7(1),8(1)	6(6)6(3)7(1),6(3)	6(6)6(3)7(1),6(3)7(1)
12	9(4)7(1)	9(4)8(1),8(1)	7(6)7(3)7(1),7(3)	7(6)7(3)7(1),7(3)7(1)
13	10(4)7(1)	10(4)8(1),9(1)	8(6)8(3)8(1),8(3)	8(6)8(3)8(1),8(3)8(1)
14			9(6)8(3)8(1),8(3)	9(6)8(3)8(1),8(3)8(1)

No. of Exponents	K (●), Ca	Sc, Ti, V, Cr, Mn, Fe, Co, Ni, Cu, Zn (⊙)	Ga, Ge, As, Se, Br, Kr (X)
5	4(2)4(2)5(1)5(1),4(2)5(1)	4(2)4(2)5(1)5(1),4(2)5(1),5(1)	4(2)4(2)5(1)5(1),4(2)5(1)5(1),5(1)
6	4(3)4(2)5(1)5(1),4(2)5(1)	4(3)4(2)5(1)5(1),4(2)5(1),5(1)	4(3)4(2)5(1)5(1),4(2)5(1)5(1),5(1)
7	5(3)4(3)5(1)5(1),4(3)5(1)	5(3)4(3)5(1)5(1),4(3)5(1),5(1)	5(3)4(3)5(1)5(1),4(3)5(1)5(1),5(1)
8	5(4)5(3)5(2)5(1),5(3)5(2)	5(4)5(3)5(2)5(1),5(3)5(2),5(2)	5(4)5(3)5(2)5(1),5(3)5(2)5(1),5(2)
9	5(5)5(4)5(2)5(1),5(4)5(2)	5(5)5(4)5(2)5(1),5(4)5(2),5(2)	5(5)5(4)5(2)5(1),5(4)5(2)5(1),5(2)
10	6(5)5(4)5(2)5(1),5(4)5(2)	6(5)5(4)5(2)5(1),5(4)5(2),5(2)	6(5)5(4)5(2)5(1),5(4)5(2)5(1),5(2)
11	6(6)6(4)6(2)6(1),6(4)6(2)	6(6)6(4)6(2)6(1),6(4)6(2),6(2)	6(6)6(4)6(2)6(1),6(4)6(2)6(1),6(2)
12	6(7)7(4)7(2)7(1),7(4)7(2)	6(7)7(4)7(2)7(1),7(4)7(2),7(2)	6(7)7(4)7(2)7(1),7(4)7(2)7(1),7(2)
13	7(7)7(4)7(2)7(1),7(4)7(2)	7(7)7(4)7(2)7(1),7(4)7(2 ,7(2)	7(7)7(4)7(2)7(1),7(4)7(2)7(1),7(2)
14	8(7)8(4)8(2)8(1),8(4)8(2)	8(7)8(4)8(2)8(1),8(4)8(2),8(2)	8(7)8(4)8(2)8(1),8(4)8(2)8(1),8(2)

[a] Each array of numbers consists of the number of even-tempered Gaussians expanding each SCFAO, n, followed by the initial value of k for $\alpha\beta^k$ in parentheses. These parameters are grouped as follows: $n_{1s}(k_{1s})n_{2s}(k_{2s})n_{3s}(k_{3s})$, ... , $n_{2p}(k_{2p})n_{3p}(k_{3p})$, ... , $n_{3d}(k_{3d})$.

It should be mentioned that an exhaustive analysis such as that for oxygen was not carried out for all the atoms of Table 7, but only for those atoms with the smallest and largest atomic number in each group. However, some of the selected expansions were examined for a few of the remaining atoms in each group and were always found to be the most economical. The validity of this approach is demonstrated in the next section.

The results reported in this table approximately obey the following results:

(i) In the most economic expansions, each SCFAO uses the same number $x(n,\ell) = x$ primitives.

(ii) The number of primitives used to represent all SCFAO's within a given ℓ- symmetry, i.e., the value of $N(\ell)$, is related to the AO expansion length x by

$$N(\ell) \approx x\{a_\ell + b_\ell[n(\ell) - \ell]\}$$

where $n(\ell)$ is the maximum value of the n-quantum number for that ℓ-value in the atom in question. Specifically,

$$N(0) = N(s) \approx x\{1.225 + 0.125\ n(s)\},$$

$$N(1) = N(p) \approx x\{1.273 + 0.053[n(p) - 1]\},$$

$$N(2) = N(d) = x.$$

(iii) Also we have $N(s) = M$, as mentioned before.

Quality of expansions

As one progresses further into the periodic table, the accuracy obtainable from an expansion based on M primitive exponents gradually

decreases. This statement encompasses three observations. First and most important, the weighted mean square deviation of the (1s) orbital deteriorates, since it becomes increasingly difficult to fit the cusp as the nuclear charge increases. Second, the quality of the fit of the outer orbitals remains about the same. Third, the TWMSQD increases because (i) the inner orbital fit is worse and (ii) a greater number of orbital deviations are added up. We shall illustrate this behavior for two types of expansions, the (M,M,M) expansions and the most effective expansions given in Table 7.

In Figure 2, the situation is illustrated for the (M,M,M) expansions of the atoms H to Ne. The average weighted mean square deviation per SCFAO

$$\overline{D}(Z,M) = [\mathrm{TWMSQD}/\Sigma_{n\ell} w(n,\ell)] \qquad (10)$$

is plotted against M. The increase of the latter quantity is indicative of the worsening 1s-fit. It is furthermore apparent from the figure that the orbital average of TWMSQD increases by an almost constant factor of about 1.2 in going from atomic number Z to atomic number Z+1, regardless of the values of Z and M. This is confirmed numerically in Table 8.

Figure 3 exhibits plots of $[\mathrm{TWMSQD}/\Sigma_{n\ell} w(n\ell)]$ versus M for the expansions given in Table 7. This figure does not contain plots for all atoms of the second and third rows since the points fall too close together for a clear display. However, the grouping of all atoms in Table 7 is substantiated by the grouping of the average orbital deviations plotted in Figure 3. The similarity of the results shown in Figure 2 and Figure 3 indicates that the dependence of the TWMSQD upon the atomic

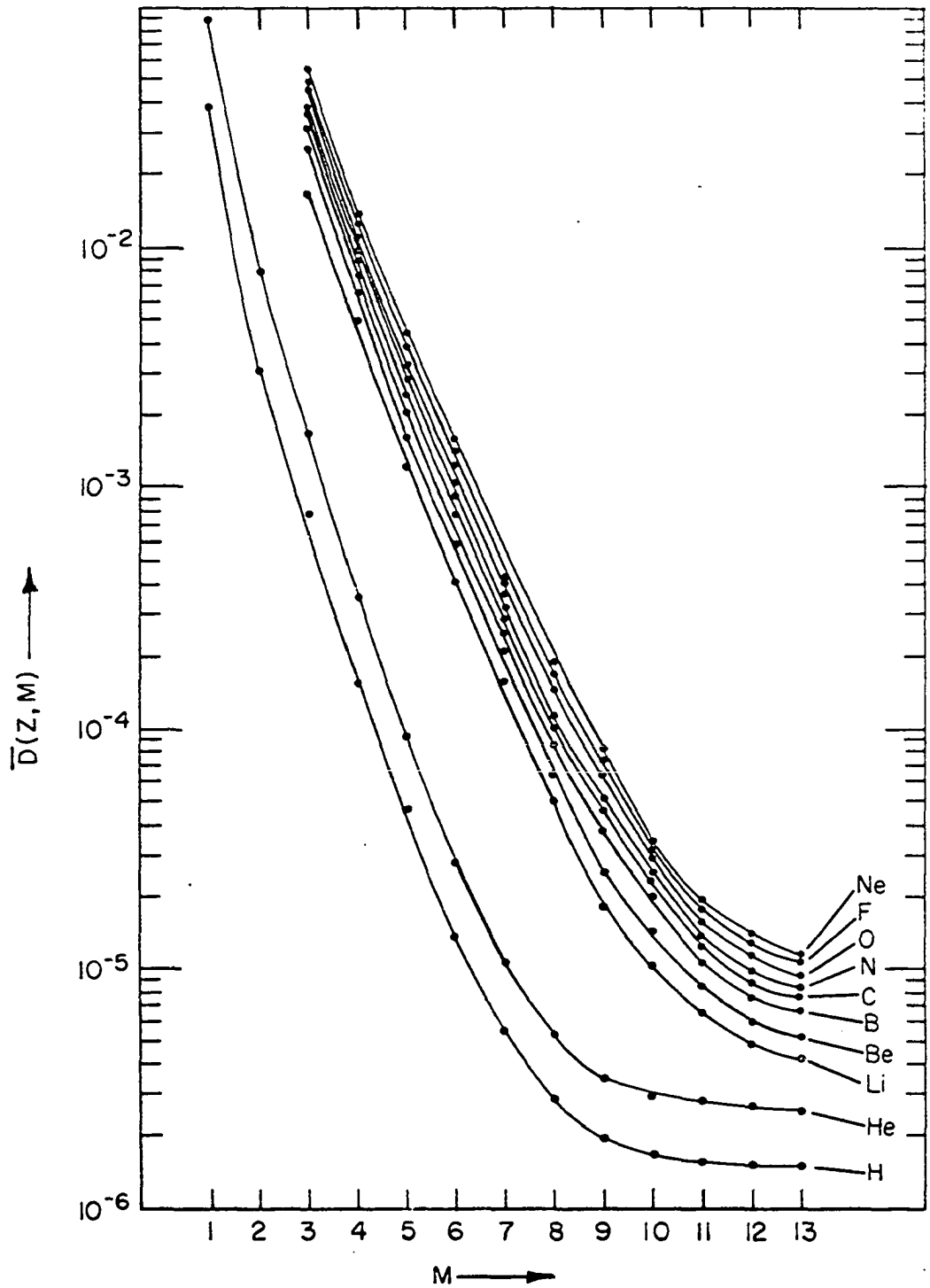

Figure 2. Average weighted mean square deviations per non-orthogonal SCFAO for the (M,M.M) even-tempered Gaussian expansions of the groundstates of H through Ne

Table 8. Ratios[a] of average values of $\bar{D}(Z,M)$ for neighboring atoms

Be/Li	B/Be	C/B	N/C	O/N	F/O	Ne/F
1.33	1.25	1.20	1.12	1.14	1.12	1.17

[a]The ratios are defined as $\bar{D}(Z+1)/\bar{D}(Z)$ where $\bar{D}(Z)$ = average of $\bar{D}(Z,M)$ over all M with $\bar{D}(Z,M)$ given in Equation (10)

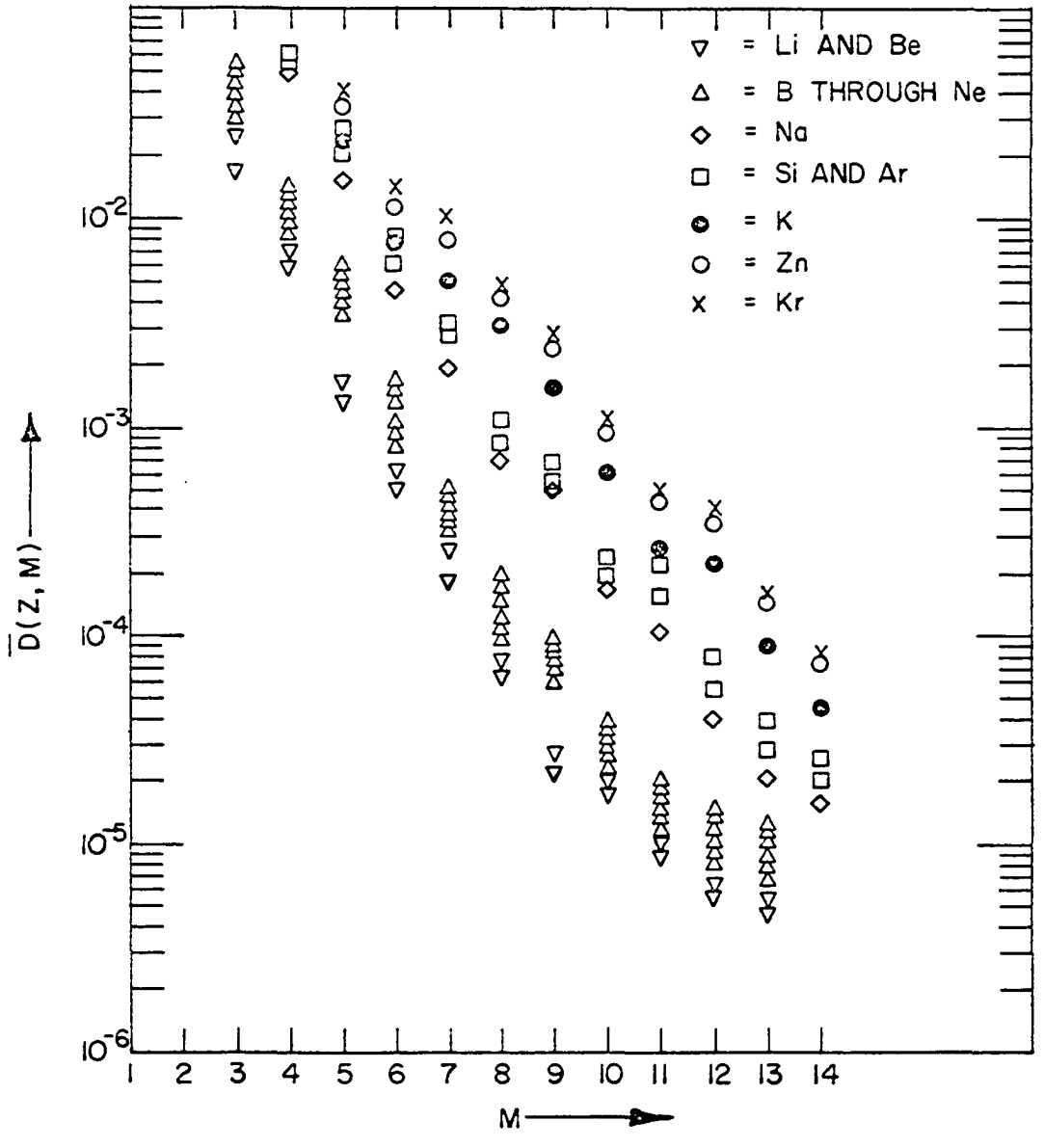

Figure 3. Average weighted mean square deviations per non-orthogonal SCFAO for even-tempered Gaussian expansions and atoms given in Table 7

number and M is of general validity.

It should also be mentioned that, to a very good approximation, the excited state SCFAO's of Clementi (18), too, may be expanded in the same bases of Table 7. As a result, the conclusions given above are expected to apply to these states also.

Even-tempered Gaussian bases with the optimal expansion length of Table 7 for the groundstates of hydrogen through krypton are available in Reference (20). These expansions were determined by minimizing Equation (7) for each ℓ value and therefore provide improved representations of the SCFAO's. For each atom the following quantities are tabulated: (1) optimal α_ℓ and β_ℓ parameter, (2) expansion coefficients, (3) mean square deviations, (4) the expectation values $\langle r^n \rangle$, n = -2, -1, 0, 1, 2, for each atomic orbital, and (5) the energies.

Regularities of exponential parameters

Figure 4 exhibits the values of all exponents $\alpha\beta^k$ for all M values in oxygen, obtained when all SCFAO's are expanded in terms of M even-tempered AO's. The pattern indicates that, with increasing number of primitives the range of exponential values covered by the even-tempered set increases and the spacing between adjacent exponents decreases. The change in α is more drastic than that in β.

This type of behavior is found in all atoms. Figure 5 shows the variation of β with atomic number Z for various M values of the bases in Table 7. A strong variation occurs only when both M and Z are small. Figure 6 shows the variation of α with the atomic number Z for groups of M values of the bases in Table 7. Since α is essentially a scale parameter,

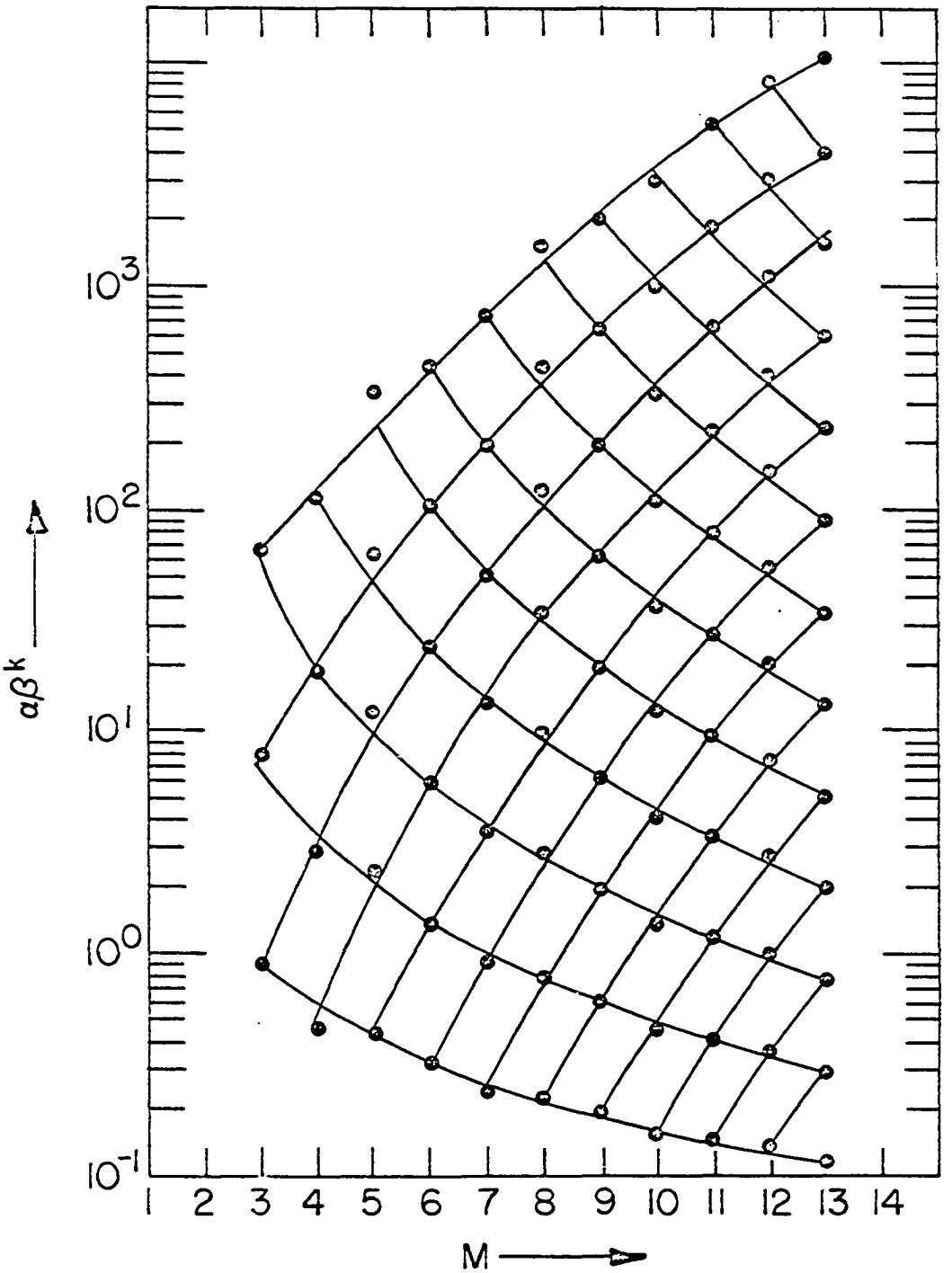

Figure 4. Exponents $\alpha\beta^k$ for the (M, M, M) even-tempered Gaussian expansions of the oxygen groundstate

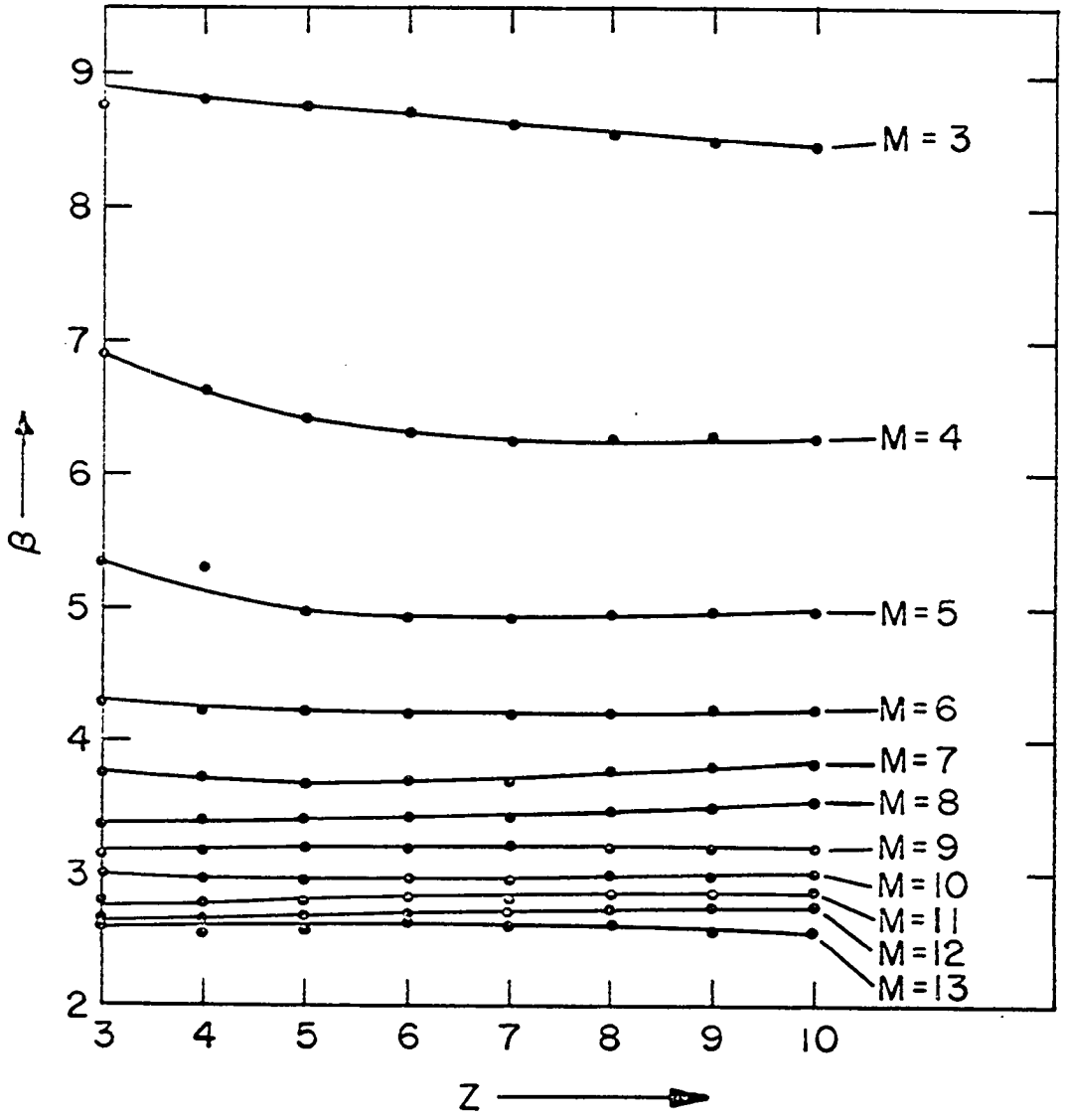

Figure 5. Variation of exponent parameter β for the expansions of Table 7

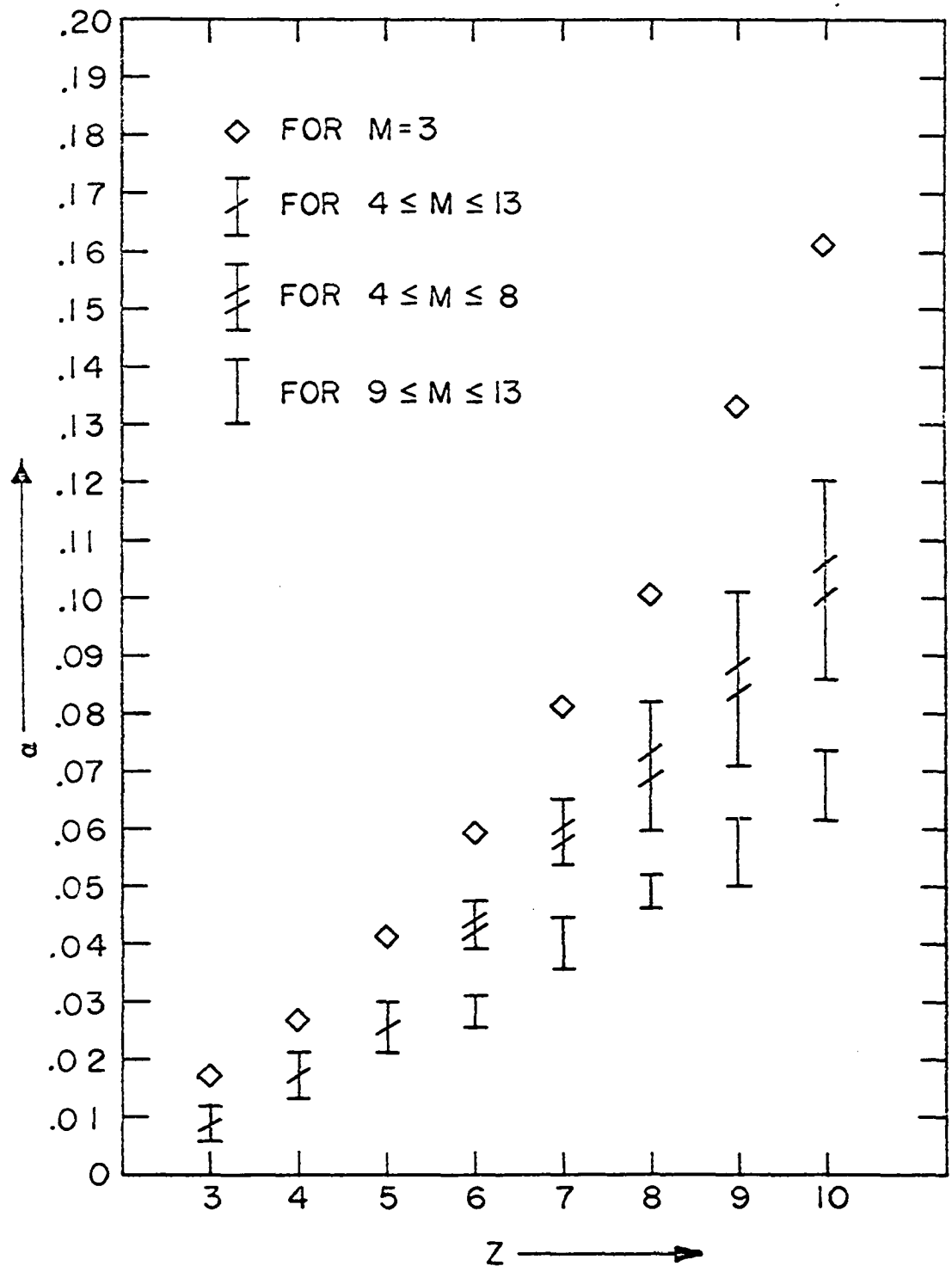

Figure 6. Variations of exponent parameter α for the expansions of Table 7

it varies more strongly with Z in order to provide the necessary contraction of the SCFAO's. Here too, the variation with Z is less pronounced when M is large.

CHAPTER II. EVEN-TEMPERED ATOMIC ORBITAL BASES WITH PSEUDO-SCALING CAPABILITY FOR MOLECULAR CALCULATIONS

Introduction

Work on many-electron systems has revealed that self-consistent-field atomic orbitals of isolated atoms form optimal minimal basis sets for molecular calculations, and that improvements beyond such minimal sets must provide for two types of further flexibility: Polarization and Contraction-Expansion. A particular form of the latter is orbital scaling, i.e., the variation of orbital exponents. Scaling optimization also guarantees the validity of the virial theorem. It is, however, an extremely time-consuming process, because it requires numerous recalculations of the energy for different orbital exponents, implying equally numerous re-evaluations of molecular integrals.

On the other hand, when a complete orbital basis is used, then the variation of all linear coefficients alone is sufficient to generate all possible variations of the orbitals, including scaling. It is, therefore, natural to inquire whether it may not be possible to construct a finite orbital basis of a character such that variation of the linear expansion coefficients will suffice to at least closely simulate the variation of orbital exponents in atomic self-consistent-field orbitals. If such linear "pseudo-scaling" should prove possible, then nonlinear variations and scaling would be unnecessary for practical purposes, and atomic orbital bases of this type would be most attractive for molecular calculations.

It is with this objective in mind that the "even-tempered" bases of

primitive atomic orbitals have been developed. It has been explained in Reference (17) why it is particularly useful for the purpose of pseudo-scaling to choose the orbital exponents within an atomic symmetry in a geometric progression, namely: if β is the ratio of the progression, then exact scaling of the primitive orbitals by β does not change this progression of exponents. The present investigation is concerned with developing a procedure for adapting an even-tempered atomic orbital basis to the task of optimally representing scaled atomic self-consistent-field orbitals. In trying to achieve this objective one can distinguish two problems: (1) The optimal choice of the even-tempered primitives and (2) the optimal choice of superpositions of such primitives to serve as "combined atomic orbitals", a device that is of particular importance in working with Gaussian-type primitives. We shall deal with both problems in turn.

The method to be described can be fully automated for application to any atom of the periodic table. For example, from a given set of accurate atomic self-consistent-field orbitals, a set of contracted Gaussian orbitals with pseudo-scaling properties and appropriate for molecular calculations can be generated in one uninterrupted computer run. An application obtained in this manner is given on pages 51-63. As is shown in Reference (21), the resulting atomic orbital bases have proved successful in molecular calculations.

Even-Tempered Primitive Basis and Atomic SCF Orbitals

In accordance with Equations (1) to (3) in Reference (17), an even-tempered basis of primitive atomic orbitals is defined by

$$p(k\ell m|\underset{\sim}{r}) = N_\ell^{\varepsilon} \cdot (\alpha_\ell \beta_\ell^{k})^{(2\ell+3)/2\varepsilon)} \cdot \exp(-\alpha_\ell \beta_\ell^{k} r^{\varepsilon}) \cdot r^{\ell} Y_{\ell m}(\Theta,\varpi). \quad (11)$$

Two choices of the power ε are of particular interest. The choice $\varepsilon = 1$ yields even-tempered exponential-type primitive atomic orbitals (ETEPAO's); the choice $\varepsilon = 2$ yields even-tempered Gaussian-type primitive atomic orbitals (ETGPAO's). The parameters α_ℓ and β_ℓ are, in general, different for different ℓ, although the possibility of using the same α and β for all orbitals in an atom will also be considered below. The symbol β_ℓ^{k} denotes the k-th power of β_ℓ. The factors N_ℓ^{ε} contain the necessary numerical normalization constants. The $Y_{\ell m}$ are spherical harmonics.

In Reference (4), close approximations to the atomic self-consistent-field orbitals in terms of ETEPAO's were discussed in detail. Corresponding approximations in terms of ETGPAO's can be similarly obtained as shown in Chapter I. For the purpose of the present investigation, it is assumed that such ETEPAO or ETGPAO representations of the SCF orbitals of an atom are available to start with, viz.,

$$\varpi(n\ell m|\underset{\sim}{r}) = \sum_{k=1}^{M} p(k\ell m|\underset{\sim}{r}) c(k|n\ell). \quad (12)$$

Our objective is to determine a set of atomic orbitals which contains these SCFAO approximations $\varpi(n\ell m)$ and, moreover, has pseudo-scaling properties in the sense discussed in the Introduction. In developing a procedure to achieve this objective, use will be made of another set of

SCFAO's which are more accurate than the $\varpi(n\ell m)$ by at least an order of magnitude, in order to assess the degree of accuracy of the pseudo-scaling basis. These orbitals will be referred to as "the accurate SCFAO's" and denoted by $\psi(n\ell m|\underset{\sim}{r})$. Most desirable for this purpose are extended expansions of $\psi(n\ell m)$ in terms of exponential-type primitive basis orbitals. Both sets, the $\psi(n\ell m)$ and the $\varpi(n\ell m)$, can be obtained by independent Hartree-Fock-type calculations. Alternatively, excellent sets $\varpi(n\ell m)$ are obtainable from the set of "accurate" $\psi(n\ell m)$ by weighted least mean squares fitting, i.e., minimizing the integral

$$\sum_n \int dV[\varpi(n\ell m|\underset{\sim}{r}) - \psi(n\ell m|\underset{\sim}{r}]^2/r, \tag{13}$$

with respect to the coefficients and the parameters α_ℓ and β_ℓ. In Reference (17), the weighting factor r^{-1} has been found to yield wave-functions ϖ that give the best energies.

As has been discussed in a separate investigation (19), there are reasons to expect that, in a molecular context, orbital scaling is more appropriate and more effective, if it is not applied to the orthogonal canonical SCFAO's, but to an equivalent set of nonorthogonal SCFAO's, which are analogous in character to Slater-type atomic orbitals. We therefore assume that the orthogonal canonical SCFAO's have been de-orthogonalized by the procedure described in Reference (19), and that these nonorthogonal SCFAO's are the ones denoted by $\varpi(n\ell m|\underset{\sim}{r})$ in Equation (12). Similarly, the "accurate" SCFAO's $\psi(n\ell m|r)$ are assumed to be transformed to nonorthogonal ones by the same deorthogonalization transformation.

All subsequent derivations hold for exponential as well as Gaussian basis sets, unless the contrary is explicitly specified.

Adaptation of Even-tempered Basis to the Representation of Scaled SCFAO's

Our first goal is to modify the original basis of primitives, so that all scaled nonorthogonal SCFAO's, $\varpi(n\ell m|\underset{\sim}{t}r)$, are represented about as accurately as the unscaled SCFAO's. This presupposes the choice of certain scaling ranges for the various SCFAO's, $T'(n\ell) \leq t \leq T''(n\ell)$, (on physical grounds and on the basis of experience) within which this goal is to be achieved. The basis modifications which will be considered are of two kinds: (1) An increase in the number of basis functions in the even-tempered sets and (2) changes in the values of the parameters α_ℓ. Because of the importance of the unscaled SCF atomic orbitals we do not change the parameters β_ℓ. The adaptation proceeds in two steps: In Step I, each SCFAO is considered separately; in Step II all SCFAO's within each symmetry are considered together.

Step I depends slightly on the method by which $\varpi(n\ell m)$ was obtained. If $\varpi(n\ell m)$ was obtained by least mean square fitting (see Equation (13)), then the accurate SCFAO $\psi(n\ell m)$ is scaled and, subsequently expanded in terms of the original even-tempered basis of Equation (11).

$$\psi(n\ell m|\underset{\sim}{t}r) \approx \varpi(t,n\ell m|\underset{\sim}{r}) \tag{14a}$$

$$\varpi(t,n\ell m|\underset{\sim}{r}) = \sum_k p(k\ell m|\underset{\sim}{r})c(k|t,n\ell). \tag{14b}$$

Here, $\underset{\sim}{t}r$ means multiplication by t but, in $(t,n\ell m)$ and $(t,n\ell)$, t is to

be considered as a fourth index. The coefficients $c(k|t,n\ell)$ are determined by least mean square fitting with the weighting function r^{-1} as in Equation (13), so that $c(k|1,n\ell)$ are the coefficients of Equation (12). On the other hand, if $\varpi(n\ell m)$ was obtained by an independent SCF calculation, then $\varpi(n\ell m)$ is scaled and expanded in terms of the original even-tempered basis:

$$\varpi(n\ell m|\underset{\sim}{tr}) \approx \varpi(t,n\ell m|\underset{\sim}{r}) \tag{15a}$$

$$\varpi(t,n\ell m|\underset{\sim}{r}) = \sum_k p(k\ell m|\underset{\sim}{r})c(k|t,n\ell) \tag{15b}$$

and again, the $c(k|1,n\ell)$ are identical to the coefficients found in Equation (12). In any event, the scaled-function-approximation contains the t-dependence in the coefficients. Now the two types of basis modifications mentioned above are introduced with the objective to obtain a basis such that the mean square deviation

$$\Delta(t,n\ell) = \int dV[\psi(n\ell m|\underset{\sim}{tr}) - \varpi(t,n\ell m|\underset{\sim}{r})]^2/r \tag{16}$$

has the same order of magnitude for all t within the scaling range,

$$T'(n\ell) \leq t \leq T''(n\ell), \tag{17}$$

which is chosen according to the requirements of the individual problem. Typically, it is required that $\Delta(t,n\ell)$ be $\lesssim 2\Delta(1,n\ell)$.

In general, the even-tempered expansion which provides the most economical representation of the nonorthogonal SCF atomic orbital to a given accuracy is inadequate to represent the scaled orbitals equally

well. For example, if Clementi's (1s) SCF atomic orbital of the ^3P state of silicon (18) is expanded in terms of seven even-tempered Gaussians, the accuracy is $\Delta(1,1s) = 8.65 \times 10^{-5}$. The even-tempered exponent parameters are $\alpha = 2.35 \times 10^{-2}$ and $\beta = 2.85$. When scaled (1s) SCF atomic orbitals are expanded in terms of these seven ETGPAO's, then the mean square deviation $\Delta(t,1s)$ has the values given in Figure 7a. The scale for the abscissa is in terms of $[2\ell n(t)/\ell n(\beta)]$; the corresponding values of t are also indicated.

If it is required that the accuracy be maintained over the scaling range $T' = 0.66 \leq t \leq 1.52 = T''$, then it is apparent that ETGPAO's with higher and lower exponents must be added to the original set of primitives. Due to the even-tempered character, ETGPAO's are readily added at either the high or low exponent end of the set. By adding ETGPAO's with large exponents or removing ETGPAO's with small exponents, or both, contraction of the orbital is favored and the fit is improved for $t > 1$. By removing ETGPAO's with large exponents or adding ETGPAO's with small exponents or both, expansion of the orbital is favored and the fit is improved for $t < 1$. If, in the case at hand, one ETGPAO is added at the upper end and one at the lower end, then the mean square deviation $\Delta(t,1s)$ has the form of Figure 7b, which is still unsatisfactory at the upper endpoint T''. However, rather than enlarge the set of ETGPAO's further by adding another function at the upper end, it is more efficient to change the parameter α from its original value of 2.35×10^{-2} to the value $\alpha' = 3.60 \times 10^{-2}$. This modification results in the curve of Figure 7c. It is readily verified that the change of α will shift

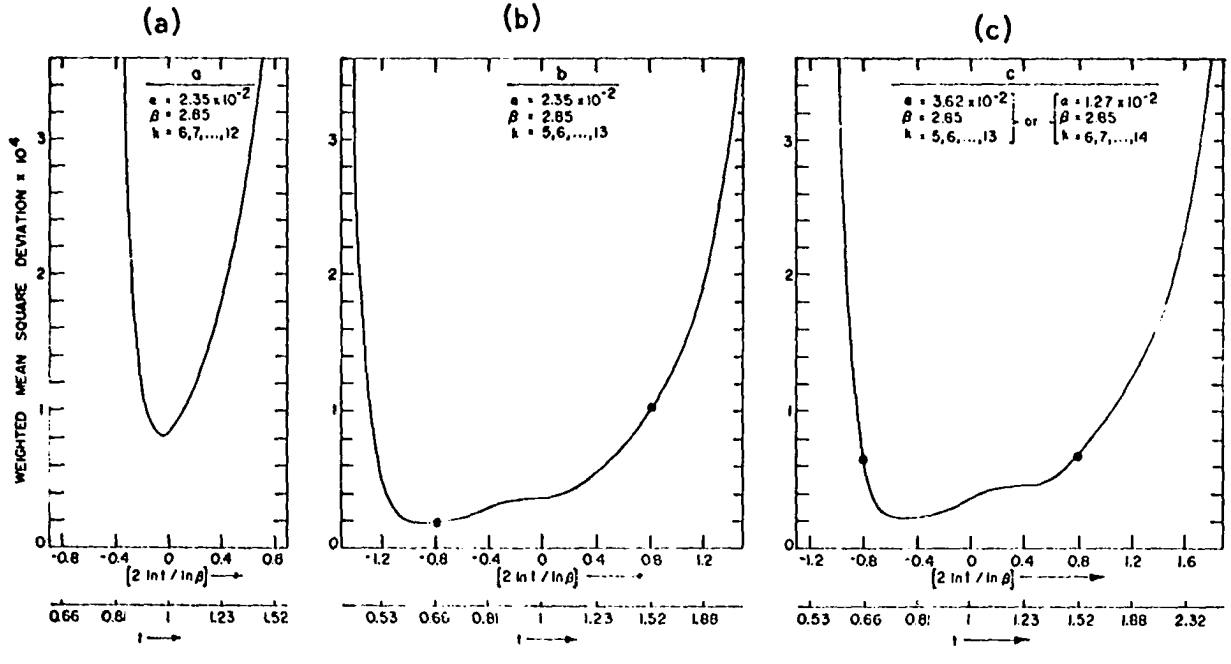

Figure 7. Weighted mean square deviations for even-tempered Gaussian expansions of scaled 1s SCFAO's of Si(^{3}P)

the curve with respect to the abscissa $[2\ell n(t)/\ell n(\beta)]$ by the amount $[\ell n(\alpha') - \ell n(\alpha)]/\ell n(\beta)$ and cause its values to be multiplied by the factor $\sqrt{\alpha'/\alpha}$. It is apparent that we have now the required accuracy in the entire scaling range. Changing the value of α therefore permits optimal positioning in the specified range.

A practical way to automatically achieve the best adjustment is as follows. First, that scaling parameter t' is determined which corresponds to the left-most point in Figure 7a for which the required accuracy is satisfied. Secondly, ETGPAO's with higher exponents are added so that the required accuracy is also satisfied for the scale parameter $t'' = t'(T''/T')$. In the example of Figure 7a, the lower endpoint, for which one has $\Delta(t',1s) = 2\Delta(1,1s) = 1.73 \times 10^{-4}$, is $t' = 0.87$. The upper endpoint is then $t'' = t'(1.52/0.66) = 2.00$, and it requires the addition of two ETGPAO's in order that $\Delta(2.00,1s) \leq 1.73 \times 10^{-4}$. Thirdly, the value of α is varied until the difference $|\Delta(T'',1s) - \Delta(T',1s)|$ is minimum. This final step brings the part of the curve which, originally, was located between t' and t'' into the desired position between T' and T''. In the example discussed this yields the value $\alpha = 1.27 \times 10^{-2}$, which results in the curve of Figure 7c. It is seen that $\Delta(t,1s)$ has practically the same value for $t = T' = 0.66$ and $t = T'' = 1.52$. It has been found that examination of about thirty equally-spaced points in the scaling range works well for carrying out an adequate adjustment.

This adjustment of the mean square deviation is performed as needed for all SCF atomic orbitals which are expected to scale. In case the scaling range of an orbital is sufficiently small, the number of ETGPAO's

in the original set may be adequate for the entire range so that only an alteration of α is required.

At this point the various scaled SCF atomic orbitals of the same symmetry have been expressed in terms of sets of primitives which differ in the value of α and in the number of ETGPAO's. For example, the ETGPAO sets for the s-type scaled orbitals of $Si(^3P)$ are found to have the parameters $(\alpha_1,\alpha_2,\alpha_3)$ given in Table 9. We now proceed to Step II, namely the elimination of this complication by determining <u>one</u> α, common to all the scaled SCF atomic orbitals in one symmetry. To this end, it is expedient <u>first</u> to change the ranges of the indices $k_1,k_2,\ldots$ so that all the parameters α_i (in one symmetry) are as close to one another as possible. The most natural procedure is to keep the smallest α_i fixed and to choose all the others close to it. For example, the sets of ETGPAO's of $Si(^3P)$ can be relabelled, so that one has the parameter values $(\alpha_1',\alpha_2',\alpha_3')$ and (k_1',k_2',k_3') also given in Table 9. It is evident that the set α_i' and k_i' describe the same expansions as the parameters α_i and k_i. <u>Next</u>, the set $(\alpha_1',\alpha_2',\alpha_3',\ldots)$ must be replaced by <u>one</u> parameter $\alpha = \alpha_1'' = \alpha_3'' = \alpha \ldots$ in such a way that the deterioration of the mean square deviation across the scaling range of each SCF atomic orbital is minimal. The optimal value of α which accomplishes this is determined by minimizing the total mean square deviation

$$\Delta(\alpha,\ell) = \sum_{n}\sum_{i} \Delta(t_i,n\ell)[T''(n\ell) - T'(n\ell)]. \qquad (18)$$

The symmetry is denoted by ℓ and the first summation $(\sum_n)$ is over all SCF

Table 9. Scaling ranges, exponent parameters, and basis size for even-tempered s-type AO's of Si(^{3}P)

Orbital	Scaling Range	β	α_i	Range of k_i	α'_i	Range of k'_i
1s	$0.95 \leq t \leq 1.05$	2.81	2.72(-2)	6-12	9.76(-3)	7-13
2s	$0.70 \leq t \leq 1.30$	2.81	2.89(-2)	3-9	1.03(-2)	4-10
3s	$0.60 \leq t \leq 1.40$	2.81	1.24(-2)	1-8	1.24(-2)	1-8

atomic orbitals in that symmetry. The summation (Σ_i) is taken over the aforementioned 30 equidistant points t_i in each scaling range, $T'(n\ell) \leq t \leq T''(n\ell)$. A reasonable initial guess of α for this optimization is the average value $\bar{\alpha}$ obtained from

$$\ell n\bar{\alpha} = (\ell n\alpha_1' + \ell n\alpha_2' + \ldots)/(\text{Number of } \alpha\text{'s}). \qquad (19)$$

For the example of $Si(^3P)$, with the set of ETGPAO's labelled by the values of (k_1', k_2', k_3') in Table 9, the optimal α value is $\alpha = 9.20 \times 10^{-3}$. With this choice the fit in the scaling range of each s-type atomic orbital becomes quite uniform, as will be shown by a detailed discussion of $Si(^3P)$ on pages 51-63.

The size of the scaling range selected for an orbital determines the number of even-tempered primitives required to approximate the scaled SCF orbital to a given accuracy. Therefore, knowledge concerning the extent of scaling which might occur in a molecular calculation is essential in keeping the even-tempered basis as small as possible.

The basis obtained by the described method evenly approximates the scaled SCF atomic orbitals $\psi(n\ell m|tr)$ and, therefore, can be used in a molecular calculation. Since this set is a rather good basis in the space of scaled SCF atomic orbitals, it is expected that no optimization of a scaling parameter would then be required in any orbital. In a molecular calculation, optimization of the expansion coefficients for the basis would automatically scale the atomic orbitals. This approach is practical in the case of an exponential-type pseudo-scaled even-tempered basis. However, in the case of Gaussians, a reasonably good

primitive basis is usually too large to be used as an explicit expansion basis, and it is therefore necessary to construct a smaller set of combined Gaussian functions which, ideally, span almost the same space as the even-tempered Gaussian primitives. Such a set consists of functions we call "Pseudo-Scaled Combined Even-tempered Gaussian Atomic Orbitals" (PSCETGAO's). The determination of this basis is the topic of the next section.

It may be added, that the method is readily extended to the case that α and β are assumed to be independent of ℓ. In this case the summation of Equation (18) must also be taken over all ℓ values.

Construction of a Reduced Pseudo-Scaling Basis by Combination of Primitives

The number of PSCETGAO's chosen to represent each SCF atomic orbital in scaled and unscaled form is a matter of judgment, weighing the accuracy to be obtained against the amount of calculation to be performed. A set consisting of three PSCETGAO's for a valence shell SCFAO, and two PSCETGAO's for an SCFAO from the next inner shell should provide good representations in most cases.

The PSCETGAO's related to a particular SCFAO $\psi(n\ell m|\underset{\sim}{r})$ should be selected to obtain optimal "pseudo-scaling" opportunity for that SCF orbital. This can be achieved as follows. One chooses, say, 20 evenly spaced values t_i of the scaling parameter in the applicable range $T'(n\ell) \leq t_i \leq T''(n\ell)$, including the value $t = 1$, and determines by least mean squares the 20 expansions

$$\psi(n\ell m|t_i,\underset{\sim}{r}) \simeq \varphi(t_i,n\ell m|\underset{\sim}{r}) \tag{20a}$$

$$\varphi(t_i,n\ell m|\underset{\sim}{r}) = \sum_k p(k\ell m|\underset{\sim}{r})c(k|t_i,n\ell), \tag{20b}$$

in terms of the primitive basis found in the previous section. These 20 nonorthogonal functions span a certain function space. In this function space, an orthogonal basis $\chi_\nu(n\ell m|\underset{\sim}{r})$ is then determined by "canonical orthonormalization" (22) which is given by

$$\chi_\nu(n\ell m|\underset{\sim}{r}) = D_\nu^{-\frac{1}{2}} \sum_i \varphi(t_i,n\ell m|\underset{\sim}{r})T_{i\nu}(n\ell). \tag{21}$$

Here, the $T_{i\nu}$ are elements of the orthogonal matrix $\underset{\sim}{T}$ and D_ν are elements of the diagonal matrix $\underset{\sim}{D}$, obtained by diagonalizing the matrix of overlap integrals

$$S_{ij} = \langle\varphi(t_i,n\ell m) \,|\varphi(t_j,n\ell m)\rangle \ ,$$

i.e., $\underset{\sim}{D}$ and $\underset{\sim}{T}$ are determined from

$$\underset{\sim}{D} = \underset{\sim}{\tilde{T}}\underset{\sim}{S}\underset{\sim}{T} \ .$$

If M is the number of primitive ETGPAO's, then (20-M) eigenvalues D_ν are rigorously zero, so that exactly M orthogonal functions span the space of the M ETGPAO's. Furthermore, however, most of the remaining M eigenvalues are small ($< 10^{-6}$), indicating that the corresponding χ_ν's are less important for the representation of the $\varphi(t_i,n\ell m)$, because from Equation (21) follows

$$\varphi(t_i,n\ell m) = \sum_\nu \chi_\nu(n\ell m)T_{\nu i}D_\nu^{\frac{1}{2}} \ . \tag{22}$$

For example, in the case of the (2s) orbital of Si(^{3}P) expanded in terms of seven ETGPAO's, the eigenvalues shown in the first row of Table 10 obtained. The first three atomic orbitals χ_ν (ν = 1,2,3) are usually found to be much more important than the rest. In any event, if z PSCETGAO's are to be generated for a given SCFAO then the z canonically orthonormalized AO's χ_ν (ν = 1,2, ... z) corresponding to the largest eigenvalues D_ν (ν = 1,2, ... z) are chosen.

If the scaling range is chosen to be nearly symmetrical around t = 1, then the orthogonal orbital χ_1 corresponding to the largest eigenvalue D_1 is very close to the unscaled SCFAO, $\varpi(t = 1,n\ell m)$. For molecular calculations it is, however, desirable that the unscaled SCFAO itself be one of the PSCETGAO's. This can be accomplished by the following modified procedure. After determining the 20 scaled SCF atomic orbital approximations $\varpi(t_i,n\ell m)$ given in Equation (20b), the approximate unscaled SCF atomic orbital is chosen as the first of the orthogonal χ_i's, i.e., $\chi_1(n\ell m) = \varpi(t = 1,n\ell m)$. Each of the remaining 19 orbitals are Schmidt orthogonalized to χ_1, which yields the orbitals

$$\tilde{\varpi}(t_i,n\ell m) = [\varpi(t_i,n\ell m) - Q_i\chi_1(n\ell m)](1-Q_i^2)^{-\frac{1}{2}}, \qquad (23a)$$

$$Q_i = \langle \varpi(t_i,n\ell m) | \chi_1(n\ell m) \rangle .$$

In the space spanned by these 19 orbitals, $\tilde{\varpi}(t_i,n\ell m)$, an orthogonal basis is now found by canonical orthogonalization as described previously. The orthogonal orbitals corresponding to the largest eigenvalues are then added as $\chi_2(n\ell m)$, $\chi_3(n\ell m)$, etc. to $\chi_1(n\ell m)$. The second row of Table 10 shows the D_ν obtained in this manner. This orthogonal PSCETGAO basis

Table 10. Eigenvalues for canonically orthonormalized (2s) AO's of Si(^{3}P)

ν	1	2	3	4	5	6	7
D_ν[a]	1.9(+1)	7.9(-1)	1.5(-2)	1.4(-4)	3.2(-7)	1.8(-10)	3.8(-15)
D_ν[b]		1.9(+1)	4.4(-1)	4.3(-3)	1.1(-5)	5.9(-9)	9.5(-14)

[a]Canonical orthonormalization including unscaled 2s AO.

[b]Canonical orthonormalization after projecting out unscaled 2s AO.

exhibits an improved fit to the scaled SCF atomic orbitals in the neighborhood of t = 1.

Application of this procedure to each SCFAO belonging to one symmetry yields a certain number of PSCETGAO's for each of them. For example, in the case of Si(^{3}P) it might be reasonable to construct the following six PSCETGAO's for a molecular calculation: $\chi_1(1s)$, $\chi_1(2s)$, $\chi_2(2s)$, $\chi_1(3s)$, $\chi_2(3s)$, $\chi_3(3s)$. The primitive basis contained 12 ETGPAO's so that this method of contraction has reduced the basis size by a factor of two. The orbitals $\chi_1(2s)$ and $\chi_2(2s)$ are mutually orthogonal and so are the orbitals $\chi_1(3s)$, $\chi_2(3s)$, and $\chi_3(3s)$. But the orbitals originating from different SCFAO's are not orthogonal to each other. In fact, they maintain the character and advantages of the nonorthogonal SCFAO's discussed previously and in Reference (19).

While the orbitals $\chi_1(3s)$, $\chi_2(3s)$, and $\chi_3(3s)$ have been chosen to provide a reasonable approximation to the scaling of the SCFAO $\chi_1(3s)$ as well as the accurate SCFAO $\psi(3s)$, additional assistance in the representations of these scaled SCFAO's is obtained in a molecular calculation from the orbitals $\chi_1(1s)$, $\chi_1(2s)$, and $\chi_2(2s)$. The same holds conversely for the orbitals $\chi_1(1s)$ and $\chi_1(2s)$. The amount of this "pseudo-scaling assistance" should be taken into account in trying to keep the number of PSCETGAO's as small as possible. The accuracy to which a specified number of PSCETGAO's approximates all scaled SCFAO's of the same symmetry can be assessed by computing the least mean square deviations for the expansions,

$$\psi(n\ell m|t_i\underset{\sim}{r}) \simeq \sum_{n\nu}\sum \chi_\nu(n\ell m|\underset{\sim}{r})C_{\nu n}(t_i) = \hat{\psi}(t_i,n\ell m). \qquad (24)$$

The deterioration resulting from the basis reduction introduced in this section can be assessed by computing the least mean square deviations for the expansions

$$\varpi(t_i,n\ell m|\underset{\sim}{r}) \simeq \sum_{\nu} \chi_{\nu}(n\ell m|\underset{\sim}{r})C'_{\nu n}(t_i) = \hat{\varpi}(t_i,n\ell m), \qquad (25)$$

where $\varpi(t_i,n\ell m)$ are the functions of Equation (20b). Inspection of the mean square deviations corresponding to these equations can be used to determine the minimum number of PSCETGAO's, consistent with a given accuracy.

Application to Silicon

As an explicit illustration of the method outlined in the preceding sections, we shall describe the quantitative results which are obtained by an application to the ^3P state of Silicon. As accurate SCFAO's, the extended expansions in terms of Slater-type exponential primitives given by Clementi (18) will be used. From these a scaling basis in terms of even-tempered Gaussian primitives will be constructed.

The first step is the deorthogonalization of the accurate SCFAO's. Table II gives the expansion of these nonorthogonal AO's and the expectation values of r^{-2}, r^{-1}, r, r^2 and $-\nabla^2/2$ for each orbital. Also given is the triangular matrix which Schmidt orthogonalizes the nonorthogonal SCFAO's back to the canonical SCFAO's.

The second step is the construction of the approximations $\varphi(n\ell m)$ of Equation (12) to the accurate nonorthogonal $\psi(n\ell m)$. In the present case, they are formed by least mean square fitting in terms of a set of seven even-tempered Gaussian primitives, according to Equation (13). The

Table II. Accurate nonorthogonal SCFAO's for silicon ^3P state

Expansions of Nonorthogonal SCFAO's in Terms of Slater-Type Basis

Basis AO's[a]	1S	2S	3S	Basis AO's[a]	2P	3P
1s	0.969154	-0.000000	0.000000	2P	0.568378	-0.000000
3s	0.031580	0.005153	0.000947	4P	0.000290	-0.001417
3s	0.019780	0.125099	-0.006414	4P	0.037140	0.004787
3s	-0.005980	0.351428	0.008854	4P	0.292719	-0.009192
3s	0.002850	0.551582	-0.047944	4P	0.229149	0.058036
3s	-0.001110	0.042041	-0.034631	4P	0.010010	0.472486
3s	0.000660	-0.013872	0.589581	4P	-0.002460	0.562153
3s	-0.000140	0.002390	0.503113	4P	0.000940	0.042021

Orbital Expectation Values

$\langle 1/r\cdot r\rangle$	372.297237	6.138804	0.356603	8.520219	0.248832
$\langle 1/r\rangle$	13.580506	2.211660	0.546804	2.456409	0.447932
$\langle 1\rangle$	1.000000	1.000000	1.000000	1.000000	1.000000
$\langle r\rangle$	0.111431	0.550695	2.156879	0.535388	2.705821
$\langle r\cdot r\rangle$	0.016701	0.360941	5.426097	0.359647	8.703871
$\langle r\cdot r\cdot r\rangle$	0.003157	0.276392	15.747461	0.293169	32.723675
$\langle -\frac{1}{2}\nabla\cdot\nabla\rangle$	92.235842	3.813916	0.285599	12.198042	0.412403

Orthogonalization Matrices[b]

1.000000	0.0	0.0	1.000000	0.0
-0.266078	1.034794	0.0	-0.212525	1.022334
0.068126	-0.277756	1.035402		

[a]Slater-type basis AO's are those of Clementi's (Ref. 18 Table I-6).

[b]Transformation by these matrices yield Clementi's orthogonal SCFAO's from the nonorthogonal ones given here.

resulting values of α and β and the expansion coefficients are shown in Table 12. Also given are the mean-square deviations from the $\psi(n\ell m)$, and the differences in the expectation values from those obtained for the $\psi(n\ell m)$.

In the third step, the even-tempered basis of Gaussian primitives is adapted to the scaled SCFAO's, as discussed on pages 38-46. The results are displayed in Table 13. For each SCFAO, seven expansions are given, corresponding to seven different values of the scale parameters. The scaling range is different for different SCFAO's as indicated. The expansion basis is that of the optimal even-tempered Gaussians, determined in this step. It should be noted that this adapted basis now consists of 13 s-type primitives, and 11 p-type primitives. The mean square deviations from the scaled $\psi(n\ell m)$'s are also listed and exhibit the desired uniformity.

In the fourth step, the procedure described in the previous section is used to find a reduced set of <u>superpositions</u> of even-tempered Gaussian AO's with pseudo-scaling character. Table 14 shows expansions for the first seven orthogonal orbitals $\chi_1(n\ell)$, $\chi_2(n\ell)$ ... $\chi_7(n\ell)$ for $(n\ell)$ = (1s), (2s), (3s), (2p), (3p). The orbitals $\chi_1(n\ell)$ are the unscaled SCFAO $\varpi(n\ell)$. The remaining ones are obtained by canonical orthogonalization after $\varpi(n\ell)$ has been projected out. For each of the latter the eigenvalues D_ν are also given, showing that $\chi_4(n\ell)$, $\chi_5(n\ell)$ ... are negligible in expanding the scaled $\varpi(n\ell)$. For this reason the functions $\chi_8(n\ell)$, $\chi_9(n\ell)$, ... $\chi_{19}(n\ell)$ are not even listed.

Table 12. Seven-term even-tempered Gaussian expansions of nonorthogonal SCFAO's for Silicon ^3P State

Expansions of Nonorthogonal SCFAO's						
Exponents[a]	1S	2S	3S	Exponents[a]	2P	3P
ζs(1)	0.0	0.0	0.382459	ζp(1)	0.0	0.308421
ζs(2)	0.0	0.0	0.725455	ζp(2)	0.0	0.555169
ζs(3)	0.0	0.073345	0.006997	ζp(3)	0.017223	0.269598
ζs(4)	0.0	0.537690	-0.195346	ζp(4)	0.254814	-0.000759
ζs(5)	0.0	0.429100	-0.013788	ζp(5)	0.481450	-0.011213
ζs(6)	0.226243	-0.086404	-0.000513	ζp(6)	0.310493	-0.004124
ζs(7)	0.472195	-0.074612	0.002183	ζp(7)	0.114874	-0.000911
ζs(8)	0.298009	-0.014046	0.0	ζp(8)	0.024641	0.0
ζs(9)	0.106088	-0.002303	0.0	ζp(9)	0.007832	0.0
ζs(10)	0.037096	0.0	0.0			
ζs(11)	0.006192	0.0	0.0			
ζs(12)	0.005272	0.0	0.0			
Δ( )[b]		Comparison of Expectation Values with Slater-type Basis				
Δ⟨1/r·r⟩	1.510518	0.000211	0.000014		0.006269	-0.000013
Δ⟨1/r⟩	-0.000134	0.000081	0.000032		0.000046	-0.000013
Δ⟨1⟩	0.000000	0.000000	-0.000000		-0.000000	0.000000
Δ⟨r⟩	0.000018	-0.000057	-0.000498		-0.000037	0.000236
Δ⟨r·r⟩	0.000015	-0.000058	-0.004604		-0.000051	0.004811
Δ⟨r·r·r⟩	0.000011	0.000097	-0.034945		0.000150	0.077502
Δ⟨$-\frac{1}{2}\nabla\cdot\nabla$⟩	-0.023209	-0.000446	-0.000034		-0.000865	-0.000069
MSQ-DEV[c]	9.38 (-5)	2.02(-5)	8.49(-6)		2.57 (-5)	1.09(-5)
		Orthogonalization Matrices				
	1.000000	0.0	0.0		1.000000	0.0
	-0.263774	1.034204	0.0		-0.211430	1.022107
	0.068068	-0.277354	1.035340			

[a] The exponents are $\zeta s(k) = \alpha_s \beta_s^{k}$ and $\zeta p(k) = \alpha_p \beta_p^{k}$, with the parameter values: α_s = 2.77079913(-2), β_s = 2.80928783, α_p = 2.14108095(-2), β_p = 2.73980558.

[b] Δ( ) denote the differences in the expectation values calculated for the expansions given in Table II and those given in this table.

[c] MSQ-DEV denotes the mean square deviation between the orbital expansions given in Table II and those of this table.

Table 13. Even-tempered Gaussian expansions of scaled non-orthogonal SCFAO's

Expansions of Scaled Nonorthogonal 1s Orbitals

Scale Parameter	t = 0.95	t = 0.97	t = 0.99
Exponents[a]			
$\zeta_s(7)$	0.240488	0.222588	0.205742
$\zeta_s(8)$	0.470674	0.472455	0.472917
$\zeta_s(9)$	0.290717	0.299952	0.309307
$\zeta_s(10)$	0.102148	0.107126	0.112077
$\zeta_s(11)$	0.035764	0.037458	0.039248
$\zeta_s(12)$	0.005911	0.006265	0.006612
$\zeta_s(13)$	0.005068	0.005327	0.005598
MSQ-DEV[b]	9.23(-5)	9.06(-5)	9.23(-5)

Expansions of Scaled Nonorthogonal 2s Orbitals

Scale Parameter	t = 0.70	t = 0.82	t = 0.94
Exponents[a]			
$\zeta_s(4)$	0.421567	0.213860	0.091180
$\zeta_s(5)$	0.642473	0.713627	0.659096
$\zeta_s(6)$	0.038486	0.209515	0.392818
$\zeta_s(7)$	-0.107620	-0.116265	-0.095494
$\zeta_s(8)$	-0.028681	-0.048239	-0.069813
$\zeta_s(9)$	-0.004112	-0.007483	-0.012729
$\zeta_s(10)$	-0.000549	-0.001147	-0.002044
MSQ-DEV[b]	1.84(-5)	1.70(-5)	1.72(-5)

Expansions of Scaled Nonorthogonal 3s Orbitals

Scale Parameter	t = 0.60	t = 0.76	t = 0.92
Exponents[a]			
$\zeta_s(1)$	0.324274	0.083136	0.004866
$\zeta_s(2)$	0.749256	0.678224	0.451140
$\zeta_s(3)$	0.060962	0.440395	0.686467
$\zeta_s(4)$	-0.197894	-0.198995	-0.051844
$\zeta_s(5)$	-0.020183	-0.086696	-0.167149
$\zeta_s(6)$	-0.000432	-0.000106	-0.008173
$\zeta_s(7)$	0.002244	0.001285	-0.000310
$\zeta_s(8)$	0.000050	0.000869	0.001937
MSQ-DEV[b]	6.12(-6)	4.96(-6)	6.52(-6)

[a] The exponents are $\zeta_s(k) = \alpha_s \beta_s^k$ and $\zeta_p(k) = \alpha_p \beta_p^k$, with the parameter values: α_s = 9.20023221(-3), β_s = 2.80928783, α_p = 7.58704242(-3), β_p = 2.73980558.

[b] MSQ-DEV denotes the mean square deviation between the scaled nonorthogonal SCFAO's and the orbital expansions of this table.

Expansions of Scaled Nonorthogonal 1s Orbitals

t = 1.00	t = 1.01	t = 1.03	t = 1.04
0.197703	0.189911	0.175052	0.167975
0.472684	0.472157	0.470270	0.468931
0.314011	0.318723	0.328150	0.332851
0.114548	0.117017	0.121957	0.124432
0.040176	0.041125	0.043083	0.044090
0.006783	0.006954	0.007293	0.007463
0.005739	0.005881	0.006175	0.006326
9.40(-5)	9.62(-5)	1.02(-4)	1.05(-4)

Expansions of Scaled Nonorthogonal 2s Orbitals

t = 1.00	t = 1.06	t = 1.18	t = 1.24
0.053467	0.027332	-0.000420	-0.006099
0.606087	0.544564	0.413831	0.350748
0.474316	0.544676	0.646649	0.677843
-0.071887	-0.039957	0.044598	0.094539
-0.080931	-0.091652	-0.109718	-0.116036
-0.015893	-0.019425	-0.027673	-0.032400
-0.002688	-0.003482	-0.005549	-0.006836
2.30(-5)	2.89(-5)	3.20(-5)	2.97(-5)

Expansions of Scaled Nonorthogonal 3s Orbitals

t = 1.00	t = 1.08	t = 1.24	t = 1.32
-0.006203	-0.008861	-0.004506	-0.001466
0.340999	0.245957	0.108561	0.064010
0.740284	0.754357	0.696389	0.640428
0.056537	0.173751	0.400427	0.498128
-0.197956	-0.216662	-0.210470	-0.185508
-0.018417	-0.033244	-0.074159	-0.098008
-0.000812	-0.001141	-0.002229	-0.003635
0.002393	0.002761	0.003298	0.003529
8.97(-6)	1.03(-5)	9.48(-6)	9.37(-6)

Table 13. (Continued)

Expansions of Scaled Nonorthogonal 2p Orbitals			
Scale Parameter	t = 0.70	t = 0.82	t = 0.94
Exponents[a]			
$\zeta_p(4)$	0.155807	0.069479	0.026132
$\zeta_p(5)$	0.457092	0.387983	0.298966
$\zeta_p(6)$	0.387761	0.447893	0.477289
$\zeta_p(7)$	0.164812	0.227982	0.289790
$\zeta_p(8)$	0.044172	0.069518	0.100181
$\zeta_p(9)$	0.009592	0.015618	0.023704
$\zeta_p(10)$	0.001629	0.002873	0.004573
$\zeta_p(11)$	0.000434	0.000727	0.001154
MSQ-DEV[b]	8.50(-6)	9.11(-6)	1.35(-5)

Expansions of Scaled Nonorthogonal 2p Orbitals			
Scale Parameter	t = 0.60	t = 0.76	t = 0.92
Exponents[a]			
$\zeta_p(1)$	0.300083	0.100561	0.018359
$\zeta_p(2)$	0.556637	0.506056	0.364197
$\zeta_p(3)$	0.275543	0.450957	0.544746
$\zeta_p(4)$	0.000856	0.089942	0.215191
$\zeta_p(5)$	-0.011350	-0.019669	-0.010973
$\zeta_p(6)$	-0.004411	-0.005628	-0.009258
$\zeta_p(7)$	-0.000685	-0.002263	-0.003636
$\zeta_p(8)$	-0.000147	-0.000262	-0.000657
MSQ-DEV[b]	6.24(-6)	3.52(-6)	9.47(-6)

Expansions of Scaled Nonorthogonal 2p Orbitals

t = 1.00	t = 1.06	t = 1.18	t = 1.24
0.014608	0.007479	0.001459	0.000817
0.254904	0.213530	0.142259	0.113032
0.480480	0.476818	0.452483	0.433708
0.319070	0.346675	0.395393	0.415944
0.116984	0.134537	0.171266	0.190146
0.028649	0.034216	0.047189	0.054558
0.005584	0.006708	0.009334	0.010858
0.001433	0.001762	0.002578	0.003071
1.49(-5)	1.54(-5)	1.53(-5)	1.59(-5)

Expansions of Scaled Nonorthogonal 3p Orbitals

t = 1.00	t = 1.08	t = 1.24	t = 1.32
0.002194	-0.004672	-0.004279	-0.001333
0.290398	0.222666	0.114337	0.074688
0.559359	0.556271	0.511100	0.475567
0.279795	0.340683	0.442530	0.481316
0.002965	0.023570	0.081973	0.117567
-0.012030	-0.015025	-0.019587	-0.020061
-0.004094	-0.004437	-0.005125	-0.005648
-0.001009	-0.001459	-0.002585	-0.003214
9.91(-6)	7.68(-6)	5.16(-6)	7.37(-6)

Table 14. Canonically orthonormalized AO's (COAO's) in terms of even-tempered Gaussians

COAO's for the Scaling of Nonorthogonal 1s SCFAO's[a]

	$\chi_1(1S)$	$\chi_2(1S)$	$\chi_3(1S)$
$\zeta_s(7)$[b]	1.977025D-01	9.3420170-01	1.674945D 00
$\zeta_s(8)$	4.726839D-01	3.964363D-02	-2.380565D 00
$\zeta_s(9)$	3.140105D-01	-5.515978D-01	7.079911D-01
$\zeta_s(10)$	1.145477D-01	-2.902590D-01	2.764489D-01
$\zeta_s(11)$	4.017597D-02	-1.098082D-01	2.985453D-01
$\zeta_s(12)$	6.783402D-03	-2.013625D-02	1.072281D-02
$\zeta_s(13)$	5.738501D-03	-1.656562D-02	4.150357D-02
Eigenvalues		1.899292D 01	7.079466D-03

COAO's for the Scaling of Nonorthogonal 2s SCFAO's[a]

	$\chi_1(2S)$	$\chi_2(2S)$	$\chi_3(2S)$
$\zeta_s(4)$[b]	5.346652D-02	5.2250150-01	-1.488977D 00
$\zeta_s(5)$	6.050859D-01	7.448024D-01	1.502681D 00
$\zeta_s(6)$	4.743164D-01	-1.057106D 00	3.745631D-01
$\zeta_s(7)$	-7.188687D-02	-3.964532D-01	-1.254530D 00
$\zeta_s(8)$	-8.093083D-02	1.496147D-01	8.229286D-02
$\zeta_s(9)$	-1.589260D-02	4.883971D-02	9.068193D-02
$\zeta_s(10)$	-2.687931D-03	1.071640D-02	2.732796D-02
Eigenvalues		1.855340D 01	4.422898D-01

COAO's for the Scaling of Nonorthogonal 3s SCFAO's[a]

	$\chi_1(3S)$	$\chi_2(3S)$	$\chi_3(3S)$
$\zeta_s(1)$[b]	-6.202819D-03	1.495946D-01	-8.047152D-01
$\zeta_s(2)$	3.409994D-01	9.809096D-01	-3.051398D-01
$\zeta_s(3)$	7.402843D-01	-3.863597D-01	1.866259D 00
$\zeta_s(4)$	5.653663D-02	-1.051227D 00	-1.356124D 00
$\zeta_s(5)$	-1.979563D-01	2.052206D-01	-4.343989D-01
$\zeta_s(6)$	-1.841730D-02	1.302316D-01	3.467421D-01
$\zeta_s(7)$	-8.123768D-04	5.694416D-03	1.262867D-03
$\zeta_s(8)$	2.392682D-03	-4.061703D-03	1.266426D-04
Eigenvalues		1.812611D 01	8.525711D-01

[a]The scaling range is the same as that examined in Table 13.

[b]The orbital exponents are identical with those in Table 13.

COAO's for the Scaling of Nonorthogonal 1s SCFAO's[a]

$\chi_4(1S)$	$\chi_5(1S)$	$\chi_6(1S)$	$\chi_7(1S)$
-1.245655D 00	5.086197D-01	5.079137D-01	-5.080627D-01
3.178394D 00	-1.765986D 00	-1.753821D 00	1.763951D 00
-3.666972D 00	3.440003D 00	3.437702D 00	-3.435051D 00
1.778262D 00	-4.186726D 00	-4.190272D 00	4.177110D 00
-7.536262D-02	2.541097D 00	2.554955D 00	-2.528426D 00
2.630769D-01	-4.379197D-01	-4.493095D-01	4.304430D-01
3.806588D-02	3.283079D-01	3.264303D-01	-3.288529D-01
7.107553D-07	1.751961D-11	1.762715D-14	1.165259D-14

COAO's for the Scaling of Nonorthogonal 2s SCFAO's[a]

$\chi_4(2S)$	$\chi_5(2S)$	$\chi_6(2S)$	$\chi_7(2S)$
-1.580343D 00	7.198530D-01	2.276391D-01	-6.546231D-02
3.377166D 00	-2.096271D 00	-7.556159D-01	2.203474D-01
-3.483714D 00	3.550167D 00	1.626943D 00	-4.788049D-01
1.659542D 00	-4.303908D 00	-2.836285D 00	9.050863D-01
3.707576D-01	3.218534D 00	4.009503D 00	-1.578779D 00
-1.523744D-01	-5.830585D-01	-3.716905D 00	2.330511D 00
-6.279230D-02	-8.095107D-02	1.087092D 00	-2.092109D 00
4.303285D-03	1.100525D-05	5.938084D-09	9.509236D-14

COAO's for the Scaling of Nonorthogonal 3s SCFAO's[a]

$\chi_4(3S)$	$\chi_5(3S)$	$\chi_6(3S)$	$\chi_7(3S)$
-1.660225D 00	-1.380786D 00	-4.802968D-01	9.774118D-02
2.494210D 00	3.213087D 00	1.374953D 00	-3.162326D-01
-1.194027D 00	-4.191417D 00	-2.430486D 00	6.574910D-01
-8.638143D-01	3.919309D 00	3.571322D 00	-1.199653D 00
1.781763D 00	-2.242204D 00	-4.488990D 00	2.081656D 00
-5.334931D-01	-9.227146D-02	4.152642D 00	-3.254873D 00
-3.185447D-02	3.399474D-01	-1.556887D 00	3.744545D 00
-4.622539D-03	-2.936325D-02	1.750535D-01	-1.404219D 00
2.101569D-02	3.053512D-04	1.050038D-06	5.304947D-10

Table 14. (Continued)

	COAO's for the Scaling of Nonorthogonal 2p SCFAO's[a]		
	$\chi_1(2p)$	$\chi_2(2p)$	$\chi_3(2p)$
$\zeta p(4)$[b]	1.460760D-02	1.914064D-01	-8.054614D-01
$\zeta p(5)$	2.549040D-01	6.947797D-01	-5.110891D-02
$\zeta p(6)$	4.804795D-01	-3.473185D-03	8.822731D-01
$\zeta p(7)$	3.190599D-01	-4.666277D-01	-2.256492D-01
$\zeta p(8)$	1.169939D-01	-2.845983D-01	-3.980368D-01
$\zeta p(9)$	2.864911D-02	-8.844987D-02	-1.825709D-01
$\zeta p(10)$	5.583926D-03	-1.806997D-02	-3.587253D-02
$\zeta p(11)$	1.433043D-03	-5.187261D-03	-1.277459D-02
Eigenvalues		1.864564D 01	3.508361D-01

	COAO's for the Scaling of Nonorthogonal 3p SCFAO's[a]		
	$\chi_1(3p)$	$\chi_2(3p)$	$\chi_3(3p)$
$\zeta p(1)$[b]	2.194449D-03	1.881059D-01	-8.163013D-01
$\zeta p(2)$	2.903981D-01	7.255120D-01	-1.587786D-02
$\zeta p(3)$	5.503594D-01	-8.034774D-02	9.058927D-01
$\zeta p(4)$	2.797950D-01	-6.427634D-01	-3.670128D-01
$\zeta p(5)$	2.954957D-03	-1.914613D-01	-5.643302D-01
$\zeta p(6)$	-1.203007D-02	2.620498D-02	3.169046D-02
$\zeta p(7)$	-4.093960D-03	4.955076D-03	-6.239514D-04
$\zeta p(8)$	-1.008512D-03	4.330660D-03	9.784300D-03
Eigenvalues		1.820300D 01	7.805860D-01

COAO's for the Scaling of Nonorthogonal 2p SCFAO's[a]

$\chi_4(2p)$	$\chi_5(2p)$	$\chi_6(2p)$	$\chi_7(2p)$
-1.3013350 00	7.9346500-01	-2.7090150-01	9.2540740-02
1.9075150 00	-1.8324810 00	8.2497340-01	-3.0865710-01
-8.6900790-01	2.3714070 00	-1.5830750 00	6.9472130-01
-3.4346040-01	-1.8439450 00	2.2712960 00	-1.2995180 00
3.6952420-01	3.8850220-01	-2.1902760 00	1.9737170 00
3.0659950-01	3.9227270-01	8.5491550-01	-2.0585880 00
6.5442100-02	2.0730850-01	3.2369200-01	8.0767060-01
2.6028230-02	4.8458930-02	1.9585120-01	5.6903630-01
3.5105530-03	1.2581170-05	6.7992550-09	4.3610520-13

COAO's for the Scaling of Nonorthogonal 3p SCFAO's[a]

$\chi_4(3p)$	$\chi_5(3p)$	$\chi_6(3p)$	$\chi_7(3p)$
-1.1979460 00	8.3252340-01	5.0755810-01	-7.7047000-02
1.5731180 00	-1.7708970 00	-1.3070490 00	2.2650900-01
-5.0779420-01	2.0957600 00	2.1021830 00	-4.5257840-01
-6.7635320-01	-1.4982410 00	-2.7091850 00	8.1854820-01
9.0514120-01	7.9610560-02	2.8153380 00	-1.4350390 00
9.9801320-02	9.6302900-01	-1.9331860 00	2.2312920 00
-1.5137890-02	-1.7887390-01	3.3065390-01	-2.2833850 00
-1.3272030-02	1.1309200-02	-5.9824360-02	4.9723540-01
1.6302020-02	1.0859340-04	9.5360240-07	1.4283840-09

From the orbitals shown in Table 14 we select $\chi_1(1s), \chi_1(2s), \chi_2(2s), \chi_1(3s), \chi_2(3s), \chi_3(3s), \chi_1(2p), \chi_2(2p), \chi_1(3p), \chi_2(3p), \chi_3(3p)$, basis of pseudo-scaling combined functions. As a test of the efficiency of this set, the expansions of Equation (25) are carried out by least mean squares fitting of the coefficients. The resulting expansions are listed in Table 15. Also listed are the corresponding least mean square deviations

$$\text{LMSQD} = \int dV\{\varpi(t_i, n\ell m) - \hat{\varpi}(t_i, n\ell m)\}^2/r.$$

Here the sum over $\nu = 1, 2, \ldots P$ extends over all basis functions from row 1 to row P, if the LMSQD's are listed in row P. Thus, the LMSQD's listed in the last row correspond to the expansion whose coefficients are listed. This does not hold, however, for the LSMQD's in the preceding rows, since the basis functions are not all orthogonal to each other.

Effectiveness of Pseudo-Scaling

It is desirable to have a test of the effectiveness of pseudo-scaling with respect to the energy. Two such tests, which moreover are closely related to the validity of the virial theorem, are the following. If an atomic orbital f(r) is truly scaled, i.e.,

$$f_t = t^{3/2} f(tr), \quad f_1 = f(r),$$

then the following relations hold

$$t^{-1}\langle f_t | r^{-1} | f_t \rangle = \langle f_1 | r^{-1} | f_1 \rangle \quad ,$$

$$t^{-2}\langle f_t | -\tfrac{1}{2}\nabla^2 | f_t \rangle = \langle f_1 | -\tfrac{1}{2}\nabla^2 | f_1 \rangle \quad ,$$

Table 15. Expansions of scaled nonorthogonal SCFAO's in terms of reduced basis for silicon ^3P state

Expansions of Scaled Nonorthogonal 1s Orbitals

	t = 0.95		t = 0.98	
	Coeffs.	MSQ-DEV	Coeffs.	MSQ-DEV
$\chi_1(1s)$	0.9759	1.9(-3)	0.9907	3.0(-4)
$\chi_1(2s)$	-0.0000	1.4(-3)	-0.0002	2.2(-4)
$\chi_2(2s)$	-0.0608	7.7(-4)	-0.0239	1.2(-4)
$\chi_1(3s)$	0.0295	7.0(-4)	0.0116	1.1(-4)
$\chi_2(3s)$	-0.0294	5.9(-4)	-0.0116	9.7(-5)
$\chi_3(3s)$	-0.0181	4.8(-4)	-0.0072	7.9(-5)

Expansions of Scaled Nonorthogonal 2s Orbitals

	t = 0.70		t = 0.88	
	Coeffs.	MSQ-DEV	Coeffs.	MSQ-DEV
$\chi_1(2s)$	0.7916	1.6(-1)	0.9749	2.1(-2)
$\chi_2(2s)$	0.2336	1.1(-2)	0.1314	1.5(-4)
$\chi_1(1s)$	0.0122	9.3(-3)	0.0035	1.1(-4)
$\chi_1(3s)$	0.1610	5.0(-3)	0.0162	7.1(-5)
$\chi_2(3s)$	-0.1341	1.8(-3)	-0.0144	4.0(-5)
$\chi_3(3s)$	-0.0643	4.0(-4)	-0.0076	1.9(-5)

Expansions of Scaled Nonorthogonal 3s Orbitals

	t = 0.60		t = 0.84	
	Coeffs.	MSQ-DEV	Coeffs.	MSQ-DEV
$\chi_1(3s)$	0.8621	3.3(-1)	0.9690	4.6(-2)
$\chi_2(3s)$	0.4778	4.9(-2)	0.2219	5.8(-4)
$\chi_3(3s)$	-0.2624	1.7(-3)	-0.0151	5.3(-5)
$\chi_1(2s)$	-0.0675	1.2(-3)	0.0121	3.8(-5)
$\chi_2(2s)$	-0.0566	6.2(-4)	0.0102	1.9(-5)
$\chi_1(1s)$	-0.0071	5.8(-4)	0.0013	1.8(-5)

Expansions of Scaled Nonorthogonal 1s Orbitals

t = 1.00		t = 1.02		t = 1.04	
Coeffs.	MSQ-DEV	Coeffs.	MSQ-DEV	Coeffs.	MSQ-DEV
1.0000	0.0	1.0088	2.8(-4)	1.0171	1.1(-3)
0.0	0.0	0.0004	2.1(-4)	0.0010	8.5(-4)
0.0	0.0	0.0233	1.2(-4)	0.0461	5.0(-4)
0.0	0.0	-0.0114	1.1(-4)	-0.0226	4.6(-4)
0.0	0.0	0.0114	9.8(-5)	0.0225	4.0(-4)
0.0	0.0	0.0070	8.1(-5)	0.0140	3.3(-4)

Expansions of Scaled Nonorthogonal 2s Orbitals

t = 1.00		t = 1.12		t = 1.24	
Coeffs.	MSQ-DEV	Coeffs.	MSQ-DEV	Coeffs.	MSQ-DEV
1.0000	0.0	0.9721	1.7(-2)	0.9097	5.9(-2)
0.0	0.0	-0.1506	2.5(-4)	-0.3017	2.5(-3)
0.0	0.0	0.0025	2.1(-4)	0.0126	1.9(-3)
0.0	0.0	0.0238	1.2(-4)	0.0701	1.2(-3)
0.0	0.0	-0.0202	4.9(-5)	-0.0611	5.9(-4)
0.0	0.0	-0.0100	1.4(-5)	-0.0315	2.4(-4)

Expansions of Scaled Nonorthogonal 3s Orbitals

t = 1.00		t = 1.16		t = 1.32	
Coeffs.	MSQ-DEV	Coeffs.	MSQ-DEV	Coeffs.	MSQ-DEV
1.0000	0.0	0.9843	3.3(-2)	0.9269	1.1(-1)
0.0	0.0	-0.1813	9.8(-4)	-0.3026	8.5(-3)
0.0	0.0	-0.0326	1.3(-6)	-0.0754	1.9(-4)
0.0	0.0	-0.0022	3.8(-7)	0.0251	1.1(-4)
0.0	0.0	-0.0012	5.3(-8)	0.0194	3.8(-5)
0.0	0.0	-0.0001	5.0(-8)	0.0021	3.5(-5)

Table 15. (Continued)

	Expansions of Scaled Nonorthogonal 2p Orbitals			
	t = 0.70		t = 0.88	
	Coeffs.	MSQ-DEV	Coeffs.	MSQ-DEV
$\chi_1(2p)$	0.8683	1.2(-1)	0.9840	1.6(-2)
$\chi_2(2p)$	0.2337	6.7(-3)	0.1154	8.4(-5)
$\chi_1(3p)$	0.1038	3.9(-3)	0.0103	6.3(-5)
$\chi_2(3p)$	-0.0901	1.6(-3)	-0.0099	3.9(-5)
$\chi_3(3p)$	-0.0480	5.4(-4)	-0.0061	2.2(-5)
	Expansions of Scaled Nonorthogonal 3p Orbitals			
	t = 0.60		t = 0.84	
	Coeffs.	MSQ-DEV	Coeffs.	MSQ-DEV
$\chi_1(3p)$	0.8632	3.0(-1)	0.9756	4.0(-2)
$\chi_2(3p)$	0.4750	4.0(-2)	0.2042	4.5(-4)
$\chi_3(3p)$	-0.2253	1.1(-3)	-0.0156	3.4(-5)
$\chi_1(2p)$	-0.0392	8.3(-4)	0.0070	2.6(-5)
$\chi_2(2p)$	-0.0367	4.0(-4)	0.0066	1.2(-5)

Expansions of Scaled Nonorthogonal 2p Orbitals

t = 1.00		t = 1.12		t = 1.24	
Coeffs.	MSQ-DEV	Coeffs.	MSQ-DEV	Coeffs.	MSQ-DEV
1.00	0.0	0.9830	1.3(-2)	0.9440	4.5(-2)
0.0	0.0	-0.1265	1.5(-4)	-0.2538	1.5(-3)
0.0	0.0	0.0151	9.3(-5)	0.0452	1.0(-3)
0.0	0.0	-0.0135	4.5(-5)	-0.0422	5.9(-4)
0.0	0.0	-0.0075	1.8(-5)	-0.0249	2.9(-4)

Expansions of Scaled Nonorthogonal 3p Orbitals

t = 1.00		t = 1.16		t = 1.32	
Coeffs.	MSQ-DEV	Coeffs.	MSQ-DEV	Coeffs.	MSQ-DEV
1.00	0.0	0.9861	2.9(-2)	0.9407	9.8(-2)
0.0	0.0	-0.1695	7.8(-4)	-0.2912	6.8(-3)
0.0	0.0	-0.0289	9.9(-7)	-0.0716	1.4(-4)
0.0	0.0	-0.0015	4.4(-7)	0.0152	9.3(-5)
0.0	0.0	-0.0011	4.4(-8)	0.0134	3.5(-5)

where the right hand side is independent of the scale parameter t. It is therefore illuminating to examine the relative deviations

$$\Delta V(n\ell) = [t^{-1}\langle\tilde{\varpi}(t,n\ell)|r^{-1}|\tilde{\varpi}(t,n\ell)\rangle - \langle\varpi(n\ell)|r^{-1}|\varpi(n\ell)\rangle]/$$

$$\langle\varpi(n\ell)|r^{-1}|\varphi(n\ell)\rangle \tag{26a}$$

$$\Delta T(n\ell) = [t^{-2}\langle\tilde{\varpi}(t,n\ell)|-\tfrac{1}{2}\nabla^2|\tilde{\varpi}(t,n\ell)\rangle - \langle\varphi(n\ell)|-\tfrac{1}{2}\nabla^2|\varphi(n\ell)\rangle]/$$

$$\langle\varpi(n\ell)|-\tfrac{1}{2}\nabla^2|\varpi(n\ell)\rangle \tag{26b}$$

as t varies over the scaling range. Here $\varpi(n\ell)$ are the even-tempered SCFAO expansions of Equation (12) and $\tilde{\varpi}(n\ell)$ are the even-tempered expansions of the scaled $\psi(n\ell m|tr)$. Such a test is displayed in Table 16 for the (1s), (2s), (3s), (2p), and (3p) orbitals of Silicon discussed in the preceding section.

Two cases are examined for $\tilde{\varpi}$. First we consider the approximations

$$\tilde{\varpi}(t,n\ell m) = \varphi(t,n\ell m) \text{ of Equations (14a), (14b),}$$

i.e., expansions of $\psi(n\ell m|tr)$ in terms of the even-tempered basis that is optimally adapted to represent scaled SCFAO's according to the discussion on pages 38-46. The corresponding deviations are listed under the heading "Full Basis." Secondly, we consider the approximations

$$\tilde{\varphi}(t,n\ell m) = \hat{\varphi}(t,n\ell m) \text{ of Equation (25),}$$

i.e., expansions of $\psi(n\ell m|tr)$ in the reduced basis PSCETGAO's obtained in the preceding section according to the procedure of pages 46-51. The

Table 16. Pseudo-scaled orbital kinetic and potential energies[a]

Scaled 2p Orbital

	T_1 = 12.2		V_1 = 2.46	
Scale	Full Basis		Reduced Basis	
Parameter	%ΔT	%ΔV	%ΔT	%ΔV
0.70	.001	.001	-1	-.5
0.82	-.001	-.0002	-.9	-.3
0.94	-.0007	-.0004	-.2	-.06
1.00	0	0	0	0
1.06	.0006	.0003	-.1	-.04
1.18	.001	.0004	-1	-.6
1.24	.001	.0002	-3	-1

Scaled 3p Orbital

	T_1 = 0.412		V_1 = 0.448	
Scale	Full Basis		Reduced Basis	
Parameter	%ΔT	%ΔV	%ΔT	%ΔV
0.60	.006	.003	4	.2
0.76	-.007	.002	.06	.001
0.92	-.006	-.002	.002	-.007
1.00	0	0	0	0
1.08	.001	.002	.01	.007
1.24	-.006	.002	-.02	-.01
1.32	-.008	-.0003	.05	-.04

[a] %ΔT and %ΔV are the relative deviations of Equations (26a) and (26b) multiplied by 100.

Scaled 1s Orbital

$T_1 = 92.3$ $V_1 = 13.6$

Scale Parameter	Full Basis %ΔT	Full Basis %ΔV	Reduced Basis %ΔT	Reduced Basis %ΔV
0.95	.002	.003	5	2
0.97	.0004	.001	3	1
0.99	-.00006	.0004	1	.5
1.00	0	0	0	0
1.01	.0002	-.0003	-1	-.5
1.03	.0009	-.0007	-3	-1
1.04	.001	-.0009	-4	-2

Scaled 2s Orbital

$T_1 = 3.81$ $V_1 = 2.21$

Scale Parameter	Full Basis %ΔT	Full Basis %ΔV	Reduced Basis %ΔT	Reduced Basis %ΔV
0.70	.002	.003	2	-.01
0.82	.002	.003	-.008	-.07
0.94	-.0009	.0009	-.1	-.02
1.00	0	0	0	0
1.06	.004	.0002	-.1	-.01
1.18	.01	.002	-2	-.2
1.24	.02	.003	-3	-.4

Scaled 3s Orbital

$T_1 = 0.286$ $V_1 = 0.547$

Scale Parameter	Full Basis %ΔT	Full Basis %ΔV	Reduced Basis %ΔT	Reduced Basis %ΔV
0.60	-.005	-.002	9	.3
0.76	.003	.002	.2	.006
0.92	-.006	0	.03	.001
1.00	0	0	0	0
1.08	.006	.0004	.02	.003
1.24	.004	.0009	.02	-.008
1.32	-.005	.0009	.2	-.02

corresponding deviations are listed under the heading "Reduced Basis."

It is apparent that the deviations ΔV and ΔT are gratifyingly small, confirming the usefulness of the method.

Remarks on Computation

The reported quantitative results were obtained by a set of computer programs which are linked together to form a fully automated system.

Input consists of the following information: (1) A set of accurate orthogonal or nonorthogonal SCFAO's, $\psi(n\ell m)$, expanded in terms of either exponential or Gaussian-type primitives; (2) The required expansion lengths, i.e., the number of even-tempered Gaussian-type primitives chosen to represent each accurate SCFAO; (3) Scaling ranges and weight factors (for LMSQ evaluations) for each SCFAO; (4) The number of superpositions of even-tempered Gaussian primitives (PSCETGAO's) which each SCFAO is to contribute to the final reduced basis.

The output is similar to that exhibited on pages 52-67, with some additional options. The program is general enough to generate a pseudo-scaling reduced basis of superpositions of even-tempered Gaussian primitives for any atom of the periodic table.

On the IBM 360/65 the double-precision program occupies 188 K bytes of main core, 54 K bytes of bulk core and several disk files. Execution time for the entire generation process increases with the atomic number; it is 10 minutes for Carbon and 25 minutes for Silicon. A restart option is provided for, in case of termination before completion. The bulk of the time is spent on the nonlinear minimizations with respect

to α and β, which are performed using Powell's conjugate directions program (23). Overlap integrals between Gaussians and exponentials are evaluated by a novel method described in Reference (24).

Chapter III. OPTIMIZATIONS OF EVEN-TEMPERED GAUSSIAN PRIMITIVE BASES BY MINIMIZING TOTAL MOLECULAR ENERGIES FOR HYDROCARBON AND OXYGEN-CONTAINING MOLECULES

Introduction

The large majority of molecular calculations made to date have utilized basis sets which were determined in the isolated atoms. Accurate computations involving the optimization of basis sets in the molecular framework have been carried out on a much more limited scale because of the much larger expenditure of computer time required for the variation of nonlinear, orbital exponent parameters. Past molecular optimizations of orbital exponents can be classified into the following categories:

1) completely unconstrained optimizations of all orbital exponents;

2) constraint of inner shell orbital exponents to optimal atomic values and variation of scaling parameters by which the optimal atomic exponents of the valence shells are multiplied;

3) method of category (2) supplemented by the variation of orbital exponents in additional polarization functions;

4) constraint of inner and valence shell orbital exponents to optimal atomic values and the variation of orbital exponents in additional polarization functions.

Each of these four categories can be applied to (a) exponential-type or (b) Gaussian-type basis functions so that eight possible cases can be distinguished. The following list classifies past work accordingly:

1a) application to minimal or near-minimal Slater-type basis (25-30);

1b) no application found;

2a) no application found;

2b) application to linear combinations of primitive Gaussians which were determined by fitting minimal bases of Slater-type atomic orbitals or by carrying out full atomic SCF calculations (31,32);

3a) no application found;

3b) application to SCFAO's expanded in terms of primitive Gaussians (33);

4a) application to Slater-type bases (34,35);

4b) application to SCFAO's expanded in terms of primitive Gaussians (36-38).

The feasibility of unconstrained basis optimizations in molecules is greatly increased by using the even-tempered basis (17). Even so, an alternative procedure to such nonlinear parameter optimizations in molecules was introduced in Chapter II and used in calculations on the trialkali ions (21). This "pseudo-scaling" approach, however, often requires an enlargement of the primitive Gaussian basis by one or two primitives which may be undesirable for certain calculations. Therefore, in the present chapter we investigate unconstrained optimizations of small, even-tempered Gaussian basis sets. As a result of these optimizations, basis sets are obtained which are optimal for molecular calculations. These optimizations are applied to the molecules hydrogen, methane, acetylene, ethylene, ethane, methyl acetylene, water, carbon monoxide, carbon dioxide, formaldehyde, and carbon suboxide.

The optimal bases are generated by a minimization procedure which is a modification of the method of continued parallel tangents (continued

Partan) described by Shah et al. (39). No derivatives are computed in this modification. In order to minimize the number of SCF energy calculations required to find the energy minimum, careful attention is given to the selection of initial parameter values and search directions.

The minimizations are first carried out on prototype molecules which contain the basic types of bonds, namely hydrogen, methane, acetylene, ethylene, ethane, water, carbon monoxide, carbon dioxide, and formaldehyde. For these, totally uncontracted basis sets are used. Then, on the basis of these results, new contracted, even-tempered Gaussian atomic orbitals optimal for molecular situations (MOGETGAO's) are constructed and the minimization procedure is modified which substantially reduces the amount of work involved in optimizations in larger molecules. Finally, the degree of transferability of the optimal parameters for the prototype molecules is determined by using this scheme on methyl acetylene and carbon suboxide which have bonding situations intermediate to those of the prototypes.

The quality of the optimal bases is ascertained by calculating equilibrium bond distances and bond angles. In addition, energy changes for reactions involving the molecules considered are calculated.

Selection of Even-Tempered Gaussian Atomic Orbital Bases for Molecular Calculations

In Reference (17), we have introduced the even-tempered Gaussian primitives (ETGPAO's)

$$g(k\ell m|r) = N_\ell \cdot (\alpha_\ell \beta_\ell^k)^{(2\ell+3)/4} \exp(-\alpha_\ell \beta_\ell^k r^2) \cdot r^\ell Y_{\ell m}(\theta,\varphi), \qquad (27a)$$

$$N_\ell = 2^{(4\ell+7)/4}\ \pi^{-\frac{1}{4}}\ [(2\ell+1)!!]^{-\frac{1}{2}} \qquad (27b)$$

where β_ℓ^k denotes the k-th power of the spacing parameter β_ℓ and $Y_{\ell m}$ are normalized spherical harmonics. Whereas the ratio β_ℓ/α_ℓ usually approximates 10^2, $\ln\alpha_\ell$ and $\ln\beta_\ell$ have similar magnitudes and will be used throughout this work.

In Chapter I, the economic deployment of Gaussian primitive bases for expanding atomic self-consistent field orbitals (SCFAO's) was discussed in detail. This extensive analysis provides a means of selecting even-tempered Gaussian primitive bases for molecular calculations. The basis sizes were determined by examining the mean square deviations in Figures 1, 2, and 3. These figures show that good approximations to carbon, oxygen, and hydrogen SCFAO's are obtained for bases with sizes at least as large as (6;4,3;3) for C or O and (3) for H. The number in parentheses from left to right are the total number of distinct ls-type primitives expanding both ls and 2s SCFAO's, the number of primitives for ls, 2s, and 2p SCFAO's. In the present investigation, we are primarily interested in the following small primitive bases: H(3), H(4), C(6;3)≡C(6;6,6;3), C(6;4)≡C(6;6,6;4), and O(6;4)≡O(6;6,6;4). However, the carbon and hydrogen bases C(8;5,5;6), C(10;7,7;6), and H(5) will also be considered.

For each of the small basis sets, a set of parameter values for $\ln\alpha_\ell$ and $\ln\beta_\ell$ computed by the methods of Chapter I for fitting SCFAO's will be used as initial guesses for optimizations in the molecules. Starting values for the large carbon and hydrogen bases are obtained by

the pseudo-scaling methods described in Chapter II.

In order to extract the maximum amount of variational information for the parameters of the small bases, uncontracted basis functions will be used in optimizations on the prototype molecules. However, MOCETGAO bases will be constructed before proceeding to methyl acetylene and carbon suboxide. For the larger carbon and hydrogen bases, the methods described in Chapter II are used to generate pseudo-scaled, contracted, even-tempered Gaussian atomic orbitals (PSCETGAO's).

For each of the above basis sets, the initial values of $\ln\alpha_\ell$ and $\ln\beta_\ell$, the orbital scaling ranges selected for pseudo-scaling, and the PSCETGAO bases are given in Table 17. For the reasons mentioned above, uncontracted functions are listed for the small hydrogen, carbon, and oxygen bases.

Procedure of Minimization for Prototype Molecules

Method of minimization and its applicability

The effectiveness of a linear search procedure not involving derivatives is judged by the number of function evaluations required to find the minimum. In this section we describe two ways of reducing this number: (1) a more appropriate choice of finding starting values for $\ln\alpha_\ell$ and $\ln\beta_\ell$ than those described in the previous section and (2) determining an effective, standard set of search directions suitable for all molecules.

The proper choice of search directions depends to a great extent on the selection of starting values for $\ln\alpha_\ell$ and $\ln\beta_\ell$. For this reason, the

Table 17. Initial atomic orbital bases for molecular optimizations

Uncontracted Bases for Hydrogen, Carbon, and Oxygen[a]

Atom and Basis Set	s primitives $\ln \alpha_0$	s primitives $\ln \beta_0$	p primitives $\ln \alpha_1$	p primitives $\ln \beta_1$
H(3)	-3.443	1.588		
H(4)	-3.460	1.380		
C(6;3)	-2.871	1.447	-3.231	1.516
C(6;4)	-2.871	1.447	-3.365	1.363
O(6;4)	-2.227	1.439	-2.813	1.374

Contracted (PSCETGA0) Bases for Hydrogen[b]

H(5)-Basis $\ell n\, \alpha_0 = -3.328$ $\ell n\, \beta_0 = 1.233$

k[c]	X_1(1s)	X_2(1s)	X_3(1s)
1	0.400351	1.206034	1.191786
2	0.510265	-0.691610	-2.260724
3	0.177597	-0.408674	1.463473
4	0.040264	-0.120256	0.015947
5	0.015093	-0.041676	0.159614

[a] Bases determined by the methods of Chapter I.

[b] Bases determined by the methods of Chapter II for the scaling range $0.90 \leq t \leq 1.10$.

[c] Index of the even-tempered primitives with the exponents $\alpha_\ell \beta_\ell^{\,k}$.

Table 17. (Continued)

Contracted (PSCETGA0) Bases for Carbon[d]

C(8;5,5;6)-Basis $\ell n\,\alpha_0 = -4.004$ $\ell n\beta_0 = 1.297$ $\ell n\,\alpha_1 = -3.949$ $\ell n\beta_1 = 1.198$

k[a]	χ_1(1s)	χ_1(2s)	χ_2(2s)	χ_1(2p)	χ_2(2p)
1	0.0	0.111557	0.727066	0.116657	0.607054
2	0.0	0.757303	0.277575	0.501980	0.363655
3	0.0	0.271697	-1.079974	0.428879	-0.475308
4	0.439068	-0.123973	0.000516	0.157407	-0.357828
5	0.494543	-0.030680	0.110583	0.032991	-0.093999
6	0.168799	0.0	0.0	0.007550	-0.024875
7	0.036570	0.0	0.0	0.0	0.0
8	0.011982	0.0	0.0	0.0	0.0

[d]Bases determined by the methods of Chapter II for the following scaling ranges: $0.95 \leq t \leq 1.05$ for the 1s orbital and $0.70 \leq t \leq 1.30$ for the 2s and 2p orbitals.

Table 17. (Continued)

C(10;7,7;6)-Basis	$\ell n\ \alpha_0 = -3.742$	$\ell n\ \beta_0 = 1.085$	$\ell n\ \alpha_1 = -3.949$	$\ell n\ \beta_1 = 1.198$		
k^a	$\chi_1(1s)$	$\chi_2(2s)$	$\chi_1(2s)$	$\chi_2(2s)$	$\chi_1(2p)$	$\chi_2(2p)$
1	0.0	0.0	0.098156	0.635477	0.116657	0.607054
2	0.0	0.0	0.604595	0.505277	0.501980	0.363655
3	0.0	0.0	0.426209	-0.921585	0.428879	-0.475308
4	0.141675	0.781684	-0.053082	-0.394729	0.157407	-0.357828
5	0.484871	0.271600	-0.076567	0.146630	0.032991	-0.093999
6	0.345730	-0.599673	-0.011800	0.040315	0.007550	-0.024875
7	0.128941	-0.297122	-0.002445	0.008987	0.0	0.0
8	0.041677	-0.122621	0.0	0.0	0.0	0.0
9	0.007744	-0.019715	0.0	0.0	0.0	0.0
10	0.005073	-0.015396	0.0	0.0	0.0	0.0

first and second directions are the most crucial. Since gradients are not calculated here, good first and second directions may be determined by minimizations on a variety of small molecules. Before attempting such minimizations, however, much of the arbitrariness in the initial direction may be eliminated by consideration of two features of the even-tempered basis. First, the assumption that the value of $\ln\alpha_\ell$ and $\ln\beta_\ell$ obtained from atomic calculations are reasonable initial guesses is supported by the results of Chapters I and II and Reference (21). Second, if this assumption is valid, the greatest gain in the energy should be achieved when $\ln\alpha_\ell$ and $\ln\beta_\ell$ do not increase or decrease together, but vary oppositely since the Gaussian exponents shouldn't become too small or too large. This means that the initial direction should have a negative slope in the $(\ln\alpha_\ell, \ln\beta_\ell)$ plane. In choosing the second direction, it is expected that $\ln\alpha_\ell$ and $\ln\beta_\ell$ will more likely increase or decrease together nearer the beginning of the minimization than later on. Thus, this direction is taken perpendicular to the first. All subsequent directions are selected by a scheme which is a suitable two-dimensional modification of the Continued Parallel Tangents (Continued Partan) method of Shah et al. (39). A more detailed discussion of this modified two-dimensional method is given in the Appendix.

Application to the hydrogen molecule

The minimization procedure is used first on H_2 at the experimental bond distance (40) to test the assumptions of the preceding paragraph as well as to determine the relative quality of the bases H(3), H(4), and

H(5). Using the method introduced above, the complete optimization for H(4) is displayed graphically in Figure 8. In accordance with the above assumptions, the direction of the initial line is chosen at an angle of 135° from the $(\ln\alpha_\ell)$-axis. Using the computer program described in the Appendix, this line is searched until a quadratic prediction satisfies the specified parameter and function convergence criteria of 10^{-2} and 10^{-3}, respectively. The distance between the first and second points is the initial stepsize with value 10^{-1}. The second and third lines are searched in the same way, except that the stepsize is now 10^{-2}. For the reasons given in the Appendix, the stepsize, parameter criterion, and function criterion for the remaining directions are now decremented to their final values of 10^{-3}, 10^{-3}, and 10^{-5}, respectively. The minimization ends after these criteria have been satisfied for the last two directions.

Figure 8 emphasizes two important aspects of the previous discussion. First, the initial direction of 135° is poor enough to increase the number of subsequent directions so that 24 function evaluations are required to reach the minimum. Second, if a line is drawn to connect the initial point to the final point, it is seen that $\ln\alpha_o$ and $\ln\beta_o$ increase together and not oppositely as assumed. It will be seen in the following work, however, that this is the exception rather than the rule. Similar graphs are obtained for the bases H(3) and H(5). For all three bases, the final values of $\ln\alpha_o$ and $\ln\beta_o$ and the energies are given in Tables 18 and 20, respectively.

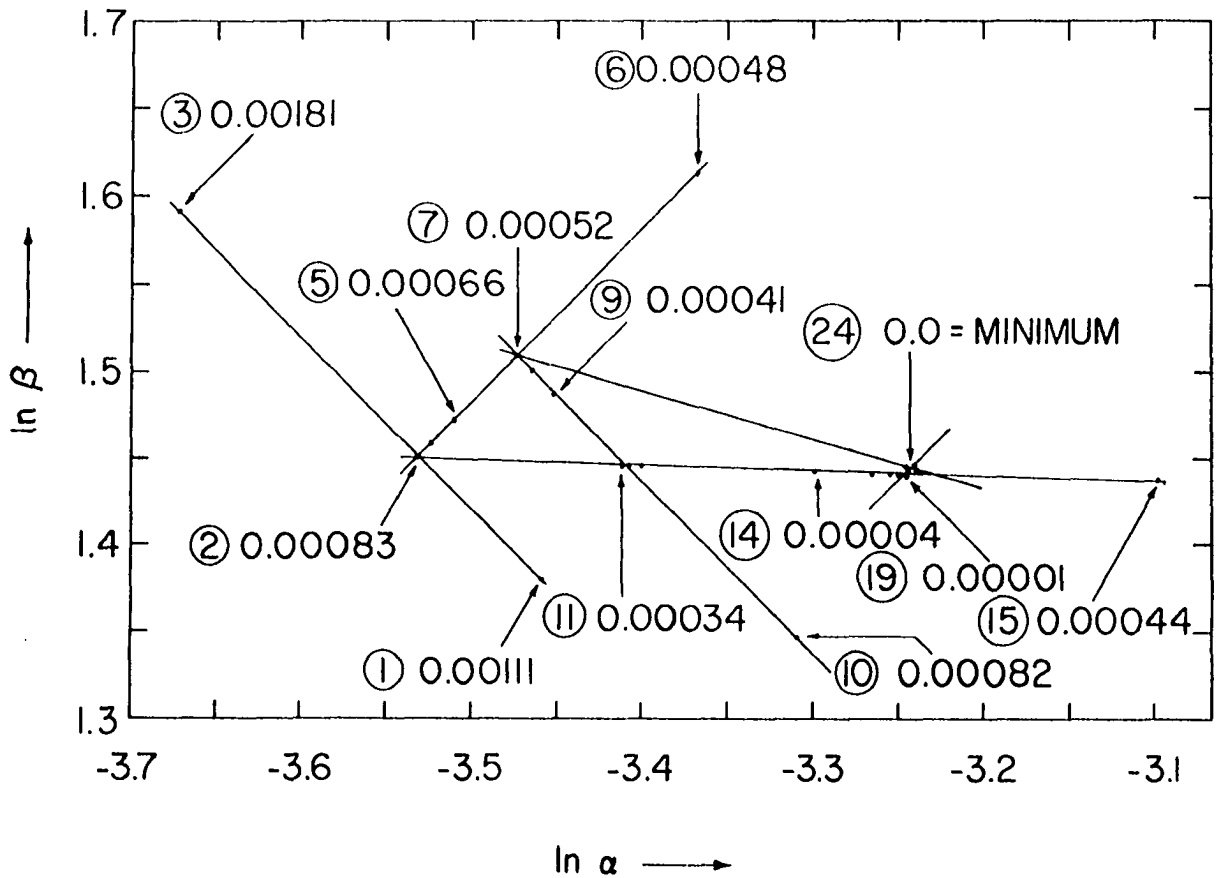

Figure 8. Progress of optimization of even-tempered parameters for H_2

Application to methane and acetylene

Next, the even-tempered parameters of CH_4 and C_2H_2 were determined for the basis C(6;3), H(4). In a first cycle, the method just described was applied separately and successively to each of the three parameter sets $(\ln\alpha_o, \ln\beta_o)$ of C, $(\ln\alpha_1, \ln\beta_1)$ of C, and $(\ln\alpha_o, \ln\beta_o)$ of H. Then, this same procedure was repeated in a second cycle to ascertain the interdependence between the three sets. The results of these successive optimizations are shown in Table 22. The negligible improvement in the second cycle shows that the three parameter sets are practically independent of each other. The carbon SCFAO fitting values of $\ln\alpha_\ell$ and $\ln\beta_\ell$ of Table 17 and the optimal values from H_2 given in Table 18 were used as initial parameter values for the optimizations in CH_4 and C_2H_2. In the first cycle, the initial search direction of 135° was employed in the optimization of each parameter set. In the second cycle, the initial directions were chosen along the lines connecting the initial points and the optimal points of the first cycle, since these lines were found to have negative slopes.

The same type of calculation was then repeated for CH_4 and C_2H_2, but with the larger basis C(6;4), H(4). In these calculations, the initial parameter values selected for the carbon and hydrogen, s-orbitals were the optimal values for the basis C(6;3), H(4) while those for the p-orbitals were taken from Table 17. The initial search directions for all sets of parameters were chosen to be along the lines connecting the previous optimal parameter points for CH_4 with those for C_2H_2.

The final parameter values and energies for both bases are given in

Table 18. Optimum values of $\ell n\, \alpha_\ell$ and $\ell n\, \beta_\ell$ for various bases[a]

Primitive Basis	Contracted Basis	Hydrogen s Orbital Parameter Values[b] H_2[c]	CH_4[c]	C_2H_2[c]	C_2H_4[c]
H(3)	H[3]	-3.230;1.597			
H(4)	H[4]	-3.236;1.441			
H(5)	H[5]	-3.232;1.318			
H(5)	H[2][d]	-3.176;1.234			
C(6;3),H(4)	C[6;3],H[4]		-3.490;1.593	-3.440;1.504	
C(6;4),H(4)	C[6;4],H[4]		-3.463;1.547	-3.270;1.470	-3.304;1.472
C(8;5,5;6),H(5)	C[1,2;2],H[3][d]				-3.228;1.233
C(10;7,7;6),H(5)	C[2,2;2],H[2][d]			-3.235;1.317	

[a]Optimal values corresponding to minimum energies of Table 20.

[b]Each entry contains the number pair $\ell n\, \alpha$; $\ell n\, \beta$.

[c]Parameter values obtained at the most recent experimental geometries given in Reference (40). See Table 41.

[d]Contracted (PSCETGAO) bases of Table 17.

Table 18. (Continued)

Primitive Basis	Contracted Basis	Carbon s and p Orbital Parameter Values[e] H_2[c]	CH_4[c]	C_2H_2[c]	C_2H_4[c]
C(6;3),H(4)	C[6;3],H[4]		-2.217;1.410 -2.096;1.387	-2.093;1.393 -3.272;1.505	
C(6;4),H(4)	C[6;4],H[4]		-2.236;1.412 -2.918;1.280	-2.023;1.384 -3.364;1.363	-2.194;1.406 -3.186;1.351
C(8;5,5;6),H(5)	C[1,2;2],H[3][d]				-4.003;1.296 -4.134;1.198
C(10;7,7;6),H(5)	C[2,2;2],H[2][d]			-3.696;1.087 -4.104;1.198	

[e]Each entry contains $\ell n\, \alpha_0$; $\ell n\, \beta_0$ in the first row and $\ell n\, \alpha_1$; $\ell n\, \beta_1$ in the second row.

Table 19. Optimum values of $\ell n\, \alpha_\ell$ and $\ell n\, \beta_\ell$ for standard-type bases[a]

Molecule	Carbon[b] s	Carbon[b] p	Oxygen[b] s	Oxygen[b] p	Hydrogen[b] s
H_2[c]					-3.236
					1.441
CH_4[c]	-2.236	-2.918			-3.463
	1.412	1.280			1.547
C_2H_2[c]	-2.023	-3.364			-3.270
	1.384	1.363			1.470
C_2H_4[c]	-2.194	-3.186			-3.304
	1.406	1.351			1.472
C_2H_6[c]	-2.215	-3.180			-3.175
	1.413	1.345			1.442
H_2O[c]			-1.836	-2.950	-2.995
			1.433	1.402	1.427
CO[c]	-2.912	-2.900	-1.689	-2.653	
	1.463	1.341	1.414	1.348	
CO_2[c]	-2.549	-3.014	-1.689	-2.612	
	1.435	1.324	1.414	1.345	
H_2CO[c]	-2.230	-3.243	-1.784	-2.814	-3.507
	1.418	1.357	1.420	1.389	1.526

[a] The standard basis type is C(6;4),O(6;4),H(4). The optimal parameter values correspond to the minimum energies of Table 21.

[b] Each entry contains $\ell n\, \alpha_\ell$ in the first row and $\ell n\, \beta_\ell$ in the second row.

[c] Parameter values obtained at the most recent experimental geometries given in Reference (40). See Table 41.

Table 19. (Continued)

Molecule[d]	Carbon[b] s	Carbon[b] p	Oxygen[b] s	Oxygen[b] p	Hydrogen[b] s
$\underline{H_3}\underline{C}CCH$[e]	-2.215	-3.180			-3.175
	1.413	1.345			1.442
$H_3\underline{C}CCH$[e]	-2.023	-3.364			
	1.384	1.363			
$H_3CC\underline{CH}$[e]	-2.023	-3.364			-3.220
	1.384	1.363			1.470
$H_3\underline{C}CCH$[f]	-2.215	-3.160			-3.205
	1.413	1.336			1.452
$H_3C\underline{C}CH$[f]	-2.023	-3.300			
	1.384	1.358			
$H_3CC\underline{CH}$[f]	-2.023	-3.364			-3.270
	1.384	1.363			1.470
$\underline{O}\underline{C}\underline{C}\underline{O}$[g]	-2.630	-3.014	-1.689	-2.612	
	1.443	1.324	1.414	1.345	
$O\underline{C}\underline{C}O$[g]	-2.140	-2.940			
	1.403	1.311			

[d] Listed parameter values correspond to underlined atoms.

[e] Parameter values obtained for the experimental bond lengths and bond angles from C_2H_2 and C_2H_6. The contracted (MOCETGAO) basis is C[3;3], H[2] of Table 34.

[f] Parameter values obtained for the theoretical equilibrium geometry of Table 41. The contracted (MOCETGAO) basis is C[3;3],H[2] of Table 34.

[g] Parameter values obtained at the linear geometry with r(C-O) = 1.20Å and r(C-C) = 1.30Å. See Reference (45). The contracted (MOCETGAO) basis is C[4;3], O[3;3] of Table 34.

Table 20. Minimum energies (Hartrees) for various bases[a]

Primitive Basis	Contracted Basis	H_2[b]	CH_4[b]	C_2H_2[b]	C_2H_4[b]
H(3)	H[3]	-1.12021			
H(4)	H[4]	-1.12645			
H(5)	H[5]	-1.12779			
H(5)	H[2][c]	-1.12749			
C(6;3),H(4)	C[6;3],H[4]		-40.12375	-76.65708	
C(6;4),H(4)	C[6;4],H[4]		-40.13762	-76.71010	-77.92006
C(8;5,5;6),H(5)	C[1,2;2],H[3][c]				-77.94388
C(10;7,7;6),H(5)	C[2,2;2],H[2][c]			-76.79052	

[a]Minimum energies correspond to the optimal parameter values of Table 18.

[b]Energies obtained at the most recent experimental geometries given in Reference (40) and Table 41.

[c]Contracted (PSCETGAO) bases of Table 17.

Table 21. Minimum energies for standard bases and comparison with other bases

Molecule[a]	Energy of Standard Basis[b]	Energy of Comparison Basis 1[c]	Energy of Comparison Basis 2[d]
H_2	-1.12645	-1.11669	-1.12673
CH_4	-40.13762	-39.72653	-40.13938
C_2H_2	-76.71010	-75.85208	-76.71059
C_2H_4	-77.92006	-77.07232	-77.92103
C_2H_6	-79.11146	-78.30603	-79.11562
H_2O	-75.88368	-74.96293	-75.90739
CO	-112.48164	-112.4680	
CO_2	-187.23283	-185.06465	-187.32796
H_2CO	-113.65848	-112.35375	-113.69209

[a]Energies obtained at the most recent experimental geometries of Reference (40), except for cases mentioned in footnotes e,f, and g.

[b]Standard basis type is C(6;4),O(6;4),H(4). In C_3H_4 it is contracted to [3;3],H[2]. In C_3O_2 it is contracted to C[4;3],O[3;3]. See Table 34. Minimum energies correspond to optimal parameter values of Table 19.

[c]Results published (except for CO and C_3O_2) by Hehre, et al. (31), (42). Results for CO given by Hopkinson, et al. (43). Results for C_3O_2 given by Sabin and Kim (44).

[d]Results published by Ditchfield, et al. (32).

Table 21. (Continued)

Molecule	Energy of Standard Basis[b]	Energy of Comparison Basis 1[c]	Energy of Comparison Basis 2[d]
C_3H_4	-115.69770	-114.44397	-115.69964
C_3H_4[e]	-115.69299		
C_3H_4[f]	-115.70039		
C_3O_2	-262.81142		
C_3O_2[g]	-262.79774	-262.19060	

[e]Energy value obtained for the experimental bond lengths and angles from C_2H_2 and C_2H_6.

[f]Energy value obtained at the theoretical equilibrium geometry of Table 41.

[g]Energy value obtained at the linear geometry with r(C-O) = 1.20Å and r(C-C) = 1.30Å. See Reference (45). Energy value for comparison basis obtained at the linear geometry with r(C-O) = 1.243Å and r(C-C) = 1.332Å of Reference (44).

Table 22. Progress of energy minimization in CH_4 and C_2H_2[a]

α_ℓ, β_ℓ Values	CH_4	C_2H_2
Initial (See Table 17) from atomic SCFAO fitting	-40.10908	-76.56184
First Cycle		
C - α_0 and β_0 optimal	-40.11307	-76.65589
C - α_1 and β_1 optimal	-40.12211	-76.65653
H - α_0 and β_0 optimal	-40.12375	-76.65708
Second Cycle		
C - α_0 and β_0 optimal	-40.12375	-76.65708
C - α_1 and β_1 optimal	-40.12375	-76.65708
H - α_0 and β_0 optimal	-40.12375	-76.65708

[a]All energies are given for the basis C[6;3],H[4].

Tables 18, 19, 20, and 21. For the basis C(6;4), H(4), the improvement in the energy of C_2H_2 is found to be 0.053 Hartree. In addition, a superior C-C band length in C_2H_2 is obtained for the larger basis at the theoretical equilibrium geometry. Thus, the smaller basis is abandoned in favor of C(6;4), H(4), which in the sequel will be called the "standard basis."

Application to other prototype molecules

The standard bases C(6;4), O(6;4), and H(4) were optimized for the remaining prototype molecules C_2H_4, C_2H_6, H_2O, CO, CO_2, and H_2CO at their experimental geometries (40) in the same manner used for CH_4 and C_2H_2. Before starting each calculation, the best straight lines were drawn through the optimal parameter points $(\ln\alpha_\ell, \ln\beta_\ell)$ for all completed molecules in order to provide refined starting directions. For all molecules, the choices of starting parameter values were made as much as possible on the basis of bonding similarities. For example, the similar directional characteristics of the C-H bonds in C_2H_4 and C_2H_6 were expected to yield similar carbon s- and p-type parameters. The starting parameter values for oxygen in subsequent optimizations were obtained from H_2O, whose initial values were taken from Table 17. The optimal parameter values and the corresponding energies are given in Tables 19 and 21, respectively, In Table 23, additional energy information is given for the prototype molecules.

The accuracy of the preceding calculations may be assessed by using the virial ratio (V/E) of Table 23 in conjunction with the molecular virial theorem (41)

Table 23. Decomposition of the minimum total molecular energies of Table 21

	Kinetic Energy	Potential Energy	Electron-Nuclear Attraction	Electron-Electron Repulsion	Nuclear-Nuclear Repulsion	Potential/Total Energy
H_2[a]	1.11867	-2.24511	-3.61106	0.65166	0.71429	1.99310
CH_4[a]	40.03481	-80.17243	-119.53888	25.97593	13.39051	1.99744
C_2H_2[a]	76.54514	-153.25524	-227.82391	49.82710	24.74157	1.99785
C_2H_4[a]	77.96827	-155.68833	-247.55793	58.50583	33.36377	1.99805
C_2H_6[a]	78.98095	-158.09240	-267.82097	67.46770	42.26087	1.99835
C_3H_4[b]	115.67031	-231.37070	-387.50015	96.85235	59.27710	1.99974
H_2O[a]	75.80057	-151.68425	-198.61387	37.73446	9.19516	1.99890
CO[a]	112.35701	-224.83865	-310.05457	62.69868	22.51724	1.99889
CO_2[a]	187.17270	-374.40553	-558.58571	125.87645	58.30373	1.99968
H_2CO[a]	113.54533	-227.20381	-330.51633	71.94092	31.37160	1.99900
C_3O_2[c]	261.82989	-524.62763	-855.66465	211.59956	119.43747	1.99632

[a]Components of the total molecular energies given only for the C[6;4],O[6;4],H[4] basis.

[b]Components of the total molecular energy given for C_3H_4 at the theoretical equilibrium geometry.

[c]Components of the total molecular energy given for C_3O_2 at r(C-O)=1.20Å and r(C-C)=1.30Å.

$$\Delta(t_1,t_2,\ldots) = 2T + V + \sum_i \vec{R}_i \cdot \left(\frac{\partial E}{\partial \vec{R}_i}\right). \tag{28}$$

In the preceding optimizations, the variable parameters t_i of Equation (28) correspond to the even-tempered exponent parameters of the primitive Gaussian basis set and the associated linear expansion coefficients. When the optimal values of t_i and nuclear position vectors $\vec{R}_i$ have been determined such that the energy E is a minimum, Equation (28) reduces to

$$0 = 2T + V \tag{29a}$$

or

$$V/E = 2. \tag{29b}$$

However, the optimizations were carried out at the experimental molecular geometries (40). Therefore, the differences between the ratios of Table 23 and Equation (29b) is essentially due to the nonzero derivatives in Equation (28). These differences are all < 0.0005 when the parameter values of Table 19 are used in calculating the theoretical equilibrium geometries.

The optimized molecular orbitals (OMO's) are given in Tables 24-32. Each column of coefficients denotes one molecular orbital and is headed by the orbital energy and a symmetry designation corresponding to the irreducible representation of the molecular point group. Primitive Gaussian designations are used to label the first to the last rows of coefficients in each block. Within a block the exponent parameters decrease in value from the first to the last rows.

The positions of the atoms in all molecules are described in Table 33

Table 24. Optimized MO for hydrogen

		$1\sigma_g$
	ε	-0.594758
H	1s4	0.014242
	1s3	0.056596
	1s2	0.274520
	1s1	0.278310
H	1s4	0.014242
	1s3	0.056596
	1s2	0.274520
	1s1	0.278310

Table 25. Optimized MO's for methane

	$1a_1$	$2a_1$	$1t_2$	$2t_2$	$3t_2$
ε	-11.199626	-0.943655	-0.544252	-0.544252	-0.544252
C 1s6	-0.013554	-0.002432	0.0	0.0	0.0
1s5	-0.054302	-0.010237	0.0	0.0	0.0
1s4	-0.270253	-0.052335	0.0	0.0	0.0
1s3	-0.611941	-0.165234	0.0	0.0	0.0
1s2	-0.224686	-0.102320	0.0	0.0	0.0
1s1	0.026103	0.615369	0.0	0.0	0.0
2px4	0.0	0.0	-0.000463	-0.020221	0.012525
2px3	0.0	0.0	-0.001822	-0.079509	0.049250
2px2	0.0	0.0	-0.006142	-0.267946	0.165972
2px1	0.0	0.0	-0.005504	-0.240103	0.148725
2py4	0.0	0.0	0.018426	-0.008227	-0.012600
2py3	0.0	0.0	0.072454	-0.032349	-0.049543
2py2	0.0	0.0	0.244170	-0.109016	-0.166961
2py1	0.0	0.0	0.218797	-0.097688	-0.149611
2pz4	0.0	0.0	0.015041	0.009456	0.015822
2pz3	0.0	0.0	0.059141	0.037180	0.062213
2pz2	0.0	0.0	0.199306	0.125299	0.209659
2pz1	0.0	0.0	0.178595	0.112278	0.187873
H 1s4	0.000101	0.004923	-0.004019	-0.009742	0.000484
1s3	-0.000482	0.026393	-0.019912	-0.048273	0.002399
1s2	-0.002305	0.109237	-0.102250	-0.247886	0.012320
1s1	-0.001709	0.108067	-0.094268	-0.228535	0.011358
H 1s4	0.000101	0.004923	-0.003683	0.004901	-0.008586
1s3	-0.000482	0.026393	-0.018249	0.024282	-0.042543
1s2	-0.002305	0.109237	-0.093711	0.124689	-0.218461
1s1	-0.001709	0.108067	-0.086396	0.114955	-0.201407
H 1s4	0.000101	0.004923	0.010523	-0.000558	-0.000511
1s3	-0.000482	0.026393	0.052139	-0.002764	-0.002533
1s2	-0.002305	0.109237	0.267738	-0.014194	-0.013008
1s1	-0.001709	0.108067	0.246837	-0.013085	-0.011993
H 1s4	0.000101	0.004923	-0.002821	0.005400	0.008613
1s3	-0.000482	0.026393	-0.013978	0.026755	0.042676
1s2	-0.002305	0.109237	-0.071776	0.137391	0.219149
1s1	-0.001709	0.108067	-0.066173	0.126665	0.202042

Table 26. Optimized MO's for acetylene

		$1\sigma_g$	$1\sigma_u$	$2\sigma_g$
	ε	-11.246599	-11.242800	-1.042469
C	1s6	0.008918	-0.008926	-0.001988
	1s5	0.034449	-0.034480	-0.008078
	1s4	0.168795	-0.168944	-0.040254
	1s3	0.417187	-0.417579	-0.133754
	1s2	0.201873	-0.203643	-0.115164
	1s1	-0.020248	0.027281	0.435457
	2px4	0.0	0.0	0.0
	2px3	0.0	0.0	0.0
	2px2	0.0	0.0	0.0
	2px1	0.0	0.0	0.0
	2py4	0.0	0.0	0.0
	2py3	0.0	0.0	0.0
	2py2	0.0	0.0	0.0
	2py1	0.0	0.0	0.0
	2pz4	-0.000334	0.000045	0.011067
	2pz3	0.001633	-0.000447	0.062282
	2pz2	0.000208	0.006701	0.112345
	2pz1	0.008494	0.011824	0.180861
C	1s6	0.008918	0.008926	-0.001988
	1s5	0.034449	0.034480	-0.008078
	1s4	0.168795	0.168944	-0.040254
	1s3	0.417187	0.417579	-0.133754
	1s2	0.201873	0.203643	-0.115164
	1s1	-0.020248	-0.027281	0.435457
	2px4	0.0	0.0	0.0
	2px3	0.0	0.0	0.0
	2px2	0.0	0.0	0.0
	2px1	0.0	0.0	0.0
	2py4	0.0	0.0	0.0
	2py3	0.0	0.0	0.0
	2py2	0.0	0.0	0.0
	2py1	0.0	0.0	0.0
	2pz4	0.000334	0.000045	-0.011067
	2pz3	-0.001633	-0.000447	-0.062282
	2pz2	-0.000208	0.006701	-0.112345
	2pz1	-0.008494	0.011824	-0.180861
H	1s4	-0.000046	0.000130	0.002451
	1s3	0.000071	-0.000555	0.010807
	1s2	0.002190	-0.000179	0.056497
	1s1	0.006194	0.009335	0.202089
H	1s4	-0.000046	-0.000130	0.002451
	1s3	0.000071	0.000555	0.010807
	1s2	0.002190	0.000179	0.056497
	1s1	0.006194	-0.009335	0.202089

$2\sigma_u$	$3\sigma_g$	$1\pi_{ux}$	$1\pi_{uy}$
-0.765781	-0.684153	-0.415242	-0.415242
-0.001276	-0.000127	0.0	0.0
-0.005259	-0.000434	0.0	0.0
-0.025795	-0.002676	0.0	0.0
-0.088027	-0.006794	0.0	0.0
-0.070298	-0.013592	0.0	0.0
0.273425	0.057210	0.0	0.0
0.0	0.0	0.026123	0.0
0.0	0.0	0.119245	0.0
0.0	0.0	0.347927	0.0
0.0	0.0	0.244610	0.0
0.0	0.0	0.0	0.026123
0.0	0.0	0.0	0.119245
0.0	0.0	0.0	0.347927
0.0	0.0	0.0	0.244610
-0.013909	-0.025226	0.0	0.0
-0.055232	-0.117952	0.0	0.0
-0.220862	-0.308327	0.0	0.0
-0.175437	-0.036626	0.0	0.0
0.001276	-0.000127	0.0	0.0
0.005259	-0.000434	0.0	0.0
0.025795	-0.002676	0.0	0.0
0.088027	-0.006794	0.0	0.0
0.070298	-0.013592	0.0	0.0
-0.273425	0.057210	0.0	0.0
0.0	0.0	0.026123	0.0
0.0	0.0	0.119245	0.0
0.0	0.0	0.347927	0.0
0.0	0.0	0.244610	0.0
0.0	0.0	0.0	0.026123
0.0	0.0	0.0	0.119245
0.0	0.0	0.0	0.347927
0.0	0.0	0.0	0.244610
-0.013909	0.025226	0.0	0.0
-0.055232	0.117952	0.0	0.0
-0.220862	0.308327	0.0	0.0
-0.175437	0.036626	0.0	0.0
0.008112	0.008193	0.0	0.0
0.035312	0.035902	0.0	0.0
0.175410	0.178852	0.0	0.0
0.082417	0.225408	0.0	0.0
-0.008112	0.008193	0.0	0.0
-0.035312	0.035902	0.0	0.0
-0.175410	0.178852	0.0	0.0
-0.082417	0.225408	0.0	0.0

Table 27. Optimized MO's for ethylene

		$1a_{1g}$	$1b_{1u}$	$2a_{1g}$	$2b_{1u}$
	ε	-11.224061	-11.222397	-1.035978	-0.792829
C	1s6	-0.009445	-0.009451	-0.001952	-0.001480
	1s5	-0.037581	-0.037586	-0.008192	-0.006235
	1s4	-0.186477	-0.186626	-0.041465	-0.031477
	1s3	-0.430238	-0.430159	-0.133105	-0.102084
	1s2	-0.166479	-0.168634	-0.085076	-0.064981
	1s1	0.017173	0.023779	0.472205	0.369512
	2px4	0.0	0.0	0.0	0.0
	2px3	0.0	0.0	0.0	0.0
	2px2	0.0	0.0	0.0	0.0
	2px1	0.0	0.0	0.0	0.0
	2py4	0.0	0.0	0.0	0.0
	2py3	0.0	0.0	0.0	0.0
	2py2	0.0	0.0	0.0	0.0
	2py1	0.0	0.0	0.0	0.0
	2pz4	0.000195	0.000007	0.006155	-0.008705
	2pz3	-0.000639	0.000100	0.032727	-0.041356
	2pz2	-0.000451	0.001897	0.079152	-0.126161
	2pz1	-0.003147	0.007217	0.064256	-0.127217
C	1s6	-0.009445	0.009451	-0.001952	0.001480
	1s5	-0.037581	0.037586	-0.008192	0.006235
	1s4	-0.186477	0.186626	-0.041465	0.031477
	1s3	-0.430238	0.430159	-0.133105	0.102084
	1s2	-0.166479	0.168634	-0.085076	0.064981
	1s1	0.017173	-0.023779	0.472205	-0.369512
	2px4	0.0	0.0	0.0	0.0
	2px3	0.0	0.0	0.0	0.0
	2px2	0.0	0.0	0.0	0.0
	2px1	0.0	0.0	0.0	0.0
	2py4	0.0	0.0	0.0	0.0
	2py3	0.0	0.0	0.0	0.0
	2py2	0.0	0.0	0.0	0.0
	2py1	0.0	0.0	0.0	0.0
	2pz4	-0.000195	0.000007	-0.006155	-0.008705
	2pz3	0.000639	0.000100	-0.032727	-0.041356
	2pz2	0.000451	0.001897	-0.079152	-0.126161
	2pz1	0.003147	0.007217	-0.064256	-0.127217

$1b_{2u}$	$3a_{1g}$	$1b_{3g}$	$1b_{3u}$
-0.643512	-0.592480	-0.501664	-0.376087
0.0	0.000111	0.0	0.0
0.0	0.000530	0.0	0.0
0.0	0.002298	0.0	0.0
0.0	0.009199	0.0	0.0
0.0	-0.000729	0.0	0.0
0.0	-0.017035	0.0	0.0
0.0	0.0	0.0	0.020471
0.0	0.0	0.0	0.095503
0.0	0.0	0.0	0.301468
0.0	0.0	0.0	0.322623
0.017497	0.0	0.016464	0.0
0.079812	0.0	0.075389	0.0
0.259871	0.0	0.244000	0.0
0.148973	0.0	0.247477	0.0
0.0	-0.022436	0.0	0.0
0.0	-0.103893	0.0	0.0
0.0	-0.328422	0.0	0.0
0.0	-0.158645	0.0	0.0
0.0	0.000111	0.0	0.0
0.0	0.000530	0.0	0.0
0.0	0.002298	0.0	0.0
0.0	0.009199	0.0	0.0
0.0	-0.000729	0.0	0.0
0.0	-0.017035	0.0	0.0
0.0	0.0	0.0	0.020471
0.0	0.0	0.0	0.095503
0.0	0.0	0.0	0.301468
0.0	0.0	0.0	0.322623
0.017497	0.0	-0.016464	0.0
0.079812	0.0	-0.075389	0.0
0.259871	0.0	-0.244000	0.0
0.148973	0.0	-0.247477	0.0
0.0	0.022436	0.0	0.0
0.0	0.103893	0.0	0.0
0.0	0.328422	0.0	0.0
0.0	0.158645	0.0	0.0

Table 27. (Continued)

		$1a_{1g}$ (cont.)	$1b_{1u}$ (cont.)	$2a_{1g}$ (cont.)	$2b_{1u}$ (cont.)
H	1s4	0.000150	-0.000065	0.003333	-0.006358
	1s3	-0.000687	0.000253	0.016849	-0.026070
	1s2	-0.000812	0.001970	0.059540	-0.126339
	1s1	-0.002646	-0.002113	0.099601	-0.090193
H	1s4	0.000150	-0.000065	0.003333	-0.006358
	1s3	-0.000687	0.000253	0.016849	-0.026070
	1s2	-0.000812	0.001970	0.059540	-0.126339
	1s1	-0.002646	-0.002113	0.099601	-0.090193
H	1s4	0.000150	0.000065	0.003333	0.006358
	1s3	-0.000687	-0.000253	0.016849	0.026070
	1s2	-0.000812	-0.001970	0.059540	0.126339
	1s1	-0.002646	0.002113	0.099601	0.090193
H	1s4	0.000150	0.000065	0.003333	0.006358
	1s3	-0.000687	-0.000253	0.016849	0.026070
	1s2	-0.000812	-0.001970	0.059540	0.126339
	1s1	-0.002646	0.002113	0.099601	0.090193

$1b_{2u}$ (cont.)	$3a_{1g}$ (cont.)	$1b_{3g}$ (cont.)	$1b_{3u}$ (cont.)
0.006684	0.005394	-0.008098	0.0
0.027662	0.022575	-0.032458	0.0
0.136564	0.112415	-0.172883	0.0
0.097287	0.113917	-0.132920	0.0
-0.006684	0.005394	0.008098	0.0
-0.027662	0.022575	0.032458	0.0
-0.136564	0.112415	0.172883	0.0
-0.097287	0.113917	0.132920	0.0
-0.006684	0.005394	-0.008098	0.0
-0.027662	0.022575	-0.032458	0.0
-0.136564	0.112415	-0.172883	0.0
-0.097287	0.113917	-0.132920	0.0
0.006684	0.005394	0.008098	0.0
0.027662	0.022575	0.032458	0.0
0.136564	0.112415	0.172883	0.0
0.097287	0.113917	0.132920	0.0

Table 28. Optimized MO's for ethane

		$1a_{1g}$	$1a_{2u}$	$2a_{1g}$	$2a_{2u}$
	ε	-11.204600	-11.204253	-1.022719	-0.838759
C	1s6	0.009233	-0.009239	-0.001754	0.001538
	1s5	0.037227	-0.037200	-0.007426	0.006516
	1s4	0.186253	-0.186441	-0.038107	0.033454
	1s3	0.432236	-0.431590	-0.122043	0.107688
	1s2	0.165364	-0.168203	-0.081007	0.071608
	1s1	-0.017420	0.022382	0.447804	-0.400459
	2px4	0.0	0.0	0.0	0.0
	2px3	0.0	0.0	0.0	0.0
	2px2	0.0	0.0	0.0	0.0
	2px1	0.0	0.0	0.0	0.0
	2py4	0.0	0.0	0.0	0.0
	2py3	0.0	0.0	0.0	0.0
	2py2	0.0	0.0	0.0	0.0
	2py1	0.0	0.0	0.0	0.0
	2pz4	0.000081	0.000093	0.003195	0.006584
	2pz3	-0.000239	-0.000565	0.016391	0.031734
	2pz2	0.001263	0.001896	0.045681	0.092654
	2pz1	0.001617	0.002964	0.044190	0.080815
C	1s6	0.009233	0.009239	-0.001754	-0.001538
	1s5	0.037227	0.037200	-0.007426	-0.006516
	1s4	0.186253	0.186441	-0.038107	-0.033454
	1s3	0.432236	0.431590	-0.122043	-0.107688
	1s2	0.165364	0.168203	-0.081007	-0.071608
	1s1	-0.017420	-0.022382	0.447804	0.400459
	2px4	0.0	0.0	0.0	0.0
	2px3	0.0	0.0	0.0	0.0
	2px2	0.0	0.0	0.0	0.0
	2px1	0.0	0.0	0.0	0.0
	2py4	0.0	0.0	0.0	0.0
	2py3	0.0	0.0	0.0	0.0
	2py2	0.0	0.0	0.0	0.0
	2py1	0.0	0.0	0.0	0.0
	2pz4	-0.000081	0.000093	-0.003195	0.006584
	2pz3	0.000239	-0.000565	-0.016391	0.031734
	2pz2	-0.001263	0.001896	-0.045681	0.092654
	2pz1	-0.001617	0.002964	-0.044190	0.080815

$1e_u$	$1e_u$	$3a_{1g}$	$1e_g$	$1e_g$
-0.603830	-0.603824	-0.497987	-0.488212	-0.488131
0.0	0.0	0.000178	0.0	0.0
0.0	0.0	0.000737	0.0	0.0
0.0	0.0	0.003887	0.0	0.0
0.0	0.0	0.012153	0.0	0.0
0.0	0.0	0.010467	0.0	0.0
0.0	0.0	-0.059013	0.0	0.0
0.011996	0.012288	0.0	0.008274	-0.014926
0.053471	0.054783	0.0	0.037461	-0.067569
0.173438	0.177378	0.0	0.119710	-0.215981
0.113592	0.115728	0.0	0.094689	-0.170791
0.012306	-0.012014	0.0	0.014927	0.008276
0.054812	-0.053509	0.0	0.067568	0.037444
0.178430	-0.174554	0.0	0.215885	0.119737
0.117911	-0.115790	0.0	0.170788	0.094679
0.0	0.0	-0.022437	0.0	0.0
0.0	0.0	-0.100677	0.0	0.0
0.0	0.0	-0.331277	0.0	0.0
0.0	0.0	-0.229607	0.0	0.0
0.0	0.0	0.000178	0.0	0.0
0.0	0.0	0.000737	0.0	0.0
0.0	0.0	0.003887	0.0	0.0
0.0	0.0	0.012153	0.0	0.0
0.0	0.0	0.010467	0.0	0.0
0.0	0.0	-0.059013	0.0	0.0
0.011996	0.012288	0.0	-0.008274	0.014926
0.053471	0.054783	0.0	-0.037461	0.067569
0.173438	0.177378	0.0	-0.119710	0.215881
0.113592	0.115728	0.0	-0.094689	0.170791
0.012306	-0.012014	0.0	-0.014927	-0.008276
0.054812	-0.053509	0.0	-0.067568	-0.037444
0.178430	-0.174554	0.0	-0.215885	-0.119737
0.117911	-0.115790	0.0	-0.170788	-0.094679
0.0	0.0	0.022437	0.0	0.0
0.0	0.0	0.100677	0.0	0.0
0.0	0.0	0.331277	0.0	0.0
0.0	0.0	0.229607	0.0	0.0

Table 28. (Continued)

		$1a_{1g}$ (cont.)	$1a_{2u}$ (cont.)	$2a_{1g}$ (cont.)	$2a_{2u}$ (cont.)
H	1s4	-0.000139	0.000031	0.003485	-0.005002
	1s3	0.000587	-0.000046	0.016811	-0.020474
	1s2	0.000907	-0.002371	0.058108	-0.091637
	1s1	0.001923	-0.000207	0.089479	-0.095088
H	1s4	-0.000139	0.000031	0.003485	-0.005002
	1s3	0.000587	-0.000046	0.016811	-0.020474
	1s2	0.000907	-0.002371	0.058108	-0.091637
	1s1	0.001923	-0.000207	0.089479	-0.095088
H	1s4	-0.000139	0.000031	0.003485	-0.005002
	1s3	0.000587	-0.000046	0.016811	-0.020474
	1s2	0.000907	-0.002371	0.058108	-0.091637
	1s1	0.001923	-0.000207	0.089479	-0.095088
H	1s4	-0.000139	-0.000031	0.003485	0.005002
	1s3	0.000587	0.000046	0.016811	0.020474
	1s2	0.000907	0.002371	0.058108	0.091637
	1s1	0.001923	0.000207	0.089479	0.095088
H	1s4	-0.000139	-0.000031	0.003485	0.005002
	1s3	0.000587	0.000046	0.016811	0.020474
	1s2	0.000907	0.002371	0.058108	0.091637
	1s1	0.001923	0.000207	0.089479	0.095088
H	1s4	-0.000139	-0.000031	0.003485	0.005002
	1s3	0.000587	0.000046	0.016811	0.020474
	1s2	0.000907	0.002371	0.058108	0.091637
	1s1	0.001923	0.000207	0.089479	0.095088

$1e_u$ (cont.)	$1e_u$ (cont.)	$3a_{1g}$ (cont.)	$1e_g$ (cont.)	$1e_g$ (cont.)
0.005432	0.005588	0.003431	0.004378	-0.007892
0.020331	0.020882	0.012541	0.015996	-0.028883
0.106147	0.109519	0.069324	0.088033	-0.158716
0.092892	0.095714	0.077343	0.098122	-0.176944
0.002069	-0.007440	0.003431	0.004646	0.007735
0.007805	-0.027946	0.012541	0.017011	0.028322
0.039906	-0.144687	0.069324	0.093435	0.155562
0.034932	-0.126839	0.077343	0.104181	0.173465
-0.007501	0.001853	0.003431	-0.009023	0.000156
-0.028136	0.007064	0.012541	-0.033007	0.000562
-0.146054	0.035168	0.069324	-0.181468	0.003154
-0.127824	0.031125	0.077343	-0.202303	0.003479
0.007501	-0.001853	0.003431	-0.009023	0.000156
0.028136	-0.007064	0.012541	-0.033007	0.000562
0.146054	-0.035168	0.069324	-0.181468	0.003154
0.127824	-0.031125	0.077343	-0.202303	0.003479
-0.005432	-0.005588	0.003431	0.004378	-0.007892
-0.020331	-0.020882	0.012541	0.015996	-0.028883
-0.106147	-0.109519	0.069324	0.088033	-0.158716
-0.092892	-0.095714	0.077343	0.098122	-0.176944
-0.002069	0.007440	0.003431	0.004646	0.007735
-0.007805	0.027946	0.012541	0.017011	0.028322
-0.039906	0.144687	0.069324	0.093435	0.155562
-0.034932	0.126839	0.077343	0.104181	0.173465

Table 29. Optimized MO's for water

		$1a_1$	$2a_1$	$1b_2$	$3a_1$	$1b_1$
	ε	-20.533870	-1.356370	-0.715966	-0.564594	-0.500608
O	1s6	-0.014656	-0.002955	0.0	-0.001092	0.0
	1s5	-0.060204	-0.012955	0.0	-0.004801	0.0
	1s4	-0.306220	-0.067744	0.0	-0.025162	0.0
	1s3	-0.625625	-0.210001	0.0	-0.079604	0.0
	1s2	-0.160245	-0.017895	0.0	-0.004273	0.0
	1s1	0.016767	0.773400	0.0	0.338250	0.0
	2px4	0.001200	-0.008019	0.0	0.042321	0.0
	2px3	0.001372	-0.031343	0.0	0.204635	0.0
	2px2	-0.000074	-0.119263	0.0	0.456308	0.0
	2px1	-0.002415	0.048427	0.0	0.421102	0.0
	2py4	0.0	0.0	0.0	0.0	0.048539
	2py3	0.0	0.0	0.0	0.0	0.234639
	2py2	0.0	0.0	0.0	0.0	0.533374
	2py1	0.0	0.0	0.0	0.0	0.443381
	2pz4	0.0	0.0	0.038071	0.0	0.0
	2pz3	0.0	0.0	0.179450	0.0	0.0
	2pz2	0.0	0.0	0.429239	0.0	0.0
	2pz1	0.0	0.0	0.196777	0.0	0.0
H	1s4	0.000162	0.005583	-0.009566	-0.005130	0.0
	1s3	-0.000532	0.025070	-0.030582	-0.018964	0.0
	1s2	-0.000958	0.097266	-0.202902	-0.103140	0.0
	1s1	-0.002420	0.142851	-0.162491	0.009994	0.0
H	1s4	0.000162	0.005583	0.009566	-0.005130	0.0
	1s3	-0.000532	0.025070	0.030582	-0.018964	0.0
	1s2	-0.000958	0.097266	0.202902	-0.103140	0.0
	1s1	-0.002420	0.142851	0.162491	0.009994	0.0

Table 30. Optimized MO's for carbon monoxide

		1σ	2σ	3σ
	ε	-20.645691	-11.350878	-1.554903
C	1s6	0.000003	0.021508	0.002340
	1s5	-0.000020	0.090829	0.010666
	1s4	0.000100	0.420492	0.051253
	1s3	-0.000499	0.582854	0.126338
	1s2	0.000321	0.036853	-0.122006
	1s1	0.007108	0.001882	-0.329654
	2px4	0.0	0.0	0.0
	2px3	0.0	0.0	0.0
	2px2	0.0	0.0	0.0
	2px1	0.0	0.0	0.0
	2py4	0.0	0.0	0.0
	2py3	0.0	0.0	0.0
	2py2	0.0	0.0	0.0
	2py1	0.0	0.0	0.0
	2pz4	-0.000041	0.000879	-0.008351
	2pz3	-0.000045	0.003252	-0.046066
	2pz2	0.002407	-0.000219	-0.152273
	2pz1	0.004536	-0.000074	-0.125949
C	1s6	0.014041	-0.000010	0.002661
	1s5	0.056113	-0.000023	0.011380
	1s4	0.282803	-0.000235	0.058313
	1s3	0.618480	-0.000228	0.188364
	1s2	0.199485	-0.000976	0.055627
	1s1	-0.023535	0.001750	-0.670458
	2px4	0.0	0.0	0.0
	2px3	0.0	0.0	0.0
	2px2	0.0	0.0	0.0
	2px1	0.0	0.0	0.0
	2py4	0.0	0.0	0.0
	2py3	0.0	0.0	0.0
	2py2	0.0	0.0	0.0
	2py1	0.0	0.0	0.0
	2pz4	-0.001025	-0.000271	0.013327
	2pz3	-0.001878	0.000684	0.050850
	2pz2	0.000481	-0.002581	0.185384
	2pz1	0.004516	0.000165	-0.055814

4σ	$1\pi_x$	$1\pi_y$	5σ
-0.777436	-0.636226	-0.636226	-0.548747
0.002545	0.0	0.0	-0.002851
0.012072	0.0	0.0	-0.012474
0.055691	0.0	0.0	-0.064188
0.153659	0.0	0.0	-0.149434
-0.181229	0.0	0.0	0.084177
-0.082834	0.0	0.0	0.832000
0.0	-0.011544	0.0	0.0
0.0	-0.054524	0.0	0.0
0.0	-0.210335	0.0	0.0
0.0	-0.187700	0.0	0.0
0.0	0.0	-0.011544	0.0
0.0	0.0	-0.054524	0.0
0.0	0.0	-0.210335	0.0
0.0	0.0	-0.187700	0.0
-0.004613	0.0	0.0	-0.016920
-0.021828	0.0	0.0	-0.093264
-0.094005	0.0	0.0	-0.301354
0.184748	0.0	0.0	-0.218163
-0.001572	0.0	0.0	0.000165
-0.006734	0.0	0.0	0.000638
-0.034606	0.0	0.0	0.003688
-0.113471	0.0	0.0	0.010163
-0.031800	0.0	0.0	0.009364
0.445541	0.0	0.0	-0.083859
0.0	-0.036399	0.0	0.0
0.0	-0.167896	0.0	0.0
0.0	-0.430725	0.0	0.0
0.0	-0.372092	0.0	0.0
0.0	0.0	-0.036399	0.0
0.0	0.0	-0.167896	0.0
0.0	0.0	-0.430725	0.0
0.0	0.0	-0.372092	0.0
0.032763	0.0	0.0	0.018311
0.156166	0.0	0.0	0.082688
0.370476	0.0	0.0	0.222215
0.400828	0.0	0.0	0.184413

Table 31. Optimized MO's for carbon dioxide

	$1\sigma_u$	$1\sigma_g$	$2\sigma_g$	$3\sigma_g$	$2\sigma_u$
ε	-20.632066	-20.631673	-11.492428	-1.557367	-1.514104
C 1s6	0.0	-0.000001	0.016860	0.002458	0.0
1s5	0.0	0.000002	0.068882	0.010896	0.0
1s4	0.0	-0.000032	0.336194	0.053389	0.0
1s3	0.0	0.000066	0.617544	0.156711	0.0
1s2	0.0	-0.001703	0.124678	-0.023675	0.0
1s1	0.0	0.010250	-0.011339	-0.571576	0.0
2px4	0.0	0.0	0.0	0.0	0.0
2px3	0.0	0.0	0.0	0.0	0.0
2px2	0.0	0.0	0.0	0.0	0.0
2px1	0.0	0.0	0.0	0.0	0.0
2py4	0.0	0.0	0.0	0.0	0.0
2py3	0.0	0.0	0.0	0.0	0.0
2py2	0.0	0.0	0.0	0.0	0.0
2py1	0.0	0.0	0.0	0.0	0.0
2pz4	0.000056	0.0	0.0	0.0	0.017075
2pz3	-0.000717	0.0	0.0	0.0	0.077698
2pz2	0.005162	0.0	0.0	0.0	0.266691
2pz1	0.007554	0.0	0.0	0.0	0.202515

$4\sigma_g$	$3\sigma_u$	$1\pi_{uy}$	$1\pi_{ux}$	$1\pi_{gx}$
-0.758907	-0.731710	-0.728992	-0.728992	-0.526908
0.001970	0.0	0.0	0.0	0.0
0.009536	0.0	0.0	0.0	0.0
0.042112	0.0	0.0	0.0	0.0
0.147873	0.0	0.0	0.0	0.0
-0.084597	0.0	0.0	0.0	0.0
-0.107110	0.0	0.0	0.0	0.0
0.0	0.0	0.0	-0.018926	0.0
0.0	0.0	0.0	-0.081518	0.0
0.0	0.0	0.0	-0.296713	0.0
0.0	0.0	0.0	-0.212951	0.0
0.0	0.0	-0.018926	0.0	0.0
0.0	0.0	-0.081518	0.0	0.0
0.0	0.0	-0.296713	0.0	0.0
0.0	0.0	-0.212951	0.0	0.0
0.0	0.018510	0.0	0.0	0.0
0.0	0.081580	0.0	0.0	0.0
0.0	0.309082	0.0	0.0	0.0
0.0	-0.229555	0.0	0.0	0.0

Table 31. (Continued)

	$1\sigma_u$ (cont.)	$1\sigma_g$ (cont.)	$2\sigma_g$ (cont.)	$3\sigma_g$ (cont.)	$2\sigma_u$ (cont.)
O 1s6	-0.009935	0.009932	-0.000007	0.001798	0.001925
1s5	-0.039680	0.039705	-0.000024	0.007606	0.008332
1s4	-0.200085	0.199973	-0.000144	0.039485	0.042057
1s3	-0.437064	0.437617	-0.000325	0.125273	0.138600
1s2	-0.141944	0.140123	-0.000278	0.043680	0.031523
1s1	0.018990	-0.014767	0.002252	-0.466675	-0.457364
2px4	0.0	0.0	0.0	0.0	0.0
2px3	0.0	0.0	0.0	0.0	0.0
2px2	0.0	0.0	0.0	0.0	0.0
2px1	0.0	0.0	0.0	0.0	0.0
2py4	0.0	0.0	0.0	0.0	0.0
2py3	0.0	0.0	0.0	0.0	0.0
2py2	0.0	0.0	0.0	0.0	0.0
2py1	0.0	0.0	0.0	0.0	0.0
2pz4	-0.000786	0.000917	-0.000032	-0.008444	-0.007716
2pz3	-0.001946	0.001309	0.000653	-0.028598	-0.034417
2pz2	0.001673	0.000266	-0.000093	-0.124106	-0.101051
2pz1	0.002230	-0.003785	0.000896	0.056367	0.025207
O 1s6	0.009935	0.009932	-0.000007	0.001798	-0.001925
1s5	0.039680	0.039705	-0.000024	0.007606	-0.008332
1s4	0.200085	0.199973	-0.000144	0.039485	-0.042057
1s3	0.437064	0.437617	-0.000325	0.125273	-0.138600
1s2	0.141944	0.140123	-0.000278	0.043680	-0.031523
1s1	-0.018990	-0.014767	0.002252	-0.466675	0.457364
2px4	0.0	0.0	0.0	0.0	0.0
2px3	0.0	0.0	0.0	0.0	0.0
2px2	0.0	0.0	0.0	0.0	0.0
2px1	0.0	0.0	0.0	0.0	0.0
2py4	0.0	0.0	0.0	0.0	0.0
2py3	0.0	0.0	0.0	0.0	0.0
2py2	0.0	0.0	0.0	0.0	0.0
2py1	0.0	0.0	0.0	0.0	0.0
2pz4	-0.000786	-0.000917	0.000032	0.008444	-0.007716
2pz3	-0.001946	-0.001309	-0.000653	0.028598	-0.034417
2pz2	0.001673	-0.000266	0.000093	0.124106	-0.101051
2pz1	0.002230	0.003785	-0.000896	-0.056367	0.025207

$4\sigma_g$ (cont.)	$3\sigma_u$ (cont.)	$1\pi_{uy}$ (cont.)	$1\pi_{ux}$ (cont.)	$1\pi_{gx}$ (cont.)
-0.001341	-0.000958	0.0	0.0	0.0
-0.005628	-0.004126	0.0	0.0	0.0
-0.029636	-0.021078	0.0	0.0	0.0
-0.094124	-0.069856	0.0	0.0	0.0
-0.036546	-0.018085	0.0	0.0	0.0
0.434617	0.263503	0.0	0.0	0.0
0.0	0.0	0.0	-0.022349	0.028866
0.0	0.0	0.0	-0.102987	0.137135
0.0	0.0	0.0	-0.274255	0.346942
0.0	0.0	0.0	-0.200095	0.370902
0.0	0.0	-0.022349	0.0	0.0
0.0	0.0	-0.102987	0.0	0.0
0.0	0.0	-0.274255	0.0	0.0
0.0	0.0	-0.200095	0.0	0.0
-0.020717	-0.023960	0.0	0.0	0.0
-0.098324	-0.117372	0.0	0.0	0.0
-0.235989	-0.272899	0.0	0.0	0.0
-0.291410	-0.267165	0.0	0.0	0.0
-0.001341	0.000958	0.0	0.0	0.0
-0.005628	0.004126	0.0	0.0	0.0
-0.029636	0.021078	0.0	0.0	0.0
-0.094124	0.069856	0.0	0.0	0.0
-0.036546	0.018085	0.0	0.0	0.0
0.434617	-0.263503	0.0	0.0	0.0
0.0	0.0	0.0	-0.022349	-0.028866
0.0	0.0	0.0	-0.102987	-0.137135
0.0	0.0	0.0	-0.274255	-0.346942
0.0	0.0	0.0	-0.200095	-0.370902
0.0	0.0	-0.022349	0.0	0.0
0.0	0.0	-0.102987	0.0	0.0
0.0	0.0	-0.274255	0.0	0.0
0.0	0.0	-0.200095	0.0	0.0
0.020717	-0.023960	0.0	0.0	0.0
0.098324	-0.117372	0.0	0.0	0.0
0.235989	-0.272899	0.0	0.0	0.0
0.291410	-0.267165	0.0	0.0	0.0

Table 31. (Continued)

	$1\pi_{gy}$		$1\pi_{gy}$ (cont.)
ε	-0.526908		
C 1s6	0.0	O 1s6	0.0
1s5	0.0	1s5	0.0
1s4	0.0	1s4	0.0
1s3	0.0	1s3	0.0
1s2	0.0	1s2	0.0
1s1	0.0	1s1	0.0
2px4	0.0	2px4	0.0
2px3	0.0	2px3	0.0
2px2	0.0	2px2	0.0
2px1	0.0	2px1	0.0
2py4	0.0	2py4	0.028866
2py3	0.0	2py3	0.137135
2py2	0.0	2py2	0.346942
2py1	0.0	2py1	0.370902
2pz4	0.0	2pz4	0.0
2pz3	0.0	2pz3	0.0
2pz2	0.0	2pz2	0.0
2pz1	0.0	2pz1	0.0
		O 1s6	0.0
		1s5	0.0
		1s4	0.0
		1s3	0.0
		1s2	0.0
		1s1	0.0
		2px4	0.0
		2px3	0.0
		2px2	0.0
		2px1	0.0
		2py4	-0.028866
		2py3	-0.137135
		2py2	-0.346942
		2py1	-0.370902
		2pz4	0.0
		2pz3	0.0
		2pz2	0.0
		2pz1	0.0

Table 32. Optimized MO's for formaldehyde

		$1a_1$	$2a_1$	$3a_1$	$4a_1$
	ε	-20.562480	-11.346069	-1.433331	-0.872135
C	1s6	-0.000001	0.013137	0.001401	-0.001991
	1s5	0.000008	0.053052	0.005986	-0.008541
	1s4	-0.000046	0.265847	0.030430	-0.043412
	1s3	0.000186	0.612272	0.097824	-0.142037
	1s2	-0.001263	0.231327	0.055779	-0.084969
	1s1	0.004060	-0.028891	-0.365023	0.526198
	2px4	0.0	0.0	0.0	0.0
	2px3	0.0	0.0	0.0	0.0
	2px2	0.0	0.0	0.0	0.0
	2px1	0.0	0.0	0.0	0.0
	2py4	0.0	0.0	0.0	0.0
	2py3	0.0	0.0	0.0	0.0
	2py2	0.0	0.0	0.0	0.0
	2py1	0.0	0.0	0.0	0.0
	2pz4	-0.000100	0.000087	-0.009980	-0.010885
	2pz3	0.000189	0.001676	-0.056472	-0.049345
	2pz2	0.002041	-0.002982	-0.135988	-0.155968
	2pz1	0.003633	0.002704	-0.128854	-0.141361
O	1s6	0.015094	-0.000006	0.002824	0.001294
	1s5	0.060557	-0.000017	0.012129	0.005550
	1s4	0.303438	-0.000150	0.062200	0.028612
	1s3	0.621118	-0.000137	0.193013	0.089338
	1s2	0.167461	-0.001138	0.022743	0.011317
	1s1	-0.018497	0.004596	-0.685640	-0.354096
	2px4	0.0	0.0	0.0	0.0
	2px3	0.0	0.0	0.0	0.0
	2px2	0.0	0.0	0.0	0.0
	2px1	0.0	0.0	0.0	0.0
	2py4	0.0	0.0	0.0	0.0
	2py3	0.0	0.0	0.0	0.0
	2py2	0.0	0.0	0.0	0.0
	2py1	0.0	0.0	0.0	0.0
	2pz4	-0.001052	0.000046	0.010963	-0.008710
	2pz3	-0.001742	-0.000525	0.047122	-0.046632
	2pz2	0.000637	-0.001924	0.151314	-0.089691
	2pz1	0.002900	-0.003728	-0.042754	-0.117952
H	1s4	-0.000033	-0.000157	-0.000809	0.007629
	1s3	0.000152	0.000744	-0.007464	0.035530
	1s2	-0.000340	0.001802	-0.011030	0.165193
	1s1	0.001499	0.003212	-0.074150	0.101027
H	1s4	-0.000033	-0.000157	-0.000809	0.007629
	1s3	0.000152	0.000744	-0.007464	0.035530
	1s2	-0.000340	0.001802	-0.011030	0.165193
	1s1	0.001499	0.003212	-0.074150	0.101027

$1b_2$	$5a_1$	$1b_1$	$2b_2$
-0.707896	-0.643223	-0.537169	-0.442283
0.0	-0.000244	0.0	0.0
0.0	-0.001268	0.0	0.0
0.0	-0.005059	0.0	0.0
0.0	-0.022739	0.0	0.0
0.0	0.007620	0.0	0.0
0.0	0.004885	0.0	0.0
0.023672	0.0	0.0	-0.011154
0.105192	0.0	0.0	-0.053735
0.348719	0.0	0.0	-0.165428
0.198572	0.0	0.0	-0.066487
0.0	0.0	0.019641	0.0
0.0	0.0	0.088964	0.0
0.0	0.0	0.289911	0.0
0.0	0.0	0.214122	0.0
0.0	0.021018	0.0	0.0
0.0	0.097288	0.0	0.0
0.0	0.314051	0.0	0.0
0.0	-0.113403	0.0	0.0
0.0	0.001131	0.0	0.0
0.0	0.004834	0.0	0.0
0.0	0.025076	0.0	0.0
0.0	0.078369	0.0	0.0
0.0	0.010535	0.0	0.0
0.0	-0.331617	0.0	0.0
0.023149	0.0	0.0	0.037213
0.112966	0.0	0.0	0.184449
0.281869	0.0	0.0	0.450602
0.157860	0.0	0.0	0.418884
0.0	0.0	0.032420	0.0
0.0	0.0	0.157629	0.0
0.0	0.0	0.397696	0.0
0.0	0.0	0.320952	0.0
0.0	-0.034325	0.0	0.0
0.0	-0.170646	0.0	0.0
0.0	-0.399157	0.0	0.0
0.0	-0.325814	0.0	0.0
-0.007359	-0.003841	0.0	0.008186
-0.037138	-0.019298	0.0	0.028528
-0.159030	-0.086052	0.0	0.213550
-0.076167	-0.175102	0.0	0.207776
0.007359	-0.003841	0.0	-0.008186
0.037138	-0.019298	0.0	-0.028528
0.159030	-0.086052	0.0	-0.213550
0.076167	-0.175102	0.0	-0.207776

Table 33. Cartesian coordinates of the atomic nuclei

Molecule[a]	Atom Symbol[b]			
H_2	H	0	0	0
	H	0	0	1.4
CH_4	C	0	0	0
	H	1.687616783119517	0	-1.193325271388037
	H	-1.687616783119517	0	-1.193325271388037
	H	0	1.687616783119517	1.193325271388037
	H	0	-1.687616783119517	1.193325271388037
C_2H_2	C	0	0	0
	C	0	0	2.279
	H	0	0	-2.005
	H	0	0	4.284
C_2H_4	C	0	0	0
	C	0	0	2.517
	H	0	1.733	3.608
	H	0	-1.733	3.608
	H	0	-1.733	-1.091
	H	0	1.733	-1.091

[a]Coordinates correspond to the experimental geometries of Reference (40) and Table 41 for all molecules except C_3H_4 and C_3O_2. For C_3H_4 the theoretical equilibrium geometry of Table 41 is used. For C_3O_2 the linear geometry with $r(C-O)=1.20\text{Å}$ and $r(C-C)=1.30\text{Å}$ of Reference (45) is used.

[b]Atom symbols for each molecule occur in the same order as those given in Tables 24-32.

Table 33. (Continued)

Molecule[a]	Atom Symbol[b]			
C_2H_6	C	0	0	-1.44935
	C	0	0	1.44935
	H	1.9506	0	-2.12835
	H	-0.9753	1.689269152621925	-2.12835
	H	-0.9753	-1.689269152621925	-2.12835
	H	0.9753	1.689269152621925	2.12835
	H	-1.9506	0	2.12835
	H	0.9753	-1.689269152621925	2.12835
H_2O	O	1.10713	0	0
	H	0	0	-1.4304
	H	0	0	1.4304
CO	C	0	0	0
	O	0	0	2.1317
CO_2	C	0	0	0
	O	0	0	-2.1954
	O	0	0	2.1954
H_2CO	C	0	0	0
	O	0	0	2.2732
	H	-1.7692	0	-1.0948
	H	1.7692	0	-1.0948
C_3H_4	C	0	0	-2.7626
	C	0	0	0
	C	0	0	2.252
	H	1.891490	0	-3.49625
	H	-0.945745	1.638073391004227	-3.49625
	H	-0.945745	-1.638073391004227	-3.49625
	H	0	0	4.215
C_3O_2	C	0	0	0
	C	0	0	-2.4565
	C	0	0	2.4565
	O	0	0	-4.7241
	O	0	0	4.7241

with reference to a right-handed external coordinate system. Wherever possible, the carbon and oxygen atoms lie on the z-axis. The labelling of the atoms of Tables 24-32 and 33 is the same. The integrals are calculated with respect to coordinate systems centered at the nuclei and displaced parallel to the above external coordinate system with no rotations. Thus, the positive lobes of all p-type atomic orbitals point in the same direction.

Comparison of standard bases with other calculations

The energies for the optimized standard bases are compared with other calculations in Table 21. The third column of this table contains the energies published by Hehre et al. (31,42), for all molecules except CO and C_3O_2, using a basis with six s-primitives and 3 p-primitives of the type C(6;3,3;3), O(6;3,3;3), H(3) contracted to a minimal basis. The primitives were obtained by fitting a minimal basis of atomic Slater-type orbitals followed by scaling the valence orbitals in small molecules. From these scaling parameters a standard set was derived for use in larger molecules. For CO and C_3O_2, larger unoptimized primitive bases of C(7;7,7;3) and O(7;7,7;3) were used by Hopkinson et al. (43) and Sabin and Kim (44). Uncontracted and contracted [5,2;3] bases were used for CO and C_3O_2, respectively. The fourth column of Table 21 contains the energies published by Ditchfield et al. (32), and Hehre et al. (42) using a basis of 8 s-primitives and 4 p-primitives of the type C(8;4,4;4), O(8;4,4;4), H(4) contracted to C[1,2;2], O[1,2;2], H[2]. The primitives were obtained by atomic SCF calculations followed by scaling of the

valence orbital contracted functions in all molecular calculations. It is seen that the energies for our standard bases are all substantially better than the minimal basis energies given in the third column of Table 21. The poorer performance of the bases of Hehre et al. (31) is not due to the number of primitives, but to the contraction to a minimal basis. However, the energies of the standard bases are all higher than those for the bases of the fourth column of Table 21 by 0.002 to 0.1 Hartree. These energies are sufficiently close so that we may question the need for a basis with eight primitives.

Relations governing optimal exponents for standard bases

The final, optimal parameter values for the standard bases of the prototype molecules are plotted in Figure 9. Also, shown are optimal values for methyl acetylene and carbon suboxide. We shall return to calculations on these molecules in the next two sections, since the methods for optimizing the even-tempered parameters are somewhat modified. Figure 9 shows that the optimal parameter values lie close to the following straight lines:

$$\text{Hs: } \ln\beta_o = -0.23\ \ln\alpha_o + 0.71,$$

$$\text{Cs: } \ln\beta_o = -0.13\ \ln\alpha_o + 1.12,$$

$$\text{Cp: } \ln\beta_1 = -0.12\ \ln\alpha_1 + 0.96,$$

$$\text{Os: } \ln\beta_o = -0.13\ \ln\alpha_o + 1.19,$$

$$\text{Op: } \ln\beta_1 = -0.17\ \ln\alpha_1 + 0.90.$$

The variation of α_ℓ from molecule to molecule is greater than β_ℓ showing the importance of scaling in molecular calculations. Moreover, a

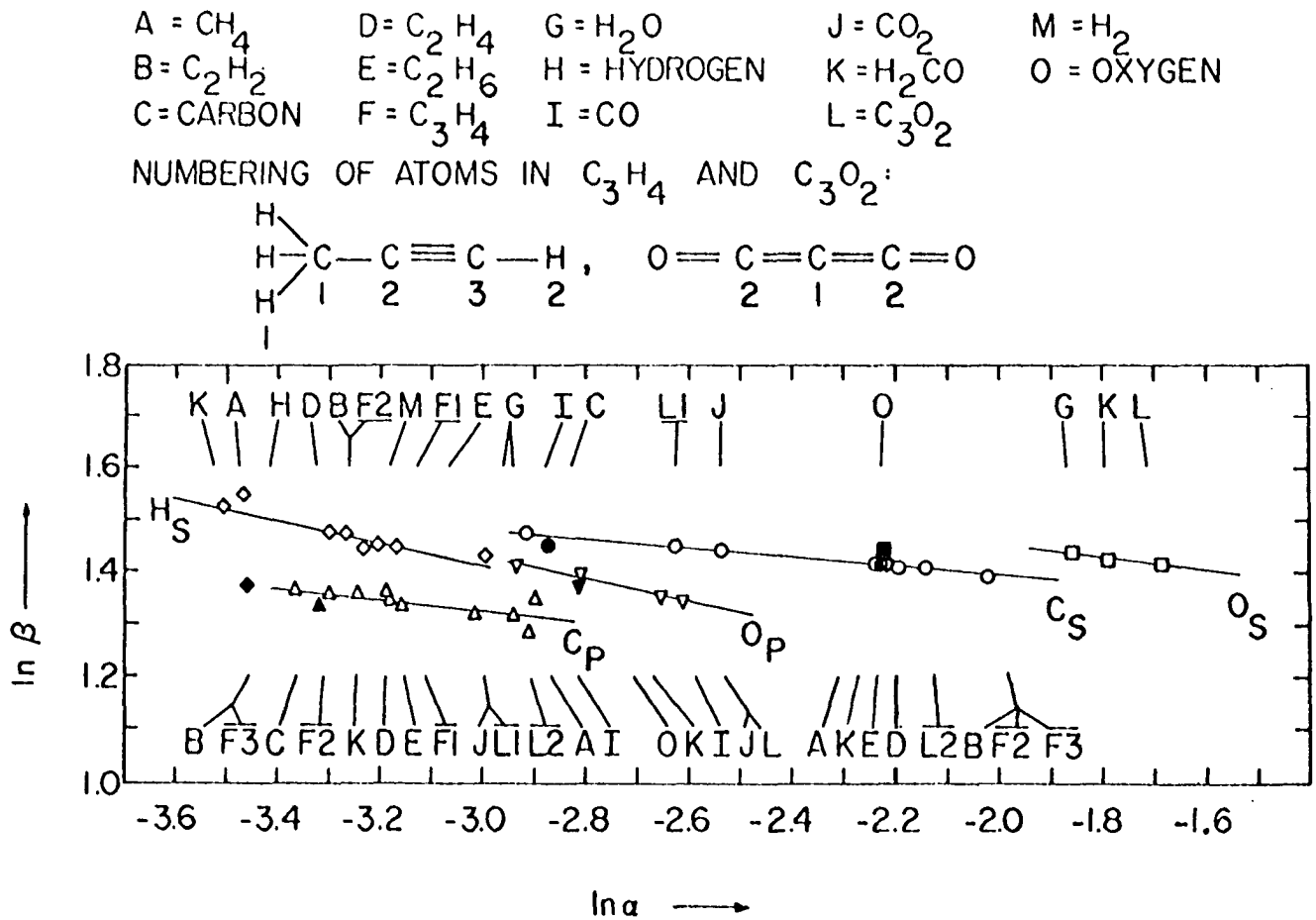

Figure 9. Optimal even-tempered parameter values for the standard bases

comparison of the fitting and optimal parameter values shows that, in general, the atomic orbitals spatially contract relative to the atoms.

These results are of great usefulness for easy optimizations not only in larger molecules containing the same atoms and similar bonds found in the prototypes, but also in molecules containing different atoms. Since for the majority of molecules optimal $(\ln\alpha_\ell, \ln\beta_\ell)$- points of a particular atom and orbitals lie very nearly on the straight line indicated in Figure 9, the most effective energy lowering is achieved by searching first along this line, using optimized parameters from related molecules as starting values. For some molecules the indicated atomic fitting values are closer to the optimal values. Nonetheless, they would be poorer starting values because of the uncertainty in the initial direction which could substantially increase the number of search directions. Once the lines of Figure 9 have been searched, additional, smaller refinements in the energy are made by searching other lines along which $\ln\alpha_\ell$ and $\ln\beta_\ell$ also vary oppositely.

Calculation of larger bases

In order to assess the quality of the standard bases, C(6;4), O(6;4), H(4), more accurate calculations were carried out on the small molecules C_2H_2 and C_2H_4, using bases C(8;5,5;6), H(5) contracted to C[3;1,2;2], H[3] for C_2H_4 and C(10;7,7;6), H(5) contracted to C[4;2,2;2], H[2] for C_2H_2. For these bases, the values of the α and β parameters determined from the pseudo-scaling procedure of Chapter II and quoted in Table 17 as "initial parameters" were very close to the optimal molecular values quoted in Table 18. This fact indicates the effectiveness of the

pseudo-scaling procedure. In this context it is also noteworthy that the optimal α_ℓ values lie inside the scaling ranges indicated in Table 17, even though β_ℓ changed slightly. For example, the ratio $\alpha_1(\text{opt})/\beta_1(\text{fitting})$ for the carbon 2p-orbital in C_2H_4 is 0.88. The minimum energies given in Table 20 were described earlier. The differences between these energies and the initial energies computed with the pseudo-scaled α_ℓ and β_ℓ values are 0.003 Hartree for C_2H_4 and 0.0003 Hartree for C_2H_2.

The minimization procedure started with the atomic pseudo-scaling α_ℓ and β_ℓ values. The first search direction was chosen parallel to the lines given in Figure 9. The second search direction was taken at 135° from the $(\ln\alpha_\ell)$-axis instead of perpendicular to the initial direction as before. Looser final parameter and energy criteria of 5×10^{-3} and 10^{-4} were used. However, the same initial stepsizes and criteria, which were used previously, were retained.

Construction of MOCETGAO's from Fully Optimized Molecular Orbitals of Prototype Molecules

In molecules larger than the prototypes and in routine calculations, it would be too time consuming to use all 6 s-primitives and 4 p-primitives as independent basis functions for the LCAO-MO-SCF procedure. Rather, experience has shown that results of almost equal quality can be obtained with a fewer number of contracted AO's which are fixed superpositions of primitives. Various schemes have been used in the past for the construction of such contracted AO's. One of these approaches was described in detail in Chapter II for constructing bases of PSCETGAO's. In contrast, the principal objective of the present section is the

determination of optimal contracted AO's in the molecular context. It is for this reason that calculations with noncontracted standard bases were made first as discussed in the preceding section. We shall now describe the derivation of optimal contracted standard bases from these uncontracted calculations. These contracted bases will be called MOCETGAO (molecular optimized contracted even-tempered Gaussian atomic orbital) bases.

In the following, the MOCETGAO's are obtained for each of the prototype molecules of the previous section with the aim of constructing optimal standard bases of maximum flexibility and transferability.

The molecular density matrix, corresponding to the minimum of the total molecular energy, contains the information concerning the MO's expanded in terms of the optimized primitive Gaussian basis. Using only the expansions of the occupied MO's in terms of the primitive Gaussians as given in Tables 24-32,

$$u_\nu = \sum_{A\,\ell\,m\,a} g(Aa\ell m|\underset{\sim}{r})\, C(Aa\ell m|\nu), \tag{30}$$

the total density matrix has the form

$$\rho(\underset{\sim}{r}|\underset{\sim}{r}') = 2\sum_\nu u_\nu(\underset{\sim}{r})\, u_\nu(\underset{\sim}{r}')$$

$$= \sum_{A\,B\,\ell\,\ell'\,m\,m'\,a\,b} g(Aa\ell m|\underset{\sim}{r})g(Bb\ell'm'|\underset{\sim}{r}')p(Aa\ell m|Bb\ell'm') \tag{31}$$

where

$$P(Aa\ell m|Bb\ell'm') = 2\sum_\nu C(Aa\ell m|\nu)\, C(Bb\ell'm'|\nu). \tag{32}$$

For the present purpose, we take all terms from Equation (31) which contain primitives from one atom A only. They form a subdensity matrix of the form

$$\rho_A(\underset{\sim}{r}|\underset{\sim}{r}') = \sum_{\ell,\ell'} \sum_{m,m'} \sum_{a,b} g(Aa\ell m|\underset{\sim}{r}) g(Ab\ell' m'|\underset{\sim}{r}') \; p(Aa\ell m|Ab\ell' m') \; . \qquad (32')$$

Since we wish to obtain contracted orbitals that are independent of m, we next form the spherically-projected, local density matrix,

$$\rho_{A,\ \text{spherical}} = \sum_{\ell} \{ \sum_{a,b} p(Aa\ell|Ab\ell) \; [\sum_{m} g(Aa\ell m) g(Ab\ell m)] \} \qquad (33)$$

where $p(Aa\ell|Ab\ell)$ is the average value of the elements $p(Aa\ell m|Ab\ell m)$, defined by

$$p(Aa\ell|Ab\ell) = \frac{1}{2\ell+1} \sum_{m} p(Aa\ell m|Ab\ell m), \qquad (34)$$

$$p(Aa\ell m|Ab\ell m) = 2\Sigma C(Aa\ell m|\nu) \; C(Ab\ell m|\nu). \qquad (34')$$

The same matrices are obtained by fragmenting each occupied MO into its atomic components and then forming local spherical density matrices from these atomic fragments. For each matrix, the elements are computed from Equations (34) and (34') by using all MO coefficients associated with the same set of primitive Gaussians.

In order to obtain MOCETGAO's, we seek those superpositions of primitives which allow the construction of the matrix of Equation (34) in the most efficient manner. To this end, the matrix is diagonalized separately

for each value of ℓ. Each matrix may then be expressed in terms of the eigenvalues $\lambda_k(\ell)$ and the elements of the orthogonal, diagonalizing matrix T,

$$p(Aa\ell|Ab\ell) = \sum_k \lambda_k(\ell)\ T_{ak}(\ell)T_{bk}(\ell). \qquad (35)$$

Substitution in Equation (33) gives

$$\rho_{A,\ \text{spherical}} = \sum_{\ell}\sum_{k} \lambda_k\ (\ell)\ [\sum_m \varphi_k(A\ell m)\varphi_k(A\ell m)] \qquad (36)$$

with the contracted AO's

$$\varphi_k(A\ell m) = \sum_a g(Aa\ell M)\ T_{ak}(\ell) \quad . \qquad (36')$$

If the eigenvalues $\lambda_k(\ell)$ are ordered according to decreasing magnitude, the contributions to Equation (36) decrease in importance as k increases. The desired MOCETGAO's are those AO's defined by Equation (36') which are required for adequate convergence of the sum over k. These MOCETGAO's and the eigenvalues λ_k are given in Table 34. The carbon s-type MOCETGAO's, φ_5 (s) and φ_6(s), and the p-type MOCETGAO, φ_4 (p), are omitted because their eigenvalues are always less than 10^{-10} and 10^{-7}, respectively.

In order to test whether MOCETGAO's represent adequate reduced bases for molecular calculations, complete LCAO-MO-SCF calculations were performed with these contracted basis functions. Table 35 lists the differences between the molecular energies obtained by this approach and the exact values of Table 21. For the basis consisting of the three most

Table 34. MOCETGAO bases and eigenvalues for the prototype molecules

H_2 MOCETGAO's

	0.704135	-0.702242	-0.025388
	0.694545	0.711938	-0.025043
	0.143191	0.0	-0.005163
	0.036033	0.0	0.999351
λ_k	1.56D-01	1.39D-17	1.08D-19

CH_4 MOCETGAO's

Carbon s-orbitals

	-0.502148	0.861423	0.063990	-0.008019
	0.305231	0.101807	0.936999	-0.026100
	0.743582	0.441406	-0.343386	-0.065947
	0.312430	0.224805	0.004203	-0.030077
	0.062562	0.045572	0.002457	0.996996
	0.015520	0.011554	-0.000001	0.000001
λ_k	6.21D-01	3.00D-01	1.45D-11	3.77D-14

Carbon p-orbitals

	0.650622	0.758943	0.025480
	0.726128	-0.612815	-0.305299
	0.215469	-0.216857	0.951916
	0.054798	-0.037908	0.0
λ_k	1.88D-01	2.93D-10	2.10D-12

Hydrogen s-orbitals

	0.671928	0.508511	-0.412987
	0.726061	-0.595297	0.273345
	0.143251	0.618413	0.664157
	0.028765	0.067844	-0.560018
λ_k	4.33D-01	4.58D-05	9.12D-08

Table 34. (Continued)

C_2H_2 MOCETGAO's

Carbon s-orbitals

	-0.382045	0.917180	0.087403	-0.071996
	0.411832	0.063699	0.834042	-0.361365
	0.768536	0.351256	-0.494238	-0.203462
	0.299684	0.173167	0.227682	0.892062
	0.061077	0.035586	0.021506	0.155822
	0.015724	0.009452	0.012709	0.052735
λ_k	5.88D-01	2.18D-01	2.24D-05	2.00D-07

Carbon p-orbitals

0.519716	0.854310	0.006231	
0.804763	-0.486981	-0.337688	
0.280217	-0.176818	0.935348	
0.061068	-0.041706	0.105132	
λ_k	2.02D-01	9.78D-03	3.41D-04

Hydrogen s-orbitals

0.779583	-0.626291	0.002818	
0.613549	0.762757	-0.197213	
0.122562	0.157017	0.979372	
0.028021	0.036146	-0.043918	
λ_k	1.53D-01	1.45D-02	4.10D-07

Table 34. (Continued)

C_2H_4 MOCETGAO's

Carbon s-orbitals

	-0.483592	0.871806	0.062866	-0.046089
	0.323379	0.102915	0.921469	-0.187016
	0.749514	0.425242	-0.379379	-0.336193
	0.309332	0.215626	0.054728	0.883566
	0.062175	0.043729	-0.003294	0.255921
	0.015525	0.011202	0.002800	0.060753
λ_k	6.18D-01	2.85D-01	2.77D-05	6.90D-09

Carbon p-orbitals

	0.609164	0.793038	-0.003143
	0.754633	-0.580834	-0.302859
	0.238348	-0.179245	0.949665
	0.051367	-0.039937	0.080015
λ_k	2.01D-01	5.14D-03	2.14D-05

Hydrogen s-orbitals

	0.637212	0.767344	-0.071615
	0.754472	-0.639840	-0.144042
	0.152913	-0.034963	0.978965
	0.036755	-0.023773	0.125506
λ_k	1.40D-01	2.09D-03	1.11D-05

Table 34. (Continued)

C_2H_6 MOCETGAO's

Carbon s-orbitals

	-0.485048	0.870599	0.064324	-0.051325
	0.323677	0.097706	0.900905	-0.270151
	0.748927	0.429541	-0.405837	-0.299686
	0.308338	0.214520	0.139348	0.881827
	0.061386	0.043213	0.007564	0.231220
	0.015145	0.010903	0.007250	0.059087
λ_k	6.17D-01	2.90D-01	4.81D-06	4.45D-08

Carbon p-orbitals

0.566665	0.819986	-0.080675	
0.785399	-0.566752	-0.245016	
0.243153	-0.073014	0.963484	
0.053996	-0.032913	0.071810	
λ_k	1.98D-01	3.32D-04	3.40D-06

Hydrogen s-orbitals

0.713870	-0.699961	-0.020972	
0.687125	0.705755	-0.169406	
0.130512	0.103409	0.980439	
0.034854	0.035648	0.097989	
λ_k	3.88D-01	1.59D-03	4.77D-05

Table 34. (Continued)

H_2O MOCETGAO's

Oxygen s-orbitals

	0.814985	0.576570	-0.023189	-0.053114
	-0.096877	0.206229	-0.355896	0.905137
	-0.524992	0.696050	-0.343291	-0.349110
	-0.220990	0.367391	0.849466	0.236702
	-0.043073	0.072509	0.175789	-0.000072
	-0.010282	0.017803	0.049573	-0.000018
λ_k	8.62D-01	4.21D-01	1.92D-06	2.68D-17

Oxygen p-orbitals

	0.571495	0.815064	-0.095128
	0.749648	-0.565587	-0.343151
	0.326783	-0.120708	0.922394
	0.068072	-0.034794	0.149624
λ_k	4.05D-01	9.26D-03	2.44D-05

Hydrogen s-orbitals

	0.643239	0.764929	-0.033564
	0.753078	-0.639860	-0.149588
	0.133124	-0.068809	0.984498
	0.037335	-0.026974	0.085213
λ_k	1.02D-01	7.74D-03	7.38D-05

Table 34. (Continued)

CO MOCETGAO's

Carbon s-orbitals

	0.861150	0.479491	-0.167978	-0.017057
	0.140769	0.076328	0.961966	-0.221258
	-0.421832	0.693715	-0.124530	-0.570255
	-0.240747	0.519178	0.171810	0.767799
	-0.050652	0.112959	0.035743	0.183918
	-0.011774	0.026771	0.010077	0.047145
λ_k	9.37D-01	4.87D-01	3.76D-02	5.52D-06

Carbon p-orbitals

0.634139	0.773110	-0.012867	
0.742209	-0.613314	-0.267035	
0.212825	-0.158630	0.962997	
0.041207	-0.031351	0.034102	
λ_k 1.18D-01	1.43D-02	4.47D-05	

Oxygen s-orbitals

0.780666	0.623805	-0.014273	-0.034979
-0.173231	0.220635	0.910686	-0.303182
-0.555638	0.668731	-0.374789	-0.321779
-0.223074	0.332171	0.171260	0.879544
-0.044035	0.066105	0.023506	0.164680
-0.010813	0.016716	0.009891	0.050964
λ_k 8.23D-01	3.95D-01	4.51D-05	1.69D-06

Oxygen p-orbitals

0.635624	0.765384	-0.100493	
0.716126	-0.633067	-0.293461	
0.281848	-0.109315	0.934213	
0.060885	-0.038271	0.176150	
λ_k 3.77D-01	1.02D-02	9.21D-06	

Table 34. (Continued)

CO_2 MOCETGAO's

Carbon s-orbitals

	-0.393732	0.909635	-0.130434	-0.022758
	0.097470	0.170327	0.941628	-0.273083
	0.811602	0.302978	-0.262237	-0.423290
	0.411359	0.222608	0.163893	0.858311
	0.084513	0.045501	0.024728	0.086747
	0.020455	0.011536	0.009149	0.038852
λ_k	6.07D-01	2.95D-01	1.01D-02	3.12D-08

Carbon p-orbitals

	0.429730	0.902395	-0.010393
	0.868572	-0.416555	-0.263600
	0.240625	-0.103526	0.964238
	0.054908	-0.023356	0.025532
λ_k	1.42D-01	4.34D-02	5.61D-06

Oxygen s-orbitals

	0.799263	0.599874	-0.010197	-0.035007
	-0.168612	0.223414	0.915683	-0.288139
	-0.534130	0.686248	-0.368961	-0.328038
	-0.213485	0.338339	0.157750	0.879922
	-0.042092	0.067366	0.018062	0.176430
	-0.010336	0.017014	0.008766	0.052449
λ_k	8.47D-01	4.02D-01	2.16D-04	2.44D-06

Oxygen p-orbitals

	0.667195	0.740243	-0.082993
	0.690511	-0.656174	-0.302202
	0.273314	-0.140273	0.943721
	0.057840	-0.042415	0.105715
λ_k	3.73D-01	1.08D-02	5.09D-05

Table 34. (Continued)

H_2CO MOCETGAO's

Carbon s-orbitals

	0.547580	0.834039	0.048222	-0.046989
	-0.301281	0.130884	0.909557	-0.254489
	-0.720273	0.478138	-0.394332	-0.311158
	-0.294849	0.237127	0.121578	0.901303
	-0.058726	0.047531	0.007874	0.146720
	-0.014420	0.011969	0.006293	0.048314
λ_k	6.43D-01	3.14D-01	2.46D-04	1.20D-06

Carbon p-orbitals

0.409476	0.912259	-0.010509	
0.868525	-0.393340	-0.296935	
0.272936	-0.111580	0.954403	
0.059157	-0.024824	0.028872	
λ_k 1.61D-01	2.34D-02	6.52D-05	

Oxygen s-orbitals

0.811111	0.582429	-0.050660	-0.017550
-0.110336	0.210457	0.828518	-0.506964
-0.527895	0.691130	-0.412100	-0.271702
-0.221830	0.364889	0.369249	0.799645
-0.043920	0.073087	0.065901	0.164367
-0.010728	0.018382	0.021842	0.049076
λ_k 8.59D-01	4.14D-01	1.61D-05	1.84D-07

Oxygen p-orbitals

0.599547	0.796544	-0.077746	
0.738390	-0.587846	-0.329728	
0.302573	-0.136132	0.930689	
0.061427	-0.037708	0.138032	
λ_k 3.81D-01	7.67D-03	4.57D-05	

Table 34. (Continued)

H_2CO MOCETGAO's

Hydrogen s-orbitals

	0.678926	0.734075	0.013887
	0.721381	-0.663422	-0.196593
	0.133147	-0.141519	0.977748
	0.030693	-0.031277	0.071885
λ_k	1.93D-01	1.16D-02	2.35D-04

Table 35. Comparison of energies for standard-type bases with energies for MOCETGAO bases[a]

Molecule[b]	C[3;3],H[2]	C[3;2],O[3;2],H[2]	C[4;2],O[3;2]
H_2	0.00000		
CH_4	0.00000	0.00000	
C_2H_2	0.00004	0.00579	
C_2H_4	0.00023	0.00073	
C_2H_6	0.00104	0.00116	
H_2O		0.00120	
CO		0.00125	
CO_2		0.00291	
H_2CO		0.00323	
C_3H_4		0.00012	
C_3O_2			0.00473

[a]Listed are the differences ΔE = (Energy for MOCETGAO basis) - (Energy for standard basis type given in Table 21) for all molecules except C_3H_4 and C_3O_2 where ΔE = (Energy for short MOCETGAO basis) - (Energy for long MOCETGAO bases given in Table 21).

[b]Experimental geometries given in Reference(40). See Table 41.

important s-type and two most important p-type MOCETGAO's, there is very little deterioration in the energies for all molecules except C_2H_2 where an additional p-type MOCETGAO is necessary to achieve equal accuracy. While the eigenvalues λ_k give a good indication of the relative importance of the MOCETGAO's in one symmetry, only representative molecular recalculations show how many of them will be routinely required.

It should be noted that none of the MOCETGAO coefficients have small enough magnitudes to permit elimination of the unimportant primitives as was possible for the isolated atoms in Chapter I. However, because of the small size of the primitive bases, such reductions are of little interest since they would yield very little savings in integral evaluation time. For example, if the two smallest coefficients of each s-type MOCETGAO in the basis C[4;2], H[2] for C_2H_4 are set equal to zero, our integrals program shows that the time saved amounts to only 0.4%.

An important question is how the MOCETGAO's of different molecules are related. First, tests may be performed to see how closely the MOCETGAO's span the same space. For this purpose, we consider the transformation matrix D of the full set of MOCETGAO's from molecule M to molecule N,

$$\varphi_i^{(N)} = \sum_k \varphi_k^{(M)} D_{ki}^{(M,N)} \tag{37a}$$

or

$$T_{ji}^{(N)} = \sum_k T_{jk}^{(M)} D_{ki}^{(M,N)} \ . \tag{37b}$$

It follows from the orthogonality of the MOCETGAO's for each molecule that

$$D_{ki}^{(M,N)} = \sum_j T_{jk}^{(M)} T_{ji}^{(N)} . \qquad (38)$$

The matrices of Equation (38) for each pair of molecules C_2H_2, C_2H_6, CO_2, and H_2O are shown in Table 36. The smallness of the s-orbital elements $D_{5,i}^{(M,N)}$ and $D_{6,i}^{(M,N)}$ for i=1 to 6 and p-orbital elements $D_{3,i}^{(M,N)}$ and $D_{4,i}^{(M,N)}$ for i=1 to 4 suggest a good degree of transferability between the molecules. This is verified by the energy comparisons of Table 37. Here the optimal primitive basis of each molecule is used, but with the coefficients $T_{jk}(\ell)$ from other molecules. These results emphasize the importance of $\varphi_4^{(N)}(s)$ for the energy when the MOCETGAO's coefficients are transferred between prototypes. Furthermore, the closer the optimal (α_ℓ,β_ℓ)-values, the better the approximation.

Next, we turn to the selection of MOCETGAO's for $(\ln\alpha_\ell, \ln\beta_\ell)$ values lying anywhere along the search directions of Figure 9. Within each group of molecules, the hydrocarbons or the oxygen-containing molecules, graphs of the MOCETGAO coefficients of Table 34 versus $\ln\alpha_\ell$ are found to closely approximate straight lines. The situation is displayed in Figure 10 for the carbon p-type orbitals of the hydrocarbons. Each line corresponds to $T_{jk}^{(M)}$ with the same (jk) subscripts as indicated. Thus, a set of linear equations,

$$T_{jk}^{(M)} = A_{jk} \cdot \ln\alpha_\ell + B_{jk}, \qquad (39)$$

may be constructed for the carbon, oxygen, and hydrogen orbitals

Table 36. Transformation matrices of the MOCETGAO's between prototype molecules

Carbon s-orbital Matrices

C_2H_2

	0.9906	-0.1055	-0.0709	0.0510	-0.0020	-0.0010
	0.1048	0.9944	-0.0048	0.0133	-0.0007	-0.0007
	0.0769	-0.0017	0.9896	-0.1217	0.0006	-0.0002
C_2H_6	-0.0426	-0.0081	0.1248	0.9881	0.0789	-0.0036
	0.0053	0.0011	-0.0106	-0.0781	0.9955	-0.0527
	0.0012	0.0006	-0.0000	-0.0005	0.0528	0.9986

C_2H_2

	0.9431	0.0046	-0.2585	0.2092	-0.0006	-0.0021
	0.0251	0.9918	0.1236	0.0176	0.0032	-0.0011
	0.2869	-0.1224	0.9415	-0.1270	0.0113	-0.0009
CO_2	-0.1660	-0.0349	0.1772	0.9677	-0.0584	-0.0043
	-0.0000	0.0004	0.0011	0.0118	0.1252	0.9921
	-0.0126	-0.0039	-0.0009	0.0571	0.9903	-0.1257

Carbon p-orbital Matrices

C_2H_2

	0.9980	0.0564	-0.0286	-0.0016
	-0.0524	0.9908	0.1247	-0.0015
C_2H_6	0.0353	-0.1230	0.9910	-0.0400
	0.0029	-0.0033	0.0398	0.9992

C_2H_2

	0.9931	-0.1007	-0.0598	-0.0037
	0.1036	0.9935	0.0470	0.0069
CO_2	0.0542	-0.0521	0.9935	-0.0851
	0.0076	-0.0117	0.0843	0.9963

Table 36. (Continued)

Oxygen s-orbital Matrices

CO_2

	0.9972	0.0291	0.0610	-0.0310	0.0014	0.0005
	-0.0274	0.9991	-0.0144	0.0291	-0.0009	-0.0008
	0.0356	-0.0289	-0.0614	0.9971	0.0044	-0.0017
H_2O	-0.0591	0.0109	0.9955	0.0638	-0.0344	-0.0098
	-0.0035	0.0013	0.0334	-0.0023	0.9952	-0.0917
	-0.0014	0.0010	0.0127	0.0022	0.0913	0.9957

Oxygen p-orbital Matrices

CO_2

	0.9922	-0.1176	0.0416	0.0013
	0.1183	0.9929	-0.0143	0.0020
H_2O	-0.0397	0.0190	0.9979	0.0476
	0.0004	-0.0027	-0.0476	0.9989

Hydrogen s-orbital Matrices

C_2H_2

	0.9951	0.0988	-0.0072	0.0031
	-0.0990	0.9942	-0.0414	0.0007
C_2H_6	0.0026	0.0414	0.9893	0.1401
	-0.0034	-0.0068	-0.1400	0.9901

Table 37. Comparison of energies for uncontracted basis with energies for carbon MOCETGAO bases transferred between molecules[a]

MOCETGAO Basis[b]	CO[c]	CO_2[c]	C_2H_6[c]
C[3(H_2CO);2],O[3;2]		.34237	
C[4(H_2CO);2],O[3;2]	.01085	.00391	
C[4(H_2CO);2(H_2CO)],O[3;2]	.01314	.00527	
C[3(C_2H_2);2(C_2H_2)],O[3;2]		.81342	.12500
C[4(C_2H_2);2(C_2H_2)],O[3;2]		.01218	.00831

[a]Listed are the differences ΔE = (Energy for MOCETGAO basis) - (Energy for standard basis type given in Table 21).

[b]The notation C[4(H_2CO);2(H_2CO)] implies that four s-type and two p-type MOCETGAO's are transferred from H_2CO and used in calculations on CO and CO_2.

[c]Experimental geometries given in Reference (40). See Table 41.

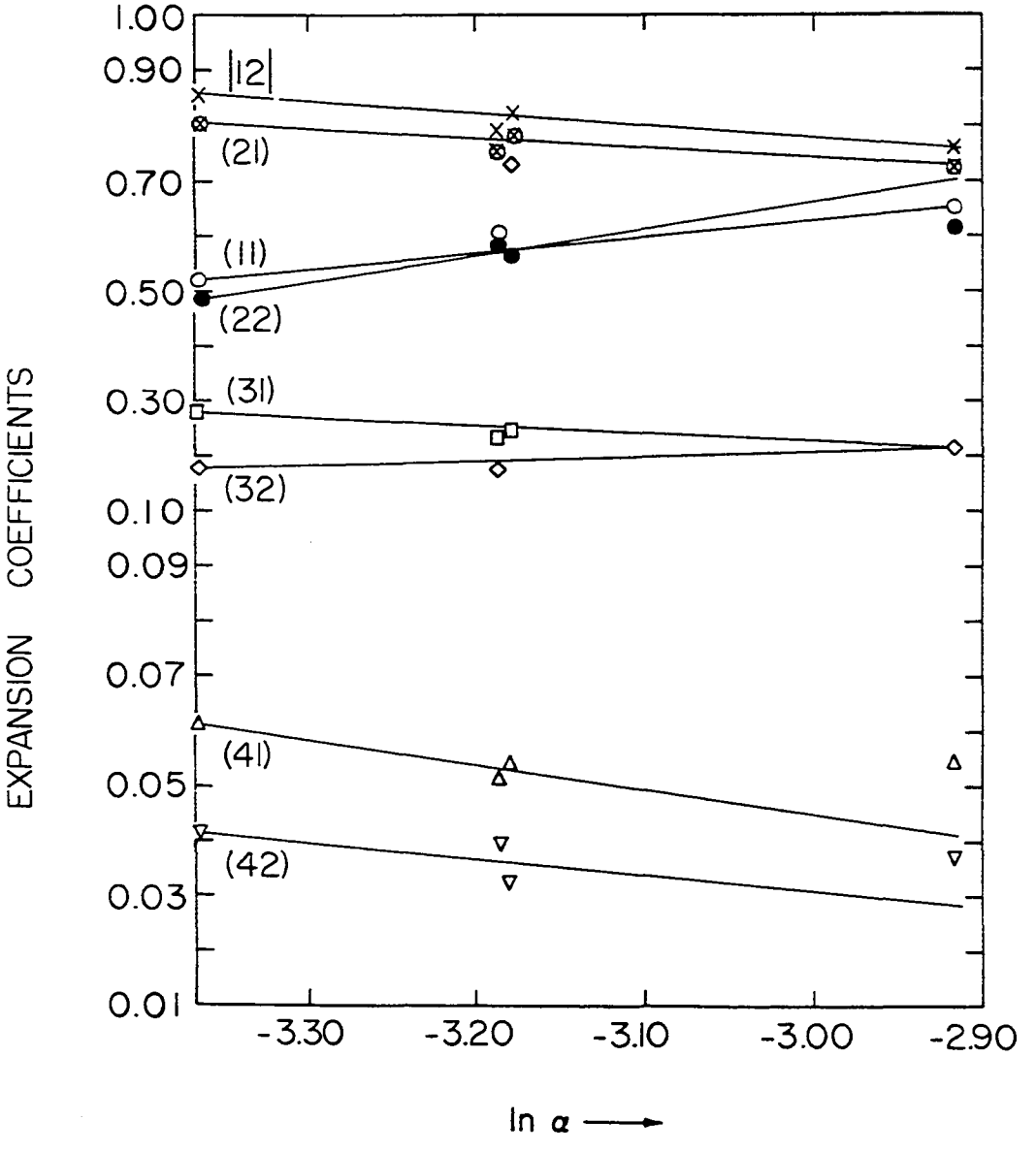

Figure 10. Variation of carbon p-type MOCETGA0 coefficients for the hydrocarbons

describing the coefficients as functions of $\ln\alpha_\ell$. It should be mentioned that polynomial equations are obtained for each carbon orbital when all molecules are considered together. However, straight line dependence between both groups is closely approached if, for each orbital, the inner and outer shell dependence are extracted from the MOCETGAO's of Table 34 by diagonalizing the matrix of the one-electron operator,

$$-\frac{1}{2}\nabla_i^2 - \sum_j \frac{Z_j}{r_{ji}} \quad ,$$

formed from the MOCETGAO's. As an example, the eigenfunctions and eigenvalues for the carbon s-orbitals in CO_2 are shown in Table 38. The eigenvalues indicate that there is one orbital representing the inner shell and three for the outer shell. Unfortunately, if the first three s-type functions and the first two p-type functions are used, the SCF energy of CO_2 increases by 0.012 Hartree above the energy of the corresponding basis size in Table 21. Therefore, a less-accurate transferable set of three s-type and two p-type MOCETGAO's is obtained from these functions. Consequently, the MOCETGAO's of Table 34 will be used in the sequel.

It is expected that the use of Equations (39) during optimizations along the directions of Figure 9 give maximum flexibility in the MOCETGAO basis. At the same time, however, these equations must be programmed and provision made to allow for changes in the signs of the coefficients. On the other hand, the results of Tables 36 and 37 imply that fixed MOCETGAO coefficients will be satisfactory for achieving most of the variation of $\ln\alpha_\ell$ and $\ln\beta_\ell$. The effectiveness of this latter approach

Table 38. Eigenvalues and eigenvectors of the one-electron Hamiltonian matrix in the basis of the carbon MOCETGAO's of CO_2

Carbon s-orbital Eigenvalues and Eigenvectors[a]				
Eigenvalues	-17.965449	-4.450777	-1.632416	19.749051
	0.018100	-0.686652	-1.645347	-0.353498
	0.098862	-0.569000	1.139885	0.720348
	0.750302	0.481741	-0.505187	-1.767519
	0.439574	0.184265	-0.231773	0.824561
	0.086864	0.031332	-0.036107	0.043685
	0.021840	0.007882	-0.009844	0.037198
Carbon p-orbital Eigenvalues and Eigenvectors[a,b]				
Eigenvalues	-4.161687	-1.788225		
	0.103629	0.918571		
	1.052374	-0.309205		
	0.287079	-0.074187		
	0.065408	-0.016670		

[a] Contracted (MOCETGAO) basis is C[4;2] of Table 34.

[b] Apply equally to (2px), (2py), (2pz).

will be tested in the next section.

Procedure of Minimization for Methyl Acetylene and Carbon Suboxide

The molecules methyl acetylene (C_3H_4) and carbon suboxide (C_3O_2) contain C-C and C-O bonds which are intermediate to the single and multiple bonds of the prototype molecules C_2H_2, C_2H_4, C_2H_6, and CO_2. Thus, the quality of the parameter values of Table 19 and the MOCETGAO's of Table 34 for use in large molecules is assessed by optimizing the even-tempered parameters of C_3H_4 and C_3O_2.

Optimizations for C_3H_4

The optimizations of carbon and hydrogen parameters are done in two stages. First, the effect of replacing the three hydrogens of C_2H_6 by the group C≡C-H (or, equivalently, replacing the single hydrogen atom of C_2H_2 by the group H_3C-C) is determined by optimizing all parameters of C_3H_4 at the experimental geometries of C_2H_2 and C_2H_6. Second, using the optimal parameters of the first stage, the equilibrium internuclear distances and bond angles of C_3H_4 are predicted. Then, all of the parameters are reoptimized at this new geometry. A detailed discussion of geometry optimizations is given in the next section.

The optimal carbon and hydrogen parameter values given in Table 19 for C_2H_2 and C_2H_6 are suitable starting values for both stages and are readily assigned to the hydrogen and outermost carbon atoms. For the central carbon atom, the assignment is made under the assumption that the triple bond is more important for the molecular energy than the "single"

bond. In this case, the starting values are taken from C_2H_2, instead of C_2H_6. The basis set for each atom is then formed from the appropriate MOCETGAO coefficients of Table 34.

According to the discussion of the previous section, the MOCETGAO basis C[4;3], H[2] is large enough so that sufficient flexibility is retained during minimization. Furthermore, it was shown for the prototype molecules that, to a good approximation, the coefficients of Table 34 may be kept constant throughout (except for a normalization constant), providing the $\ln\alpha_\ell$ and $\ln\beta_\ell$ values don't change substantially from those of C_2H_2 and C_2H_6. Since this analysis was based on comparisons for the prototype molecules which contain quite different bonding characteristics, even better approximations are expected for C_3H_4.

These implications are tested on C_3H_4 at the experimental geometries of C_2H_2 and C_2H_6. Optimizations are first carried out for the s-type orbitals of the central carbon atom since the largest adjustment of parameters should occur for this atom. The appropriate line of Figure 9 and a second direction at 135° are searched by calculating the energies at points located at distances of $\Delta\ln\alpha_o=0.05$ on each side of the optimal points indicated for C_2H_2. It is found that one quadratic prediction for each direction is sufficient to establish convergence. The parameter values and energies for both predictions are such that $|\vec{p}_f - \vec{p}_i| < 5\times10^{-3}$ and $0 < (E_f - E_i) < 10^{-4}$ where $E_i = -115.69300$ Hartrees. These results indicate that the basis size may be reduced to C[3;3], H[2] for all atoms in the molecule before proceeding further. An additional reduction of the number of carbon p-type MOCETGAO's is not made since the largest variation

of even-tempered parameters is expected for $\ln\alpha_1$ and $\ln\beta_1$. Using this basis, optimizations for the 2p-orbital of the central carbon atom and all orbitals of the remaining atoms are carried out in the same way. Again, all parameters are unchanged from those of C_2H_2 and C_2H_6. The minimum energy is given in Table 21.

We now examine the changes which the parameters undergo when optimizations are performed at the theoretical equilibrium geometry of C_3H_4. The equilibrium bond lengths and bond angles used are given in Table 41 of the next section. The previous search directions, initial parameter values of C_2H_2 and C_2H_6, and criteria are also used here. Calculation shows that the parameters for all carbon s-orbitals, the acetylene-like and carbon 2p-orbital, and the acetylene-like hydrogen 1s orbital are constant. However, the 2p-orbital parameters for the ethane-like and middle carbon atoms do change, corresponding to an energy lowering of 0.0002 Hartree to -115.70035 Hartrees. These adjustments occur entirely along the initial directions of Figure 9. Convergence along the second direction is considered sufficient to end the search for each orbital because of the closeness of the initial and final parameter values. The final results are given in Table 19 and 21 and plotted in Figure 9.

Optimizations for C_3O_2

The optimizations of carbon and oxygen parameters for C_3O_2 are performed only for the linear geometry $D_{\infty h}$ where the bond lengths, r(C-C) = 1.3Å and r(C-O) = 1.2Å, are taken from Cotton and Wilkinson (45). Although these distances are too large and differ from experiment (46) by

$\Delta r(C\text{-}C) = 0.02\text{Å}$ and $\Delta r(C\text{-}O) = 0.04\text{Å}$, the results obtained for C_3H_4 indicate that the two sets of optimal parameters would not be substantially different.

Selections of the starting parameters for C_3O_2 may be made on the basis of the relative electronegativities of the atoms. We assume, then, that the presence of the oxygen atoms at both ends of the molecule is the overwhelmingly dominant influence so that the optimal parameters and MOCETGAO coefficients of CO_2 should be used exclusively. Since the oxygen atom is expected to be especially important for the energy, optimizations are first carried out in order to determine the importance of the fourth oxygen s-type MOCETGAO in the basis O[4;3], C[4;3]. Proceeding in the same way as for C_3H_4, it is found after one quadratic prediction for each direction that the parameter values for oxygen and the molecular energies for both predictions are such that $|\vec{p}_f - \vec{p}_i| < 5 \times 10^{-3}$ and $0 < (E_f - E_i) < 10^{-4}$ where $E_i = -262.76696$ Hartrees. The basis size is now reduced to O[3;3], C[4;3] and optimizations performed on the outer carbon atoms. The initial energy is -262.76681 Hartrees. By far, the largest variation occurs for the s-orbitals as seen in Figure 9. For the s-orbitals, three energy calculations in addition to the initial calculation are required to reach the point at $\ln\alpha_o = -2.192$ where the energy increases by 0.005 Hartree from the last point to -262.76772 Hartrees. These points are located at distances of $\Delta\ln\alpha_o = 0.05$, 0.15, and 0.35 along the line from the initial point. It is now evident that the CO_2 parameters for the s-orbitals are poor starting values and that those for C_2H_4 are better. Replacing the carbon

s-orbital MOCETGAO coefficients for CO_2 with those for C_2H_4, the energy of C_3O_2 is calculated to be -262.79264 Hartrees at the point corresponding to C_2H_4 of Figure 9. An additional seven energy calculations along this direction and the one at 135° are required to reach the minimum. In the case of the p-orbitals, it is seen in Figure 9 that the optimal parameter values and MOCETGAO coefficients of the outer carbon atoms are similar to those of CO_2. Turning now to the central carbon atom, the final parameters shown in Figure 9 indicate that the combined effect of the C=O groups on this atom is similar to that of the oxygen atom in CO_2. Completion of the optimizations results in an overall energy lowering of 0.031 Hartree to the final value -262.79774 Hartrees.

Conclusions concerning the optimizations on C_3H_4 and C_3O_2

The following conclusions may be drawn from the optimizations for C_3H_4 and C_3O_2. First, most of the energy improvement is achieved by first searching the lines of Figure 9. This is so even if a poor selection of initial parameter values is made from the prototype molecules. In fact, the need for a second search direction is substantially reduced and may be eliminated unless greater accuracy is desired. Second, the high degree of transferability of prototype optimal parameters indicates that with a careful choice of parameters and MOCETGAO coefficients, the electronic distribution of a large molecule is sufficiently well represented so that only very few optimizations are required. Third, the MOCETGAO coefficients of Table 34 may be used for optimizations of α_ℓ and β_ℓ. Moreover, for the same type of atom, two sets of coefficients

which differ in symmetry (different ℓ value) and molecular origin may be mixed and the corresponding parameters then optimized.

The optimal molecular orbitals for C_3H_4 and C_3O_2 are given in Tables 39 and 40. The labelling of the MO's and selection of coordinate systems are the same as described previously, except that here each row of coefficients is labelled by the MOCETGAO designations of Table 34. The coordinates of the atoms are given in Table 33.

Molecular Equilibrium Geometries

General results

A complete geometry optimization for a molecule containing more than two atoms requires the variation of all bond lengths and angles so that the best values corresponding to the correct symmetry point group yield the lowest energy. However, in view of the existing experimental and theoretical data for the molecules considered in this paper, no attempt was made here to alter any of the symmetry point groups except for C_3O_2 where some question has remained. A one-dimensional search procedure, using quadratic predictions, similar to the method used previously was sufficient for calculations on CH_4, CO_2, and CO. For the other molecules, the geometric parameters were optimized two at a time going through as many cycles as needed. The choice of these pairs and the sequence in which they were considered for the various molecules is as follows (AB denotes the bond length A-B, ABC denotes the angle between the bonds A-B and B-C, the number indicates the required number of cycles):

Table 39. Optimized MO's for methyl acetylene

		$1a_1$	$2a_1$	$3a_1$	$4a_1$
	ε	-11.236841	-11.236070	-11.215853	-1.066956
C1	φs1	-0.644031	-0.330836	0.004142	-0.342407
	φs2	-0.364257	-0.183611	0.009573	0.363717
	φs3	-0.000431	-0.001188	-0.001176	-0.003299
	φpx1	0.0	0.0	0.0	0.0
	φpx2	0.0	0.0	0.0	0.0
	φpx3	0.0	0.0	0.0	0.0
	φpy1	0.0	0.0	0.0	0.0
	φpy2	0.0	0.0	0.0	0.0
	φpy3	0.0	0.0	0.0	0.0
	φpz1	0.001580	0.002560	0.005434	0.125219
	φpz2	0.000778	-0.001358	0.002509	0.035985
	φpz3	-0.000714	-0.001450	-0.000972	-0.005376
C2	φs1	-0.364637	0.712816	-0.086191	-0.386306
	φs2	-0.131515	0.255221	-0.023142	0.395181
	φs3	0.000214	0.000304	-0.000359	-0.000232
	φpx1	0.0	0.0	0.0	0.0
	φpx2	0.0	0.0	0.0	0.0
	φpx3	0.0	0.0	0.0	0.0
	φpy1	0.0	0.0	0.0	0.0
	φpy2	0.0	0.0	0.0	0.0
	φpy3	0.0	0.0	0.0	0.0
	φpz1	0.011421	0.000900	0.016686	0.090891
	φpz2	0.001853	0.000504	0.007231	0.046333
	φpz3	-0.002934	0.000273	-0.001362	0.015102
C3	φs1	-0.026522	0.075331	0.801173	-0.289701
	φs2	-0.018333	0.029813	0.286130	0.300049
	φs3	0.000875	0.000130	0.000213	-0.001360
	φpx1	0.0	0.0	0.0	0.0
	φpx2	0.0	0.0	0.0	0.0
	φpx3	0.0	0.0	0.0	0.0
	φpy1	0.0	0.0	0.0	0.0
	φpy2	0.0	0.0	0.0	0.0
	φpy3	0.0	0.0	0.0	0.0
	φpz1	0.011294	-0.011374	0.007688	-0.252067
	φpz2	0.004372	-0.006645	0.000296	-0.081837
	φpz3	-0.001178	0.000057	-0.002535	-0.012804
H1	φs1	-0.002385	-0.002391	0.003256	0.145883
	φs2	-0.000839	0.000029	-0.001779	-0.020560
H1	φs1	-0.002385	-0.002391	0.003256	0.145883
	φs2	-0.000839	0.000029	-0.001779	-0.020560
H1	φs1	-0.002385	-0.002391	0.003256	0.145883
	φs2	-0.000839	0.000029	-0.001779	-0.020560
H2	φs1	-0.009768	0.009993	-0.001793	0.236765
	φs2	0.003608	-0.003360	0.002154	-0.064921

$5a_1$	$6a_1$	$7a_1$
-0.973700	-0.725296	-0.628701
-0.390343	0.086981	-0.037701
0.387673	-0.099372	0.038093
0.005976	0.002411	-0.000350
0.0	0.0	0.0
0.0	0.0	0.0
0.0	0.0	0.0
0.0	0.0	0.0
0.0	0.0	0.0
0.0	0.0	0.0
-0.076281	0.149370	-0.525448
-0.032695	-0.030150	0.002103
0.006214	0.004648	-0.003019
0.132306	-0.208875	0.140916
-0.139336	0.200905	-0.162151
0.001041	0.002561	0.002296
0.0	0.0	0.0
0.0	0.0	0.0
0.0	0.0	0.0
0.0	0.0	0.0
0.0	0.0	0.0
0.0	0.0	0.0
-0.399464	-0.112227	0.458947
-0.034652	-0.058142	-0.090969
-0.009100	0.020400	-0.001067
0.298509	0.221878	-0.037068
-0.291663	-0.231814	0.021957
-0.001917	0.000216	0.002571
0.0	0.0	0.0
0.0	0.0	0.0
0.0	0.0	0.0
0.0	0.0	0.0
0.0	0.0	0.0
0.0	0.0	0.0
0.097312	-0.513749	-0.210377
-0.006073	0.038978	0.085541
0.018887	0.009495	-0.013344
0.132913	-0.105599	0.150865
0.018657	0.010214	0.008636
0.132913	-0.105599	0.150865
0.018657	0.010214	0.008636
0.132913	-0.105599	0.150865
0.018657	0.010214	0.008636
-0.124680	-0.395982	-0.239176
0.001510	-0.047467	0.013324

Table 39. (Continued)

		1e	2e	3e	4e
	ε	-0.596474	-0.596463	-0.392439	-0.392434
C1	φs1	0.0	0.0	0.0	0.0
	φs2	0.0	0.0	0.0	0.0
	φs3	0.0	0.0	0.0	0.0
	φpx1	0.113424	0.581209	0.201236	0.039180
	φpx2	-0.001320	-0.007111	0.028190	0.005472
	φpx3	-0.000007	-0.000005	-0.000910	-0.000173
	φpy1	0.581297	-0.113360	-0.039253	0.201309
	φpy2	-0.007105	0.001376	-0.005523	0.028234
	φpy3	-0.000018	0.000006	0.000161	-0.000918
	φpz1	0.0	0.0	0.0	0.0
	φpz2	0.0	0.0	0.0	0.0
	φpz3	0.0	0.0	0.0	0.0
C2	φs1	0.0	0.0	0.0	0.0
	φs2	0.0	0.0	0.0	0.0
	φs3	0.0	0.0	0.0	0.0
	φpx1	0.034050	0.174502	-0.572020	-0.111597
	φpx2	-0.004665	-0.023847	-0.028547	-0.005654
	φpx3	-0.000045	-0.000226	0.002051	0.000379
	φpy1	0.174467	-0.034024	0.111537	-0.572013
	φpy2	-0.023821	0.004662	0.005532	-0.028551
	φpy3	-0.000214	0.000049	-0.000437	0.002055
	φpz1	0.0	0.0	0.0	0.0
	φpz2	0.0	0.0	0.0	0.0
	φpz3	0.0	0.0	0.0	0.0
C3	φs1	0.0	0.0	0.0	0.0
	φs2	0.0	0.0	0.0	0.0
	φs3	0.0	0.0	0.0	0.0
	φpx1	0.020073	0.103322	-0.585725	-0.113951
	φpx2	-0.000197	-0.001131	-0.012513	-0.002332
	φpx3	0.000202	0.001004	0.001514	0.000309
	φpy1	0.103363	-0.020148	0.114137	-0.585747
	φpy2	-0.001115	0.000215	0.002534	-0.012577
	φpy3	0.000992	-0.000219	-0.000057	0.001470
	φpz1	0.0	0.0	0.0	0.0
	φpz2	0.0	0.0	0.0	0.0
	φpz3	0.0	0.0	0.0	0.0
H1	φs1	0.076041	0.390524	0.191237	0.037375
	φs2	0.003300	0.016643	-0.007306	-0.001430
H1	φs1	0.300089	-0.261208	-0.127886	0.146871
	φs2	0.012817	-0.011135	0.004884	-0.005593
H1	φs1	-0.376130	-0.129316	-0.063351	-0.184246
	φs2	-0.016117	-0.005508	0.002422	0.007023
H1	φs1	0.0	0.0	0.0	0.0
	φs2	0.0	0.0	0.0	0.0

Table 40. Optimized MO's for carbon suboxide

		$1\sigma_u$	$1\sigma_g$	$2\sigma_u$	$2\sigma_g$
	ε	-20.635119	-20.635111	-11.449290	-11.448833
C1	$\varphi s1$	0.0	-0.004988	0.0	-0.001505
	$\varphi s2$	0.0	0.012787	0.0	0.018489
	$\varphi s3$	0.0	-0.003080	0.0	-0.003362
	$\varphi s4$	0.0	0.000051	0.0	0.000308
	$\varphi px1$	0.0	0.0	0.0	0.0
	$\varphi px2$	0.0	0.0	0.0	0.0
	$\varphi px3$	0.0	0.0	0.0	0.0
	$\varphi py1$	0.0	0.0	0.0	0.0
	$\varphi py2$	0.0	0.0	0.0	0.0
	$\varphi py3$	0.0	0.0	0.0	0.0
	$\varphi pz1$	-0.004895	0.0	0.014752	0.0
	$\varphi pz2$	-0.000918	0.0	0.010547	0.0
	$\varphi pz3$	0.001533	0.0	-0.001445	0.0
C2	$\varphi s1$	-0.000941	-0.001272	-0.518198	0.512143
	$\varphi s2$	0.001525	0.002108	-0.273362	0.284453
	$\varphi s3$	-0.000179	-0.000368	-0.012865	0.010504
	$\varphi s4$	0.000005	-0.000003	0.006964	-0.007167
	$\varphi px1$	0.0	0.0	0.0	0.0
	$\varphi px2$	0.0	0.0	0.0	0.0
	$\varphi px3$	0.0	0.0	0.0	0.0
	$\varphi py1$	0.0	0.0	0.0	0.0
	$\varphi py2$	0.0	0.0	0.0	0.0
	$\varphi py3$	0.0	0.0	0.0	0.0
	$\varphi pz1$	-0.006481	-0.006416	0.004344	-0.001654
	$\varphi pz2$	-0.003916	-0.004120	0.002552	-0.003153
	$\varphi pz3$	0.001047	0.000944	-0.000351	-0.000764
C2	$\varphi s1$	0.000941	-0.001272	0.518198	0.512143
	$\varphi s2$	-0.001525	0.002108	0.273362	0.284453
	$\varphi s3$	0.000179	-0.000368	0.012865	0.010504
	$\varphi s4$	-0.000005	-0.000003	-0.006964	-0.007167
	$\varphi px1$	0.0	0.0	0.0	0.0
	$\varphi px2$	0.0	0.0	0.0	0.0
	$\varphi px3$	0.0	0.0	0.0	0.0
	$\varphi py1$	0.0	0.0	0.0	0.0
	$\varphi py2$	0.0	0.0	0.0	0.0
	$\varphi py3$	0.0	0.0	0.0	0.0
	$\varphi pz1$	-0.006481	0.006416	0.004344	0.001654
	$\varphi pz2$	-0.003916	0.004120	0.002552	0.003153
	$\varphi pz3$	0.001047	-0.000944	-0.000351	0.000764

$3\sigma_g$	$3\sigma_u$	$4\sigma_g$	$5\sigma_g$	$4\sigma_u$
-11.265947	-1.496649	-1.492346	-1.110511	-0.948637
0.790018	0.0	0.155911	-0.480147	0.0
0.355460	0.0	-0.337654	0.588129	0.0
0.001078	0.0	0.059374	0.002902	0.0
0.019046	0.0	-0.001578	-0.003015	0.0
0.0	0.0	0.0	0.0	0.0
0.0	0.0	0.0	0.0	0.0
0.0	0.0	0.0	0.0	0.0
0.0	0.0	0.0	0.0	0.0
0.0	0.0	0.0	0.0	0.0
0.0	0.0	0.0	0.0	0.0
0.0	0.132617	0.0	0.0	-0.469564
0.0	0.080917	0.0	0.0	-0.045150
0.0	-0.015281	0.0	0.0	-0.009473
-0.005191	0.193610	0.225695	-0.256211	-0.309535
0.000523	-0.184696	-0.238047	0.260464	0.298601
-0.000266	-0.004076	0.002595	-0.006833	0.001680
0.0	-0.001023	-0.000252	0.001478	0.002193
0.0	0.0	0.0	0.0	0.0
0.0	0.0	0.0	0.0	0.0
0.0	0.0	0.0	0.0	0.0
0.0	0.0	0.0	0.0	0.0
0.0	0.0	0.0	0.0	0.0
0.0	0.0	0.0	0.0	0.0
0.001018	0.247939	0.241023	0.230077	0.246258
0.001687	0.095739	0.087388	-0.014899	0.011122
0.000508	-0.001827	-0.002140	-0.002775	0.005506
-0.005191	-0.193610	0.225695	-0.256211	0.309535
0.000523	0.184696	-0.238047	0.260464	-0.298601
-0.000266	0.004076	0.002595	-0.006833	-0.001680
0.0	0.001023	-0.000252	0.001478	-0.002193
0.0	0.0	0.0	0.0	0.0
0.0	0.0	0.0	0.0	0.0
0.0	0.0	0.0	0.0	0.0
0.0	0.0	0.0	0.0	0.0
0.0	0.0	0.0	0.0	0.0
0.0	0.0	0.0	0.0	0.0
-0.001018	0.247939	-0.241023	-0.230077	0.246258
-0.001687	0.095739	-0.087388	0.014899	0.011122
-0.000508	-0.001827	0.002140	0.002775	0.005506

Table 40. (Continued)

		$1\sigma_u$ (cont.)	$1\sigma_g$ (cont.)	$2\sigma_u$ (cont.)	$2\sigma_g$ (cont.)
O	φs1	-0.304914	-0.304895	-0.001252	0.001456
	φs2	0.559041	0.559066	-0.000996	0.001248
	φs3	0.000246	0.000220	0.000183	-0.000305
	φpx1	0.0	0.0	0.0	0.0
	φpx2	0.0	0.0	0.0	0.0
	φpx3	0.0	0.0	0.0	0.0
	φpy1	0.0	0.0	0.0	0.0
	φpy2	0.0	0.0	0.0	0.0
	φpy3	0.0	0.0	0.0	0.0
	φpz1	-0.002468	-0.002355	-0.003163	0.003428
	φpz2	-0.001266	-0.001145	-0.000476	0.001210
	φpz3	0.002102	0.002110	0.000423	-0.000222
O	φs1	0.304914	-0.304895	0.001252	0.001456
	φs2	-0.559041	0.559066	0.000996	0.001248
	φs3	-0.000246	0.000220	-0.000183	-0.000305
	φpx1	0.0	0.0	0.0	0.0
	φpx2	0.0	0.0	0.0	0.0
	φpx3	0.0	0.0	0.0	0.0
	φpy1	0.0	0.0	0.0	0.0
	φpy2	0.0	0.0	0.0	0.0
	φpy3	0.0	0.0	0.0	0.0
	φpz1	-0.002468	0.002355	-0.003163	-0.003428
	φpz2	-0.001266	0.001145	-0.000476	-0.001210
	φpz3	0.002102	-0.002110	0.000423	0.000222

$3\sigma_g$ (cont.)	$3\sigma_u$ (cont.)	$4\sigma_g$ (cont.)	$5\sigma_g$ (cont.)	$4\sigma_u$ (cont.)
0.000598	-0.414011	-0.419003	-0.102876	-0.140537
0.000747	-0.254372	-0.259992	-0.066524	-0.093054
-0.000207	-0.003301	-0.002249	-0.001265	-0.000822
0.0	0.0	0.0	0.0	0.0
0.0	0.0	0.0	0.0	0.0
0.0	0.0	0.0	0.0	0.0
0.0	0.0	0.0	0.0	0.0
0.0	0.0	0.0	0.0	0.0
0.0	0.0	0.0	0.0	0.0
-0.000245	-0.081627	-0.087470	0.031158	0.088078
0.000109	0.068819	0.062940	0.016055	0.014094
0.000124	-0.001187	-0.002127	-0.001179	-0.000501
0.000598	0.414011	-0.419003	-0.102876	0.140537
0.000747	0.254372	-0.259992	-0.066524	0.093054
-0.000207	0.003301	-0.002249	-0.001265	0.000822
0.0	0.0	0.0	0.0	0.0
0.0	0.0	0.0	0.0	0.0
0.0	0.0	0.0	0.0	0.0
0.0	0.0	0.0	0.0	0.0
0.0	0.0	0.0	0.0	0.0
0.0	0.0	0.0	0.0	0.0
0.000245	-0.081627	0.087470	-0.031158	0.088078
-0.000109	0.068819	-0.062940	-0.016055	0.014094
-0.000124	-0.001187	0.002127	0.001179	-0.000501

Table 40. (Continued)

		$6\sigma_g$	$5\sigma_u$	$1\pi_{ux}$	$1\pi_{uy}$
	ε	-0.737549	-0.727560	-0.660346	-0.660346
C1	φs1	-0.239638	0.0	0.0	0.0
	φs2	0.442818	0.0	0.0	0.0
	φs3	-0.046289	0.0	0.0	0.0
	φs4	-0.001685	0.0	0.0	0.0
	φpx1	0.0	0.0	0.234545	0.0
	φpx2	0.0	0.0	0.010670	0.0
	φpx3	0.0	0.0	0.000933	0.0
	φpy1	0.0	0.0	0.0	0.234545
	φpy2	0.0	0.0	0.0	0.010670
	φpy3	0.0	0.0	0.0	0.000933
	φpz1	0.0	-0.271525	0.0	0.0
	φpz2	0.0	-0.103054	0.0	0.0
	φpz3	0.0	-0.000846	0.0	0.0
C2	φs1	0.140572	0.105270	0.0	0.0
	φs2	-0.129500	-0.112835	0.0	0.0
	φs3	-0.002494	0.001863	0.0	0.0
	φs4	-0.001410	-0.000310	0.0	0.0
	φpx1	0.0	0.0	0.334032	0.0
	φpx2	0.0	0.0	0.053597	0.0
	φpx3	0.0	0.0	0.000073	0.0
	φpy1	0.0	0.0	0.0	0.334032
	φpy2	0.0	0.0	0.0	0.053597
	φpy3	0.0	0.0	0.0	0.000073
	φpz1	0.106767	0.161262	0.0	0.0
	φpz2	-0.176818	-0.185637	0.0	0.0
	φpz3	-0.001035	-0.002214	0.0	0.0
C2	φs1	0.140572	-0.105270	0.0	0.0
	φs2	-0.129500	0.112835	0.0	0.0
	φs3	-0.002494	-0.001863	0.0	0.0
	φs4	-0.001410	0.000310	0.0	0.0
	φpx1	0.0	0.0	0.334032	0.0
	φpx2	0.0	0.0	0.053597	0.0
	φpx3	0.0	0.0	0.000073	0.0
	φpy1	0.0	0.0	0.0	0.334032
	φpy2	0.0	0.0	0.0	0.053597
	φpy3	0.0	0.0	0.0	0.000073
	φpz1	-0.106767	0.161262	0.0	0.0
	φpz2	0.176818	-0.185637	0.0	0.0
	φpz3	0.001035	-0.002214	0.0	0.0

$^1\pi_{gx}$	$^1\pi_{gu}$	$^2\pi_{ux}$	$^2\pi_{uy}$
-0.624172	-0.624172	-0.400619	-0.400619
0.0	0.0	0.0	0.0
0.0	0.0	0.0	0.0
0.0	0.0	0.0	0.0
0.0	0.0	0.0	0.0
0.0	0.0	-0.633668	0.0
0.0	0.0	-0.198573	0.0
0.0	0.0	-0.004697	0.0
0.0	0.0	0.0	-0.633668
0.0	0.0	0.0	-0.198573
0.0	0.0	0.0	-0.004697
0.0	0.0	0.0	0.0
0.0	0.0	0.0	0.0
0.0	0.0	0.0	0.0
0.0	0.0	0.0	0.0
0.0	0.0	0.0	0.0
0.0	0.0	0.0	0.0
0.0	0.0	0.0	0.0
-0.289560	0.0	-0.156707	0.0
-0.045750	0.0	-0.004752	0.0
0.000204	0.0	0.001557	0.0
0.0	-0.289560	0.0	-0.156707
0.0	-0.045750	0.0	-0.004752
0.0	0.000204	0.0	0.001557
0.0	0.0	0.0	0.0
0.0	0.0	0.0	0.0
0.0	0.0	0.0	0.0
0.0	0.0	0.0	0.0
0.0	0.0	0.0	0.0
0.0	0.0	0.0	0.0
0.0	0.0	0.0	0.0
0.289560	0.0	-0.156707	0.0
0.045750	0.0	-0.004752	0.0
-0.000204	0.0	0.001557	0.0
0.0	0.289560	0.0	-0.156707
0.0	0.045750	0.0	-0.004752
0.0	-0.000204	0.0	0.001557
0.0	0.0	0.0	0.0
0.0	0.0	0.0	0.0
0.0	0.0	0.0	0.0

Table 40. (Continued)

		$6\sigma_g$ (cont.)	$5\sigma_u$ (cont.)	$1\pi_{ux}$ (cont.)	$1\pi_{uy}$ (cont.)
O	φs1	0.258958	0.230583	0.0	0.0
	φs2	0.174407	0.153761	0.0	0.0
	φs3	0.000348	0.000856	0.0	0.0
	φpx1	0.0	0.0	0.454712	0.0
	φpx2	0.0	0.0	-0.008702	0.0
	φpx3	0.0	0.0	-0.001224	0.0
	φpy1	0.0	0.0	0.0	0.454712
	φpy2	0.0	0.0	0.0	-0.008702
	φpy3	0.0	0.0	0.0	-0.001224
	φpz1	-0.535402	-0.539940	0.0	0.0
	φpz2	-0.020788	-0.023951	0.0	0.0
	φpz3	-0.000538	-0.001389	0.0	0.0
O	φs1	0.258958	-0.230583	0.0	0.0
	φs2	0.174407	-0.153761	0.0	0.0
	φs3	0.000348	-0.000856	0.0	0.0
	φpx1	0.0	0.0	0.454712	0.0
	φpx2	0.0	0.0	-0.008702	0.0
	φpx3	0.0	0.0	-0.001224	0.0
	φpy1	0.0	0.0	0.0	0.454712
	φpy2	0.0	0.0	0.0	-0.008702
	φpy3	0.0	0.0	0.0	-0.001224
	φpz1	0.535402	-0.539940	0.0	0.0
	φpz2	0.020788	-0.023951	0.0	0.0
	φpz3	0.000538	-0.001389	0.0	0.0

$1\pi_{gx}$ (cont.)	$1\pi_{gy}$ (cont.)	$2\pi_{ux}$ (cont.)	$2\pi_{uy}$ (cont.)
0.0	0.0	0.0	0.0
0.0	0.0	0.0	0.0
0.0	0.0	0.0	0.0
-0.562157	0.0	0.463423	0.0
-0.001524	0.0	0.030634	0.0
0.002217	0.0	-0.003987	0.0
0.0	-0.562157	0.0	0.463423
0.0	-0.001524	0.0	0.030634
0.0	0.002217	0.0	-0.003987
0.0	0.0	0.0	0.0
0.0	0.0	0.0	0.0
0.0	0.0	0.0	0.0
0.0	0.0	0.0	0.0
0.0	0.0	0.0	0.0
0.0	0.0	0.0	0.0
0.562157	0.0	0.463423	0.0
0.001524	0.0	0.030634	0.0
-0.002217	0.0	-0.003987	0.0
0.0	0.562157	0.0	0.463423
0.0	0.001524	0.0	0.030634
0.0	-0.002217	0.0	-0.003987
0.0	0.0	0.0	0.0
0.0	0.0	0.0	0.0
0.0	0.0	0.0	0.0

C_2H_2: (CC,CH); 2 cycles

C_2H_4 and C_2H_6: (CC,CH); (CH,HCH); 2 cycles

H_2O: (OH,HOH); 3 cycles

H_2CO: (CO,CH), (CH,HCH); 2 cycles

$H_3CC'C''H'$: (CC',C'C''), (CC',CH), (C'C'',C''H');
2 cycles for (CC', C'C'') only

OCC'CO: (CC', CO) at angles of OCC' = 180° and
CC'C = 180°; 2 cycles
(CC', CO) at angles of OCC' = 180° and
CC'C = 150° and 170°.

For the two-dimensional searches, the following method was employed. First, six energies were calculated at six points arranged as shown in Figure 11. These energy values are sufficient to determine a quadratic function, given by the Lagrange interpolation formula (47),

$$f(x_o + ph, y_o + qk) = q^2 \left[\frac{1}{2} (f_{0,1} + f_{0,-1}) - f_{0,0} \right]$$

$$+ p^2 \left[\frac{1}{2} (f_{1,0} + f_{-1,0}) - f_{0,0} \right] + q \left[\frac{1}{2} (f_{0,1} - f_{0,-1}) \right]$$

$$+ p \left[\frac{1}{2} (f_{1,0} - f_{-1,0}) \right] + pq \, (f_{0,0} + f_{1,1} - f_{1,0} - f_{0,1}) + f_{0,0}$$

$$+ O(h^3) \qquad (40)$$

where $O(h^3)$ is the error as a function of h^3. Second, the minimum was

predicted by setting the derivatives of Equation (40) equal to zero. Numerical testing on some of the smaller molecules revealed that h and k as well as the distance between the evenly-spaced points in the one-dimensional searches should be assigned maximum values of 0.01Å or 1.5° in order that $0(h^3)$ be negligible.

The general spatial contraction of the atomic orbitals around the nuclei in the molecules as shown in Figure 9 suggest that the electronic charge is attenuated in the bond regions so that theoretical bond lengths will underestimate experiment. This assumption was verified by testing on some of the small molecules. Thus, in all succeeding bond-length optimizations, the experimental bond lengths were assigned to the point $(x_o + h, y_o + k)$ of Figure 11 rather than (x_o, y_o) so that improved predictions could be made. On the other hand, the initial pairs of parameters involving bond lengths and bond angles were assigned to (x_o, y_o) since no definite trend could be found for the angles. In the second cycle, as many of the previously computed energies as possible were used with the predicted minimum of the first cycle assigned to (x_o, y_o). Often, five new energies had to be calculated. With the exception of H_2O, only two cycles were needed for each pair. Even then, the second predicted point was found to differ from the first only by amounts < 0.005 Å or 0.5°. The corresponding energy gain was < 10^{-4} Hartree. In the case of C_3H_4, recycling through all pairs was found to be unnecessary because the C-C bonds didn't change in the second cycle. Additional testing in most molecules showed that the accuracies of the bond lengths and bond angles are $\leq$ 0.001 Å and < 1°, respectively.

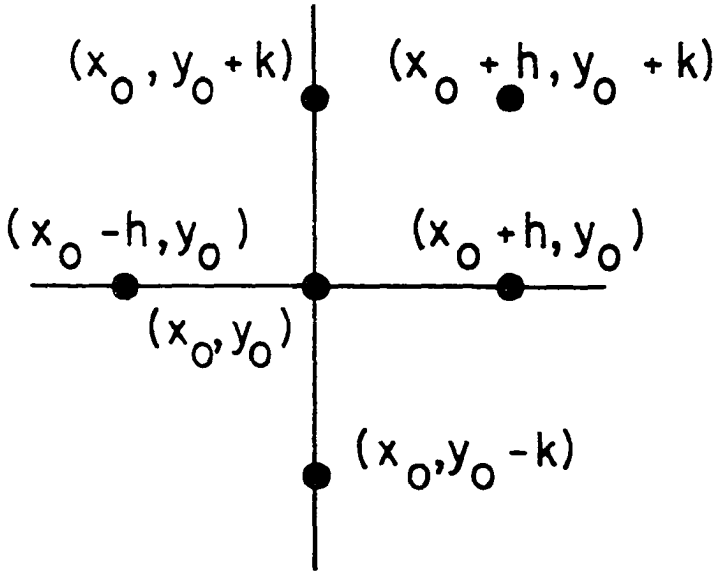

Figure 11. Arrangement of six points for molecular geometry optimizations

The optimal bond lengths and angles are given in Table 41, and the corresponding energy lowerings are given in Table 42. It is seen that quantitative agreement with experiment is quite good for all molecules except H_2O. The largest errors are 0.031 Å for the ethane-like C-H bond in C_3H_4 and 8.2° in H_2O. It is interesting to note that the addition of a single, optimized p-orbital to hydrogen in H_2O improves the H-O-H angle by only 2°. The addition of d-type Gaussian polarization functions to oxygen in H_2O should improve the angle even more. The accuracies of these bond lengths and angles of Table 41 are comparable to those found by Newton et al. (48) and Hehre et al. (49).

The geometry of C_3O_2

The structure of carbon suboxide has been previously investigated by a variety of experimental and theoretical techniques. While infrared and Raman spectrum studies (50,51) have given strong evidence in favor of a linear structure, the possibility of a nonlinear conformation could not be entirely eliminated. An ab initio calculation was made by Sabin and Kim (44), who varied the C-C-C angle from 180° to 170°, while keeping the C-C-O angle at 180°. Their results are indicated by a triangle (Δ) in Figure 12 and predict the linear configuration as the most stable. Very recently, Weimann and Christoffersen (52) have made another ab initio calculation involving drastic simplifications and constraints. They varied the C-C-C angle from 180° to 90° and the C-C-O angle from 180° to 172° and found that a zig-zag structure with a C-C-C angle of 125° and a C-C-O angle of 176° to be the most stable. Under the constrained C-C-O angle of 180°, they obtained a minimum at the C-C-C angle of 125°.

Table 41. Comparison of theoretical and experimental geometries

Molecule[b,c]	Bond Lengths and Bond Angles[a] r(C-C)	r(C-O)	r(C-H)	r(O-H)	θ(HCH)	θ(HOH)
$CH_4(T_d)$			0.003			
			1.085			
$C_2H_2(D_{\infty h})$	0.013		0.021			
	1.203		1.061			
$C_2H_4(D_{2h})$	0.010		0.002		-0.3	
	1.330		1.076		115.6	
$C_2H_6(D_{3d})$	0.010		0.028		1.25	
	1.534		1.093		109.75	
$H_3\underline{C}CCH(C_{3v})$[d]	0.004		0.031		1.1	
	1.459		1.105		108.7	
$H_3C\underline{C}CH(C_{3v})$[d]	0.014		0.017			
	1.206		1.056			
$H_2O(C_{2v})$				0.020		-8.20
				0.957		104.52
$CO(C_{\infty v})$		0.021				
		1.128				
$CO_2(D_{\infty h})$		0.011				
		1.160				
$C_3O_2(D_{\infty h})$	0.026	0.005				
	1.28	1.16				
$H_2CO(C_{2v})$		-0.005	0.030		2.0	
		1.203	1.101		116.5	

[a] Each entry contains the difference Δr = r(experiment) - r(theoretical) or $\Delta\theta$ = θ(experimental) - θ(theoretical) in the first row and the experimental value of Reference (40) in the second row.

[b] Symmetry point group is given in parentheses. Each point group was maintained during the optimizations.

[c] Contracted (MOCETGAO) basis C[3;2],O[3;2],H[2] is used for all molecules except C_3O_2 where C[4;2],O[3;2] is needed.

[d] Each entry pertains to the bonds connecting the underlined atoms.

Table 42. Energy lowerings corresponding to theoretical equilibrium geometries of Table 41

Molecule[a]	ΔE[b]
CH_4	0.00051
C_2H_2	0.00122
C_2H_4	0.00074
C_2H_6	0.00109
H_2O	0.00259
CO	0.00115
CO_2	0.00005
H_2CO	0.00151
C_3H_4	0.00261
C_3O_2	0.00217

[a] Contracted (MOCETGAO) basis C[3;2],O[3;2],H[2] is used for all molecules except C_3O_2 where C[4;2],O[3;2] is used.

[b] Energy lowering ΔE = (Energy for MOCETGAO basis obtained from Table 35 at experimental geometries) - (Energy for MOCETGAO basis at theoretical equilibrium geometry).

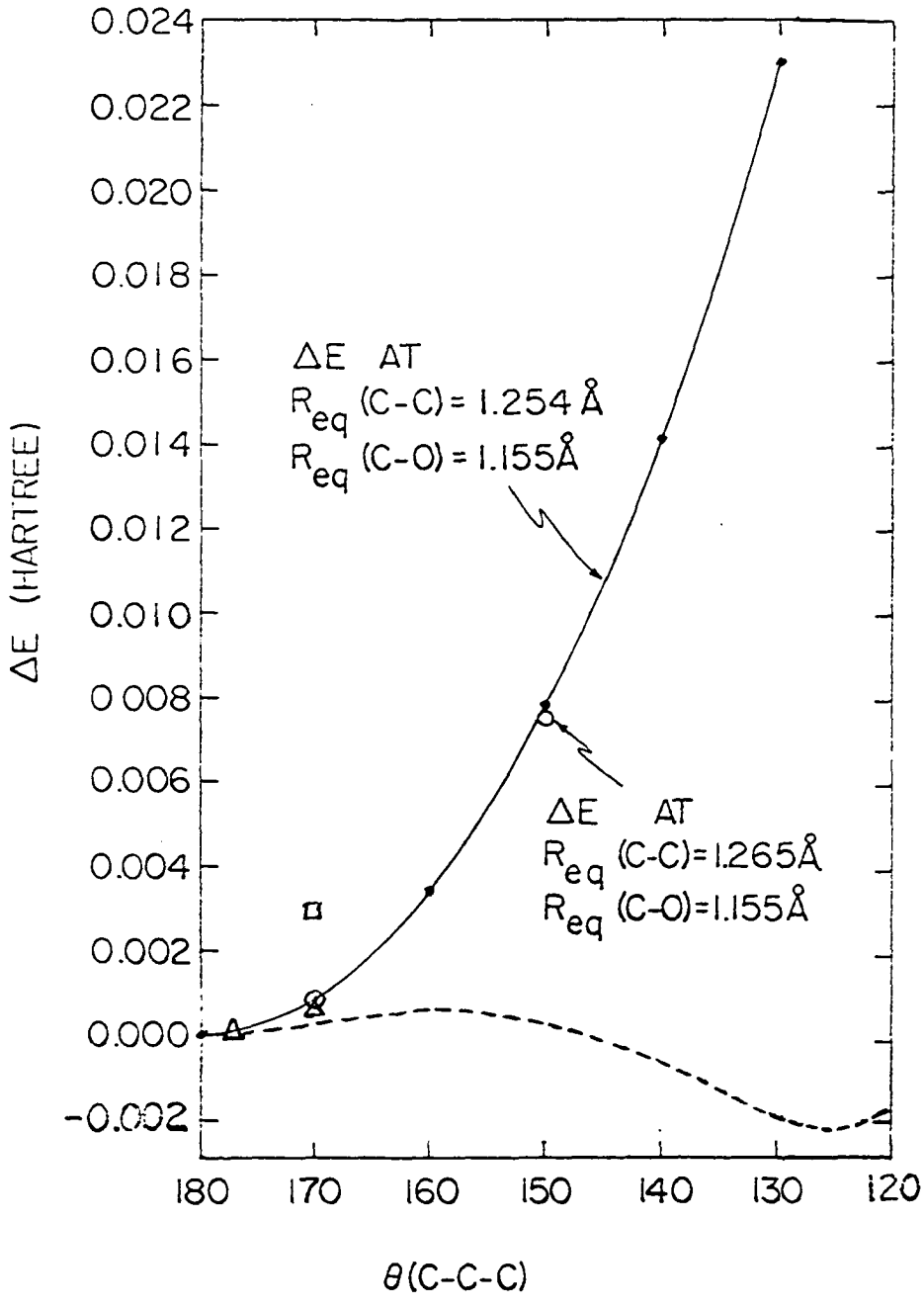

Figure 12. Variation of total energy of C_3O_2 with geometry, relative to the total energy of linear C_3O_2

These results are indicated by the dashed curve in Figure 12. In view of these inconsistencies, it was considered of interest to investigate the molecular energy of C_3O_2 as a function of all the geometrical parameters by the present approach, using the MOCETGAO bases C[4;2], O [3;2] constructed from Tables 19 and 34.

The solid curve in Figure 12 gives our results as a function of the C-C-C angle with the C-C and C-O bond lengths fixed at the equilibrium values for the C-C-C angle of 180° and with the C-C-O angle constrained at 180°. For the fixed C-C-C angle of 170°, the C-C-O angle was changed to 175° to yield a zig-zag structure, which further increased the energy to the value indicated by a square (□) in Figure 12. For the C-C-C angles of 170° and 150° and C-C-O angle of 180°, the two bond lengths were reoptimized, yielding the energies indicated by circles in Figure 12. The bond lengths were found to be unchanged at 170°, whereas at 150°, the C-O and C-C lengths were found to be 1.15 Å and 1.26 Å, respectively. In the context of an ab initio calculation with the reliability of the one performed here, the substantial energy increase for decreasing C-C-C angle seems to us to be conclusive evidence for a linear conformation.

The orbital energies for linear C_3O_2 are given in Table 43. The accuracy of the present calculation is illustrated by using Koopmans' theorem (54) to compare the theoretical and experimental first ionization potentials. The experimental value is 10.60 eV (44), whereas from Table 43, the orbital energy for $2\pi_u$ is 10.88 eV. In addition, the orbital energies of Table 43 and those over the range of angles are plotted in Figures 13 and 14. The atomic and overlap populations are given in

Table 43. Orbital energies for C_3O_2 at theoretical equilibrium geometry[a]

Orbital Symmetry	Orbital Energy
$1\sigma_u$	-20.625100
$1\sigma_g$	-20.625093
$2\sigma_u$	-11.429803
$2\sigma_g$	-11.429394
$3\sigma_g$	-11.246111
$3\sigma_u$	- 1.525928
$4\sigma_g$	- 1.522778
$5\sigma_g$	- 1.122235
$4\sigma_u$	- 0.955428
$6\sigma_g$	- 0.741335
$5\sigma_u$	- 0.735470
$1\pi_u$	- 0.679373
$1\pi_g$	- 0.640035
$2\pi_u$	- 0.399820

[a]Contracted (MOCETGAO) basis set is C[4;2],O[3;2].

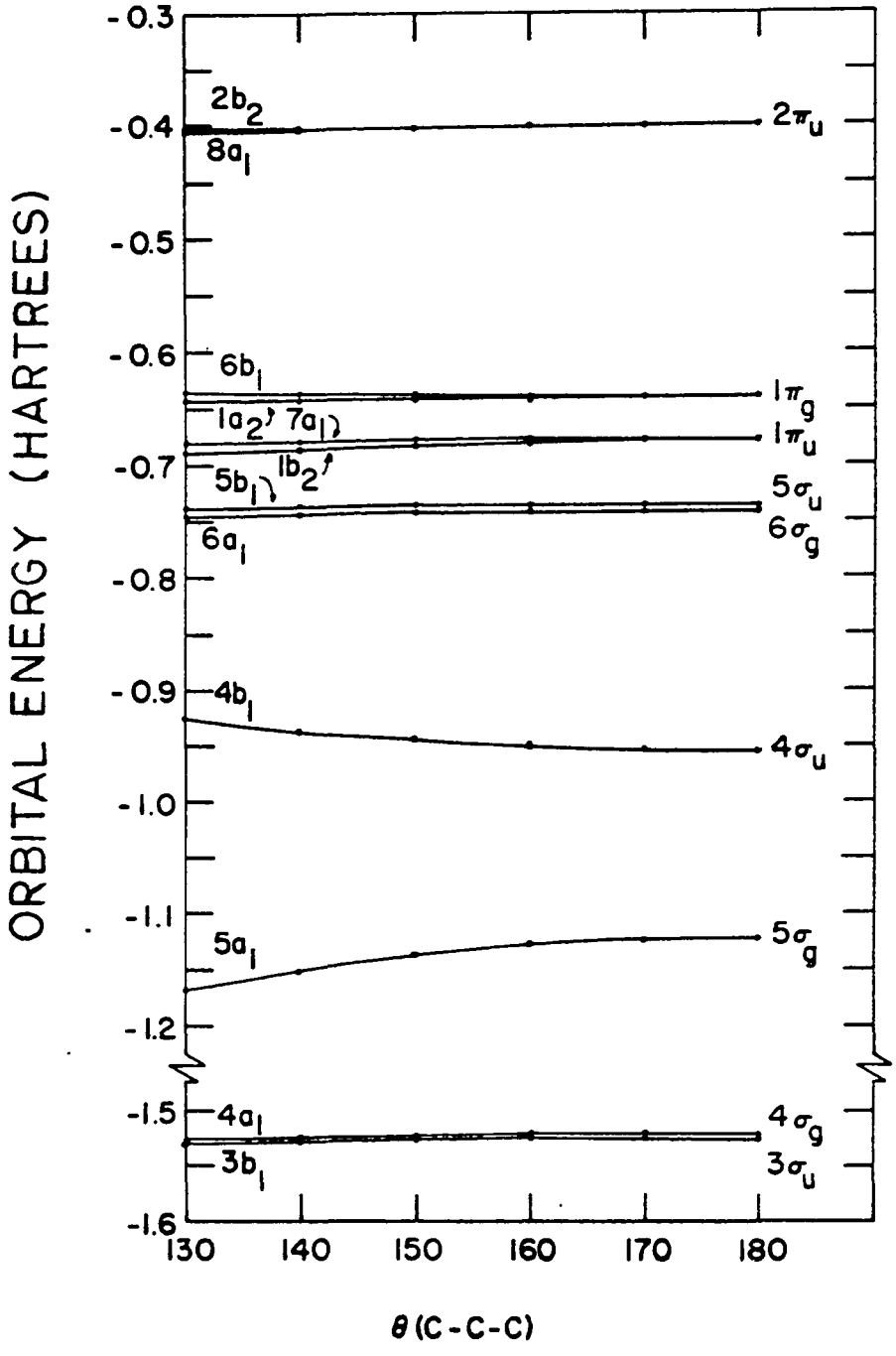

Figure 13. Variation of valence orbital energies with the CCC angles of C_3O_2

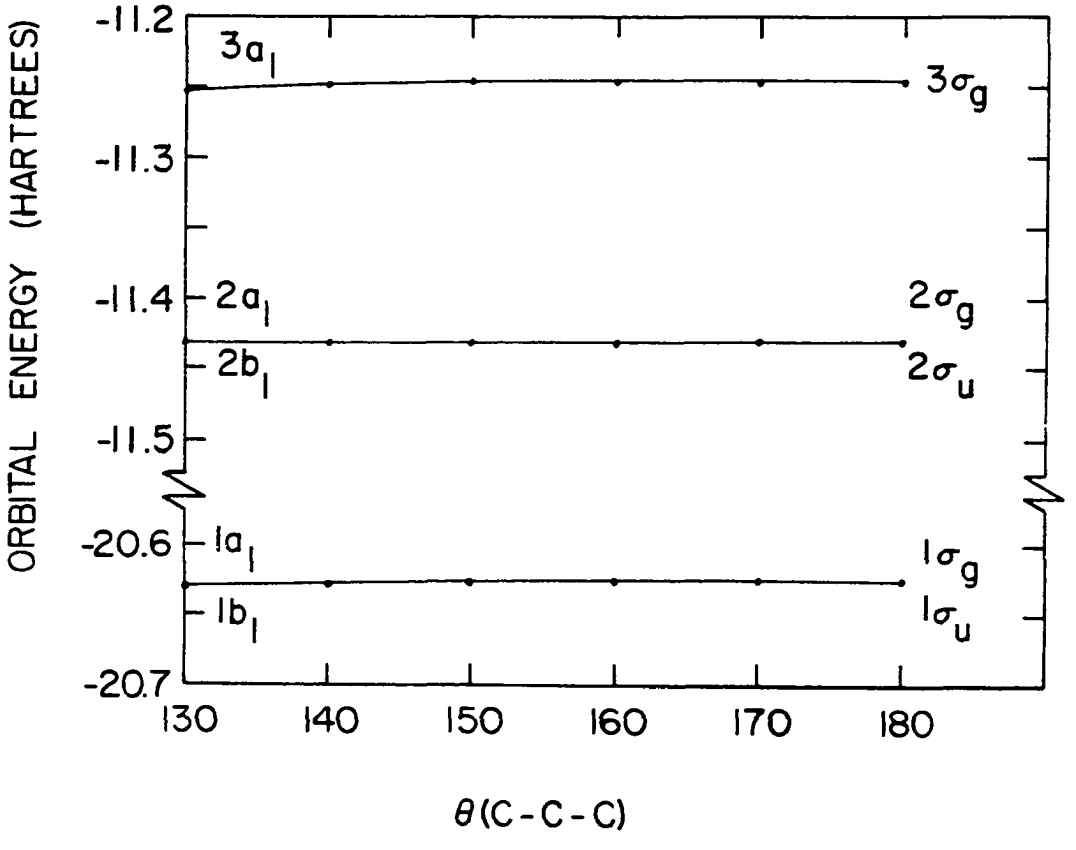

Figure 14. Variation of inner shell orbital energies with the CCC angle of C_3O_2

Table 44. These results may fit in with an explanation given by Smith and Leroi (53), pertaining to the relative ease of bending at the central carbon. According to this explanation, the relatively low vibrational frequency of 63 cm^{-1} is due to the presence of the $2\pi_u$ orbital which, during bending, maintains a sufficiently high charge density on the central carbon atom in spite of the presence of a $1\pi_g$ orbital of lower energy. The energy of $2\pi_u$ remains nearly constant because of the low atomic population on the two carbon atoms which are neighbors to the center of bending.

Reaction Energies

The accuracy with which reaction energies ΔE are computed, using approximate Hartree-Foch wavefunctions (HF app.) and energies, is determined by the magnitudes of the second and third terms in

$$\Delta E \text{ (experiment)} = \Delta E(\text{HF app.}) + \Delta[E(\text{HF exact}) - E(\text{HF app.})] + \Delta E \text{ (correlation)} + \Delta[E(\text{translation}) + E(\text{vibration}) + E(\text{rotation})]. \quad (41)$$

The second term approaches zero as the Gaussian basis set approaches completeness, and it will be small if a judicious choice of basis set is made. The correlation correction, ΔE (correlation), will be present no matter what the size of the basis set. However, its value is often small or even negligible for a variety of reactions of chemical interest where the number of paired electrons is conserved between reactants and products. In order to ascertain the magnitudes of these errors, investigations have been carried out by Snyder and Basch (55), Hehre et al. (42,49),

Table 44. Mulliken population analysis for C_3O_2[a,b]

C-C-C Angle	Gross Atomic C_1	Gross Atomic C_2	Gross Atomic O	Net Atomic C_1	Net Atomic C_2	Net Atomic O	Overlap C_1-C_2	Overlap C_2-O
				Core Shells				
180	2.0092	1.9963	1.9990	1.9981	1.9872	1.9953	0.0109	0.0073
170	2.0091	1.9964	1.9990	1.9981	1.9874	1.9953	0.0108	0.0073
150	2.0089	1.9965	1.9991	1.9982	1.9877	1.9953	0.0105	0.0073
130	2.0087	1.9966	1.9991	1.9984	1.9879	1.9953	0.0102	0.0074
				Valence Shells				
180	4.9372	3.5594	5.9720	4.1286	2.1727	5.1762	0.9977	1.7817
170	4.9329	3.5614	5.9721	4.1197	2.1756	5.1778	1.0007	1.7773
150	4.8838	3.5857	5.9723	4.0506	2.2005	5.1846	1.0172	1.7613
130	4.7813	3.6370	5.9724	3.9327	2.2526	5.1930	1.0310	1.7460

[a]Carbon atoms in C_3O_2 are numbered as $O = C_2 = C_1 = C_2 = O$.

[b]The O-C-C angle is fixed at 180°.

and Hariharan and Pople (33), using a variety of Gaussian bases of different sizes and optimal character. In Reference (21), accurate dissociation energies for the trialkali ions were obtained, using even-tempered Gaussian basis sets of modest size.

The study of heats of reaction is now extended to include the standard and MOCETGAO bases of Tables 19 and 34. For these bases, the total energies of Table 21 are used to compute the reaction energies given in Table 45. Also listed in Table 45 are theoretical reaction energies obtained by other authors, and the corrected experimental heats of reaction at 0°K corresponding to stationary nuclei. Since both ΔE (translation) and ΔE (rotation) vanish, these corrections are obtained by subtracting ΔE (vibration) $= \Delta[\frac{1}{2} h \sum_i \nu_i]$ from ΔE (experiment) where the summation is made over the normal vibrational modes of each molecule involved in the reaction.

The reactions of Table 45 are divided into two groups--(1) hydrogenation reactions and (2) those reactions for which the deficiencies of the basis for both reactants and products are such that the second and third terms of Equation (41) are smaller than for group 1. A comparison of the heats for the various MOCETGAO bases shows that little deterioration results in choosing the smallest basis. For the reactions involving only hydrocarbon and hydrogen molecules, the reaction energies are seen to approximate experiment as well as those for the comparison bases in column two. Poorer energies are obtained for reactions involving oxygen-containing molecules, especially for group 1.

An explanation for this deterioration may be as follows. The more

Table 45. Comparison of reaction energies (kcal/mole) at 0°K

Reaction	Standard-type and MOCETGAO bases C[6;4],H[4] C[3;3],H[2] C[3;2],O[3;2]H[2]			Comparison bases[a]			Exptl.[b]
	Group I Reactions (Hydrogenation)						
$H_2+C_2H_6 \rightarrow 2CH_4$	-23.4	-24.1	-24.1	-19.0	-22.9	-24.9	-18.1
$2H_2+C_2H_4 \rightarrow 2CH_4$	-64.2	-64.3	-64.6	-92.5	-65.4	-66.5	-57.2
$3H_2+C_2H_2 \rightarrow 2CH_4$	-116.6	-116.6	-120.2	-157.5	-118.0	-120.9	-105.4
$4H_2+C_3H_4 \rightarrow 3CH_4$	-131.4	-131.4	-135.0	-105.9	-132.8		-116.3
$H_2+C_2H_2 \rightarrow C_2H_4$	-52.4	-52.3	-55.5	-64.9	-52.5	-54.5	-48.2
$H_2+C_2H_4 \rightarrow C_2H_6$	-40.8	-40.3	-40.5	-73.4	-42.6	-41.6	-39.1
$2H_2+H_2CO \rightarrow CH_4+H_2O$	-69.1		-70.3	-64.2	-63.5	-70.2	-57.3
$3H_2+CO \rightarrow CH_4+H_2O$	-100.7		-100.6			-81.5	-63.9
$4H_2+CO_2 \rightarrow CH_4+2H_2O$	-104.5		-104.7	-75.9	-74.8	-91.3	-56.7

[a] First and second columns obtained from Hehre *et al.* (42) and energies of Table 21 corresponding to the bases of footnotes c and d of that table. Third column obtained from results published by Snyder and Basch (55), using a basis with 10 s-primitives and 5 p-primitives of the type C(10;10,10;5),O(10;10,10;5),H(4) contracted to C[4,4;2],O[4,4;2],H[2].

[b] Corrected experimental values obtained from the extensive tabulations of both references in footnote a. Zero point vibrational corrections were obtained from Reference (42).

Table 45. (Continued)

Reaction	Standard-type and MOCETGAO bases C[6;4],H[4]	C[3;3],H[2]	C[3;2],O[3;2],H[2]	Comparison Bases[a]			Exptl.[b]
			Group 2 Reactions				
$2CH_4+C_2H_4 \rightarrow 2C_2H_6$	-17.3	-16.2	-16.3	-54.4	-19.7	-16.7	-21.0
$2CH_4+C_2H_2 \rightarrow C_2H_6+C_2H_4$	-29.0	-28.2	-31.4	-45.9	-29.7	-29.5	-30.1
$CH_4+C_3H_4 \rightarrow C_2H_6+C_2H_2$	8.6	9.3	9.3	7.8	8.0		7.2
$CH_4+CO_2 \rightarrow 2H_2CO$	33.6		35.8	52.5	52.2	49.0	57.9
$2CH_4+H_2CO \rightarrow C_2H_6+\frac{1}{2}C_2H_4+H_2O$	-13.5		-13.8	1.1	-7.9	-12.0	-10.6
$2CH_4+CO \rightarrow C_2H_6+H_2CO$	-8.2		-6.2			13.5	11.5
$2CH_4+CO_2 \rightarrow C_2H_6+H_2O+CO$	19.7		20.1			15.1	25.3

nearly alike are the discrepancies in the basis sets for reactants and products, the greater will be the cancellation of errors in the molecular energies. This is the case for reactions involving only the hydrocarbon molecules as is seen for both groups in Table 45. Additional evidence for the bases themselves is ascertained from Figure 9. On the other hand, the discrepancies of the basis sets may not be similar in the hydrocarbons and oxygen-containing molecules. As a result, less cancellation is expected in reactions involving these molecules. The results of Table 45 and Figure 9 suggest that the major part of the error may be in the inner shells of carbon and oxygen. The bases used for comparison in Table 45 all contain fixed atomic orbital representations of inner shells whereas the outer shells are allowed to scale. The corresponding reaction energies are generally superior. However, it is seen in Figure 9 that optimization of the inner shell even-tempered parameters leads to carbon values for CO and CO_2 which are quite different from those of the hydrocarbons and leads to oxygen values for H_2O different from those of CO and CO_2. Therefore, it may be that sufficient flexibility should be maintained in the valence orbitals, but the inner shells should be such that a nearly constant error is introduced. This problem will be taken up in future work with the even-tempered basis.

LITERATURE CITED

1. Slater, J. C. Quantum Theory of Atomic Structure. Vol. 1. New York, N.Y., McGraw-Hill Book Co., Inc. 1960.

2. Fock, V. Näherungsmethode zur Lösung des quantenmechanischen Mehrkörperproblems. Z. Physik. 61, 126 (1930).

3. Steinborn, O. and Ruedenberg, K. Rotation and translation of regular and irregular solid spherical harmonics. In Löwdin, P. O., editor. Advances In Quantum Chemistry. Vol. 7. pp. 1-81. New York, N.Y., Academic Press, Inc. 1973.

4. Raffenetti, R. C. Even-tempered atomic orbitals II. Atomic SCF wavefunctions in terms of even-tempered exponential bases. J. Chem. Phys. [in press ca. 1973].

5. Shavitt, I. The Gaussian function in calculations of statistical mechanics and quantum mechanics. In Alder, B., Fernbach, S., and Rotenberg, M., eds. Methods in Computational Physics. Vol. 2. pp. 1-45. New York, N.Y., Academic Press, Inc. 1963.

6. Roothaan, C. C. J. New developments in molecular orbital theory. Rev. Mod. Phys. 23, 69 (1951).

7. Huzinaga, S. Approximate Atomic Functions. Vols. 1 and 2. Division of Theoretical Chemistry, Department of Chemistry, the University of Alberta. 1971.

8. Veillard, A. Gaussian basis set for molecular wavefunctions containing second-row atoms. Theoret. Chim. Acta (Berlin) 12, 405 (1968).

9. Petke, J. D., Whitten, J. L., and Douglas, A. W. Gaussian lobe function expansions of Hartree-Fock solutions for the second-row atoms. J. Chem. Phys. 51, 256 (1969).

10. Whitman, D. R. and Hornback, C. J. Optimized Gaussian basis SCF wavefunctions for first-row atoms. J. Chem. Phys. 51, 398 (1969).

11. Basch, H., Hornback, C. J., and Moskowitz, J. W. Gaussian orbital basis sets for the first-row transition-metal atoms. J. Chem. Phys. 51, 1311 (1969).

12. Roos, B. and Siegbahn, P. Gaussian basis sets for the first and second row atoms. Theoret. Chim. Acta (Berlin) 17, 209 (1970).

13. Wachters, A. J. H. Gaussian basis set for molecular wavefunctions containing third-row atoms. J. Chem. Phys. 52, 1033 (1970).

14. Ditchfield, R., Hehre, W. J., and Pople, J. A. Self-consistent molecular orbital methods. VI. Energy optimized Gaussian atomic orbitals. J. Chem. Phys. 52, 5001 (1970).

15. Stewart, R. F. and Hehre, W. J. Small Gaussian expansions of atomic orbitals: second-row atoms. J. Chem. Phys. 52, 5243 (1970).

16. Claxton, T. A. and Smith, N. A. Small Gaussian basis sets for second-row atoms. Theoret. Chim. Acta (Berlin) 22, 378 (1971).

17. Ruedenberg, K. Raffenetti, R. C. and Bardo, R. D. Even-tempered orbital bases for atoms and molecules. Proceedings of the Summer Conference in Theoretical Chemistry. Boulder, Colorado. 1972.

18. Clementi, E. Tables of Atomic Functions. IBM J. Res. Develop. 9 (Supplement), 2 (1965).

19. Raffenetti, R. C. and Ruedenberg, K. Non-orthogonal atomic self-consistent field orbitals. J. Chem. Phys. [in press ca. 1973].

20. Bardo, R. D. and Ruedenberg, K. Even-tempered Gaussian expansions of self-consistent field atomic orbitals. Technical Report, Ames Laboratory-USAEC, Iowa State University [in preparation ca. 1973].

21. Raffenetti, R. C. and Ruedenberg, K. Even-tempered atomic orbitals V. SCF calculations of trialkali ions with pseudo-scaled, non-orthogonal AO bases. J. Chem. Phys. [in press ca. 1973].

22. Lowdin, P. O. Quantum theory of cohesive properties of solids. Adv. Phys. 5, 1 (1956).

23. Powell, M. J. D. An efficient method for finding the minimum of a function of several variables without calculating derivatives. Computer J. 7, 155 (1964).

24. Bardo, R. D. and Ruedenberg, K. Numerical analysis and evaluation of normalized repeated integrals of the error function and related functions. J. Comp. Phys. 8, 167 (1971).

25. Ransil, B. J. Studies in molecular structure. I. Scope and summary of the diatomic molecule program. Rev. Mod. Phys. 32, 239 (1960).

26. Ransil, B. J. Studies in molecular structure. I. LCAO-MO-SCF wavefunctions for selected first-row diatomic molecules. Rev. Mod. Phys. 32, 245 (1960).

27. Pitzer, R. M. Optimized molecular orbital wavefunctions for methane constructed from a minimum basis set. J. Chem. Phys. 46, 4871 (1967).

28. Cade, P. E. and Huo, W. M. Electronic structure of diatomic molecules. VI.A. Hartree-Fock wavefunctions and energy quantities for the ground states of the first-row hydrides, AH. J. Chem. Phys. 47, 614 (1967).

29. Aung, S., Pitzer, R. M., and Chan, S. I. Approximate Hartree-Fock wavefunctions, one-electron properties, and electronic structure of the water molecule. J. Chem. Phys. 49, 2071 (1968).

30. Stevens, R. M., Switkes, E., Laws, E. A., and Lipscomb, W. N. Self-consistent-field studies of the electronic structures of cyclopropane and benzene. J. Am. Chem. Soc. 93, 2603 (1971).

31. Hehre, W. J., Stewart, R. F., and Pople, J. A. Self-consistent molecular-orbital methods. I. Use of Gaussian expansions of Slater-type atomic orbitals. J. Chem. Phys. 51, 2657 (1969).

32. Ditchfield, R., Hehre, W. J., and Pople, J. A. Self-consistent molecular-orbital methods. IX. An extended Gaussian-type basis for molecular-orbital studies of organic molecules. J. Chem. Phys. 54, 724 (1971).

33. Hariharan, P. C. and Pople, J. A. The influence of polarization functions on molecular orbital hydrogenation energies. Unpublished paper. Pittsburgh, Pennsylvania, Department of Chemistry, Carnegie-Mellon University. ca. 1973).

34. Yoshimine, M. and McLean, A. D. Ground states of linear molecules: dissociation energies and dipole moments in the Hartree-Fock approximation. Intern. J. Quantum Chem. 1S, 313 (1967).

35. McLean, A. D. and Yoshimine, M. Tables of Linear Molecule Wave Functions. IBM J. Res. Develop. 12 (Supplement), 206 (1968).

36. Roos, B. and Siegbahn, P. Polarization functions for first and second row atoms in Gaussian-type MO-SCF calculations. Theoret. Chim. Acta (Berlin) 17, 199 (1970).

37. Dunning, T. H., Jr. Gaussian basis functions for use in molecular calculations. IV. The representation of polarization functions for the first row atoms and hydrogen. J. Chem. Phys. 55, 3958 (1971).

38. Rothenberg, S. and Schaefer, H. F., III. Methane as a numerical experiment for polarization basis function selection. J. Chem. Phys. 54, 2764 (1971).

39. Shah, B. V., Buehler, R. J., and Kempthorne, O. Some algorithms for minimizing a function of several variables. J. Soc. Indust. Appl. Math. 12, 74 (1964).

40. Sutton, L. E. Tables of Interatomic Distances and Configuration in Molecules and Ions, Supplement 1956-1959. London, England, The Chemical Society. 1965.

41. Wassermann, A. L. Deviations from the virial relationship in many-center variational functions. J. Chem. Phys. 40, 1812 (1964).

42. Hehre, W. J., Ditchfield, R., Radom, L., and Pople, J. A. Molecular orbital theory of the electronic structure of organic compounds. V. Molecular theory of bond separation. J. Am. Chem. Soc. 92, 4796 (1970).

43. Hopkinson, A. C., Holbrook, N. K., Yates, K., and Csizmadia, I. G. Theoretical study on the proton affinity of small molecules using Gaussian basis sets in the LCAO-MO-SCF framework. J. Chem. Phys. 49, 3597 (1968).

44. Sabin, J. R. and Kim, H. Ab initio calculation of the electronic structure of carbon suboxide. J. Chem. Phys. 56, 2195 (1972).

45. Cotton, F. A. and Wilkinson, G. Advanced Inorganic Chemistry. 2nd Ed. p. 307. New York, N.Y., Interscience Publishers. 1967.

46. Livingston, R. L. and Rao, C. N. R. The molecular structure of carbon suboxide. J. Am. Chem. Soc. 81, 285 (1959).

47. Abramowitz, M. and Stegun, I. A., Handbook of Mathematical Functions. p. 882. National Bureau of Standards Applied Math. Ser. 55, Washington, D. C. 1970.

48. Newton, M. D., Lathan, W. A., Hehre, W. J. and Pople, J. A. Self-consistent molecular orbital methods. V. Ab initio calculation of equilibrium geometries and quadratic force constants. J. Chem. Phys. 52, 4064 (1970).

49. Hehre, W. J., Ditchfield, R., and Pople, J. A. Self-consistent molecular orbital methods. XII. Further extensions of Gaussian-type basis sets for use in molecular orbital studies of organic molecules. J. Chem. Phys. 56, 2257 (1972).

50. Lafferty, W. J., Maki, A. G., and Plyler, E. K. High-resolution infrared determination of the structure of carbon suboxide. J. Chem. Phys. 40, 224 (1964).

51. Miller, F. A., Lemmon, D. H., and Witkowski, R. E. Observation of the iowest bending frequencies of carbon suboxide, dicyanoacetylene, diacetylene and dimethylacetylene. Spectrochim. Acta 21, 1709 (1965).

52. Weimann, L. J. and Christoffersen, R. E. Ab initio calculations on large molecules using molecular fragments. Cumulenes and related molecules. Unpublished paper. Lawrence, Kansas, Department of Chemistry, University of Kansas. ca. 1973.

53. Smith, W. H. and Leroi, G. E. Correlation of electronic structure and bending force constants in some linear molecules. J. Chem. Phys. 45, 1784 (1966).

54. Koopmans, T. A. Über die Zuordnung von Wellenfunktionen and Eigenwerten zu den einzelnen Elektronen eines Atoms. Physica, 1 104 (1934).

55. Snyder, L. C. and Basch, H. Heats of reaction from self-consistent field energies of closed-shell molecules. J. Am. Chem. Soc. 91, 2189 (1969).

56. Raffenetti, R. C. Even-tempered atomic orbitals in quantum chemical ab initio calculations: Light atoms, heavy atoms, triatomic alkali ions. Unpublished Ph.D. thesis. Ames, Iowa, Library, Iowa State University of Science and Technology. 1971.

ACKNOWLEDGMENTS

The author gratefully acknowledges the opportunity to have worked under Professor Klaus Ruedenberg, and wishes to thank him for his guidance and many helpful discussions during the course of this work.

The author thanks Dr. Richard C. Raffenetti for helpful discussions. The use of his molecular SCF computer program is greatly appreciated.

The service and help provided by the programming and operating staffs of the ISU Computation Center are greatly appreciated.

APPENDIX: DESCRIPTION OF METHODS AND COMPUTER PROGRAMS USED IN THE MOLECULAR OPTIMIZATIONS

The exponent optimizations discussed previously were carried out with a set of computer programs consisting of a minimization package and an SCF molecular program which are linked together to form a fully automated system. The SCF molecular program is a highly modified version of the one described in Reference (56). This reference may be consulted for the essential features of the program. The following discussion gives the structure of the minimization package and the methods employed in each of the subprograms.

Subroutine EXPOPT

This routine oversees the entire minimization package. It is called by the SCF molecular program. Information pertinent to the progress of the minimization is stored on peripheral devices after each function evaluation. A restart option is included so that information from a previous run may be retrieved and used to restart the minimization at the exact point where the program ended. Loss of information is thus minimized. Subprograms in which the molecular integrals and SCF calculations are performed are called here.

Subroutine PARTNB

This routine is second in command to EXPOPT and is called by EXPOPT. It contains the Partan scheme, calls MINOL (see below), decides in conjunction with DECRMT when to decrement the criteria, and calls DECRMT.

Thus, the routine controls minimization on a "global" scale.

The method of Partan consists of cycles, each of which contains parallel (p) and acceleration (a) search directions in the order $p_1^i \rightarrow a_1^i \rightarrow p_2^i \rightarrow a_2^i$ where the p_1^i search direction of the ith cycle is parallel to the first acceleration search direction a_1^{i-1} of the (i-1)th cycle, and p_2^i is parallel to a_2^{i-1}. The direction of a_1^i is determined from the minima along the directions a_1^{i-1} and p_1^i. The direction a_2^i is similarly obtained from a_2^{i-1} and p_1^i. The initial search direction is arbitrary, but should be chosen as skillfully as possible as emphasized in Chapter III. If in doubt, it may be chosen at 45° to the coordinate axes or chosen as one of the coordinate directions. The second direction may be chosen perpendicular to the initial direction. Denoting the first and second directions by p_1^1 and a_1^1, respectively, each cycle spells "papa."

Decrementation of the intial function and parameter criteria, FSTPML and PSTPML, and the stepsize STEP to their final values FSTPMN, PSTPMN, and STEPMN is important for the following reasons. First, the total number of function evaluations is reduced if, initially, the criteria and stepsize are set quite loose and tightened at some appropriate point in the procedure. Second, at the beginning of minimization the number of directions chosen is more important than a detailed investigation along each direction for reaching the neighborhood of the minimum. In the vicinity of the minimum, a detailed search becomes important so that the criteria must be stricter.

The amount by which a criterion and stepsize is tightened depends on the distance from the minimum and the nature of the surface (e.g.

degree of flatness, etc.). As a result, decrementation must proceed in stages. The greater the distance from the minimum, the smaller must be the decrementing factor for each stage. The values of the function, parameter, and stepsize decrementation factors, DF, DP, and DS, are to be chosen such that FSTPMN, PSTPMN, and STEPMN are reached in an integral number of steps.

The following decrementation scheme has been found to work satisfactorily for various surfaces. The decision whether or not to decrement is made in PARTNB whereas actual decrementation is carried out in DECRMT. The following condition must be met before entering DECRMT. The input and output functions and points for MINOL must satisfy $|\text{input} - \text{output}| <$ FSTPML and PSTPML for two successive directions. In the event that either FSTPML or PSTPML is satisfied, but not both, DECRMT is not entered. Instead, the criterion that is not satisfied is loosened to assume the average value of the differences between input and output function values or points of MINOL for the two directions under consideration, i.e.,

$$\frac{1}{2}\left[\,|\text{input}_1 - \text{output}_1| + |\text{input}_2 - \text{output}_2|\,\right].$$

This requirement eliminates the likelihood of increasing the number of function evaluations due to premature decrementation of one of the criteria. Thus, the criteria can change during the course of the minimization so that they become more suited to the nature of the surface by approaching commensurability. The stepsize is decremented when the above conditions are satisfied for the criteria.

It frequently happens that PSTPML is satisfied for pairs of directions far in advance of FSTPML. This situation arises because the parameter values obey a linear relationship whereas the function values undergo more drastic, nonlinear changes. As a consequence, the function criterion may be loosened so much that it will be satisfied too soon, resulting in decrementation and an increased number of function evaluations. This circumstance is remedied by introducing an additional criterion PDECR as input which specifies how close the initial and final function values must be along a particular direction before decrementation.

An extremely loose value of PSTPML will also lead to the situation discussed in the previous paragraph. A loose value of PSTPML could also cause MINOL to end without finding a new minimum. As a consequence, Partan might not yield a new direction which could result in again searching a previous line. In order to eliminate this possibility, PARTNB forces MINOL to find a new minimum. If, after five quadratic predictions no new point is found, PARTNB avoids researching the direction by choosing a direction which bisects the quadrant currently being investigated unless Partan can choose a new direction.

In spite of the adjustments discussed previously, decrementation for both criteria may not proceed simultaneously or at all. It is possible that only one criterion may require decrementation. In this case, FSTPMN or PSTPMN must be already satisfied in both directions.

The minimization ends when FSTPMN and PSTPMN are simultaneously satisfied for two successive directions.

Subroutine MINOL

This routine finds the function minimum along a direction chosen in PARTNB. It proceeds by quadratic prediction and accelerated stepping. MINOL returns to PARTNB with its best point and function value when either a parameters criterion or a function criterion has been satisfied.

Quadratic fitting requires three function values (F_1, F_2, F_3) and their associated points along the search direction

$$S_i = (x_{ni} - x_{no})/u_n \qquad (i = 1,2,3\ ) \tag{42}$$

where x_{ni} is the nth component of the ith vector in the parameter space of the function, and u_n is the nth component of the unit vector giving the search direction. S_i is always measured from the origin of the search direction. The minimum of the quadratic is determined from the equation

$$S_4 = \frac{(S_2^2 - S_3^2)\ F_1 + (S_3^2 - S_1^2)\ F_2 + (S_1^2 - S_2^2)\ F_3}{2[(S_2-S_3)\ F_1 + (S_3-S_1)F_2 + (S_1-S_2)F_3]} . \tag{43}$$

Concavity or convexity of the surface is obtained from the second derivative

$$\left(\frac{\partial^2 f}{\partial s^2}\right)_{S_4} \equiv \frac{-2\ [(S_2-S_3)F_1 + (S_3-S_1)F_2+(S_1-S_2)F_3]}{(S_2-S_3)(S_3-S_1)(S_1-S_2)} . \tag{44}$$

Accelerated stepping is used to bracket the minimum along the direction in as few function evaluations as possible. This permits full utilization of the benefits of quadratic fitting by rapidly forcing the

search into the immediate vicinity of the minimum. Since acceleration is combined with quadratic-fitting to guarantee a downhill search, the point at the minimum of the quadratic, Equation (43), is used to determine the acceleration step. The comparison of this point with additional points is demonstrated in the flow diagram (left-hand side) of Figure 15. Succeeding function evaluations are made at the indicated points, depending on which of the inequalities are satisfied. It can be seen that the flatter the surface, the larger the stepsize chosen. Accelerated stepping ends when the first bracketing function is determined, i.e. when $F_3 > F_2$. In case Equation (44) is negative, $(S_4 < S_2)$, the new point $S_3' = S_3 + 5\ (S_3 - S_2)$ is chosen. This acceleration has been found to permit rapid exit from the region of convexity.

After the first bracketing is achieved, the routine continues with bracketing situations until one of the criteria is satisfied as shown on the right-hand side of the flow diagram. Each time, the function is computed at S_4 and the best three of the four points are kept.

Provision is made to eliminate the first bracketing function value if it is much larger than the other values and will likely continue forcing the quadratic prediction substantially away from the minimum. This function value must satisfy

$$F_3 - F_2 < \text{FBIGF}\ (F_1 - F_2),\ \text{FBIGF} = 10^3 \qquad (45)$$

if it is to be retained.

If Equation (45) is not satisfied, the smallest three of the four function values, which are not necessarily bracketing, are retained for

In the diagram, $x_1<x_2<x_3$ and $f_i>f_2$.
ST=Distance between second and third points, $|x_2-x_3|$.
PC=Parameter criterion; FC=Function criterion.

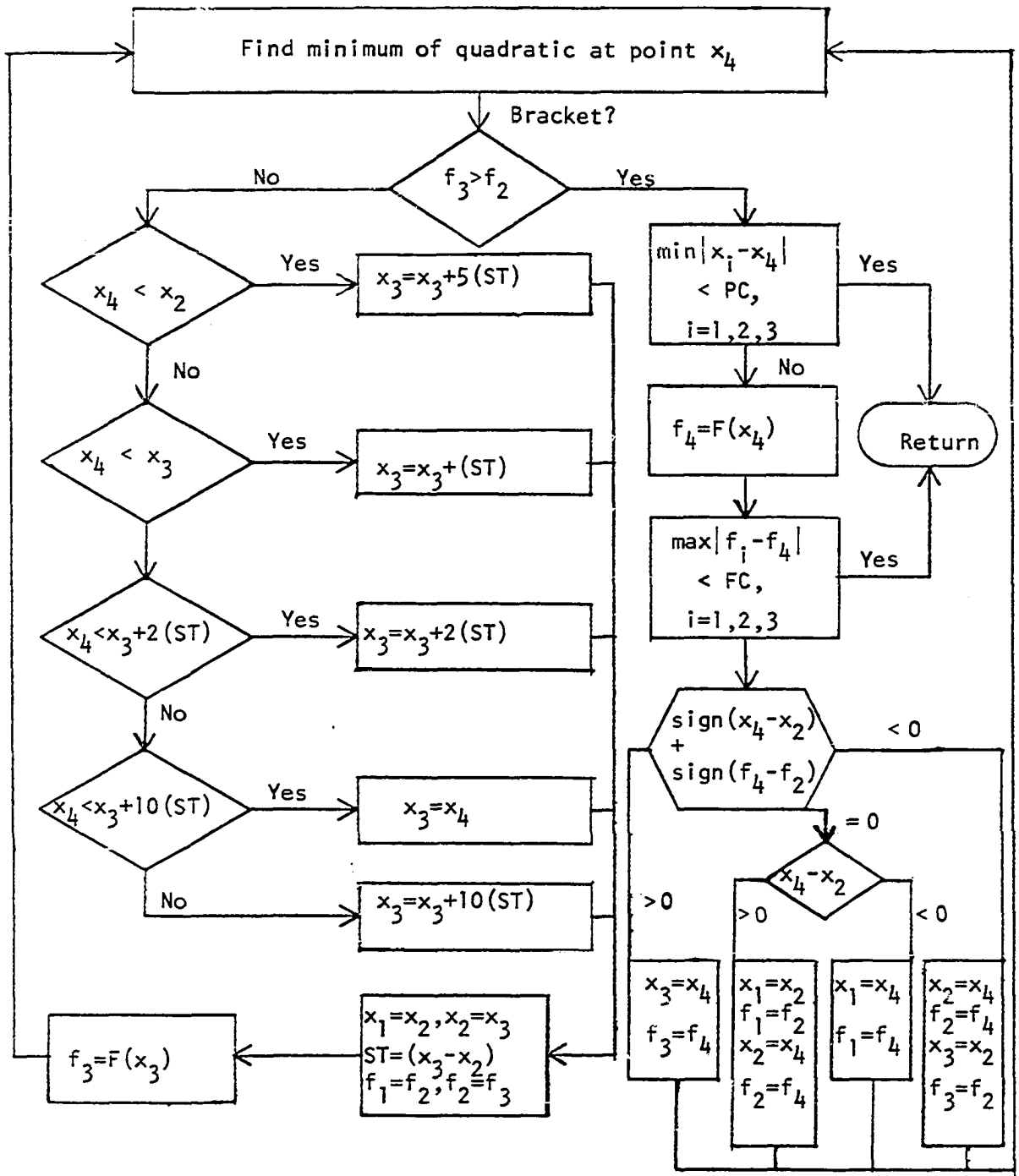

Figure 15. Partial flow diagram for MINOL

the remaining quadratic fittings. In case a poor quadratic prediction is obtained after elimination of F(big) and S(big) so that $S_4 > S(big)$ a return to bracketing is made by setting

$$S_3^{new} = S_3^{old} + FCTR\,[S_3(big) - S_2^{old}], \quad FCTR = \frac{1}{2} \text{ or } \frac{3}{4} \tag{46}$$

and calculating F_3^{new}. If bracketing is impossible, MINOL returns the best values found.

In case of convexity, S_4 is chosen as

$$S_4 \equiv S(4) = NFAIL * DXN * [S(3) - S(1)] + S(MIN) \tag{47}$$

where NFAIL is the number of consecutive times the surface has appeared convex and DXN is the direction away and downhill from the best point found so far, S(MIN). The maximum value NFAIL assumes before MINOL returns with the best values is five.

Both the parameter and function criteria need not be satisfied in MINOL. Since use of the function criterion requires additional function evaluations, the parameter criterion PMNL is always checked preferentially.

The parameter and function criteria are given as follows:

$$\begin{aligned} &\min[|S_i - S_4|] \leq PMNL, \quad i = 1,2,3, \\ &\max[|F_i - F_4|] \leq FSTPML, \quad i = 1,2,3. \end{aligned} \tag{48}$$

However, <u>both</u> the parameter and function criteria need not be satisfied in MINOL. Since use of the function criterion requires additional function evaluations, the parameter criterion PMNL is always checked

preferentially. The sufficiency of one or the other is possible because quadratic fitting guarantees closeness for both. Thus, convergence in the Cauchy sense occurs which means that if S_1, S_2, S_3 and S_4 are getting close together in value, then they must be getting close (converging) to something.

Theoretically, the parameter criterion (PMNL) in MINOL should be equal to PSTPML in PARTNB. However, due to the importance placed on PMNL in MINOL, it is best to make it smaller than PSTPML, but never smaller than PSTPMN. The following relation has been found to be satisfactory for a variety of surfaces,

$$\text{PMNL} = \text{PSTPML}/10 \ . \tag{49}$$

The function criterion is equal to that in PARTNB.

The choice of stepsize (STEP) is also important, but somewhat arbitrary. A compromise must be achieved between calculating three function values which provide too much detail about the surface or too little at the start of MINOL. From the previous discussion it is evident that stepsize will determine the rate of accelerated stepping.

Both PMNL and STEP are decremented in DECRMT as Partan progresses. However, PMNL never becomes smaller than PSTPMN.

Note: this version of MINOL may be used in conjunction with a many-parameter minimization program. In addition, it may be entered with two or three points according to the value of NPNTS (see above).

Subroutine DECRMT

Decrementation of the criteria and stepsize is carried out in this routine. Refer to PARTNB for details concerning the method of decrementation.